HABITAT FRAGMENTATION BY LAND-USE CHANGE: ONE-HORNED RHINOCEROS IN NEPAL AND RED-COCKADED WOODPECKER IN TEXAS

Vivek Thapa, M.S.

Dissertation Prepared for the Degree of

DOCTOR OF PHILOSOPHY

UNIVERSITY OF NORTH TEXAS

December 2010

APPROVED:

Miguel F. Acevedo, Major Professor
Paul F. Hudak, Committee Member
Pete A.Y. Gunter, Committee Member
Pinliang Dong, Committee Member
Ricardo Rozzi, Committee Member
Art J. Goven, Department Chair of Biological Sciences
James D. Meernik, Acting Dean of the Robert B. Toulouse School of Graduate Studies

Thapa, Vivek. Habitat fragmentation by land-use change: One-horned rhinoceros in Nepal and red-cockaded woodpecker in Texas. Doctor of Philosophy (Environmental Science), December 2010, 135 pp., 18 tables, 55 illustrations, references, 163 titles.

This research focuses on the spatial analysis of the habitat of two vulnerable species, the one-horn rhinoceros in the grasslands of southern Nepal, and the red-cockaded woodpecker in the Piney woods of southeast Texas, in the USA. A study sites relevant for biodiversity conservation was selected in each country: Chitwan National Park in Nepal, and areas near the Big Thicket National Preserve in Texas. Land-use differs in the two study areas: the first is still undergoing agrarian development while the second is in a technological phase and undergoing urbanization processes. Satellite remote sensing images were used to derive land-cover maps by supervised classification. These maps were then processed by Geographic Information Systems methods to apply habitat models based on basic resources (food and cover) and obtain habitat suitability maps. Several landscape metrics were computed to quantify the habitat characteristics especially the composition and configuration of suitable habitat patches. Sensitivity analyses were performed as the nominal values of some of the model parameters were arbitrary. Development potential probability models were used to hypothesize changes in land-use of the second study site. Various scenarios were employed to examine the impact of development on the habitat of red-cockaded woodpecker. The method derived in this study would prove beneficial to guide management and conservation of wildlife habitats.

ACKNOWLEDGEMENTS

For the research conducted in Nepal I acknowledge the assistance of several individuals such as the staff of National Trust for Nature Conservation (Formerly known as King Mahendra Trust for Nature Conservation), especially Mr. P. Khanal and the guides who offered immense help during the adventurous field trip in the year of 2004–2005. Special thanks are due to Kul Limbu, who participated in this field trip and collaborated in many aspects of the rhino research.

The research on the woodpecker was possible due to the help of many people. I would like to thank Maxine Johnston (Big Thicket Association), Arlene Kalmbach (TPWD-Texas Parks and Wildlife Department), Wendy Ledbetter (The Nature Conservancy), Steve Marietta and David Green (Hancock Forest Management), and Theresa and Wade Taylor (Hardin and Jefferson County Appraisal District). These individuals provided valuable information such as maps of timber lands, parcel and GIS data. I am also grateful for partial funding received for the research reported in Chapters 3 and 4 that was conducted as part of a Biocomplexity in the Environment (Coupled Natural Human Systems) project funded by grant CNH BCS-0216722 from the U.S. National Science Foundation. Chapter 3 benefitted from the input of Prof. J.B. Callicott, Philosophy department. I would also like to thank Otilia Sanchez, editor College of Engineering, for constructive and extensive editorial comments on Chapters 2 and 3.

Many thanks are due to the University of North Texas faculty who served in my doctoral committee, Paul Hudak, Ricardo Rozzi, Pete Gunter, and Pinliang Dong, as well as in my M.S. committee Jim Kennedy and Earl Zimmerman. Special thanks to Miguel F. Acevedo, my major professor, for his support during my graduate studies at the University of North Texas.

TABLE OF CONTENTS

LIST OF TABLES

LIST OF FIGURES

CHAPTER 1

INTRODUCTION

With ever increasing world population (current 1.3% growth rate) coupled with constant change in technologies, we are becoming urban species and as a result our effects on the environment are also increasing (Cincotta et al., 2000; Botkin & Keller, 2003). Economic development is the precursor of urbanization; urban areas expand and rural area decreases. With urban sprawl, environmentally sensitive lands such as forests, wetlands, floodplains and grasslands are lost forever. According to Botkin and Keller (2003), currently about 75% of population in the developed world live in urban areas and 25% in rural areas. In contrast, only 38% of people are city dwellers in developing countries. However, urbanization trends indicate that by 2025 almost two-thirds (~ 5 billion) of the world's population will live in cities and megacities. A megacity is a city with more than 8 million inhabitants. And by 2015, there will be 36 megacities of which 23 will be in the developing world especially in the Asian continent (Botkin & Keller, 2003).

Further, Huston (2005) described three phases of human-induced alteration of landscapes; agrarian, transportation and communication. The agrarian phase is driven by primary and secondary productivity of a particular area and has been a part of hunter-gatherer culture of human history (Huston 2005). In this phase, both primary and secondary productivity leads to population growth that in turn leads to agricultural culture. However, net primary productivity (NPP, plant mass) is the ultimate driver of this phase as well as the fundamental constraint that determines animal densities of a particular place including humans. In other words, high plant productivity can support high animal mass and vice-versa. Global cultivation patterns also suggest that high proportions of agriculture activities are found where soils are fertile and thus

carry high human populations. Due to this inevitable correlation between NPP and human population density, the impacts of the agrarian phase are restricted to landscapes with high NPP such as riparian and alluvial areas, productive grasslands, and productive forests on fertile soils. For example, forests in the prairie areas of the United States of America (USA) and alluvial floodplains of Chitwan Valley in Nepal have been converted to cropland thus eliminating large native herbivores such as elk and bison from their historic range and shrinking the once abundant habitat of rhinoceroses in Chitwan Valley.

The second or transportation phase weakened the connection of population to local NPP. With the expansion of transportation networks such as highways, waterways and railways, humans were able to move foods efficiently and population began to shift towards locations where transportation concentrated food and other resources called as transportation nodes. Sometimes, these places could be areas with low NPP and have escaped impact during the agrarian stage that now can be heavily affected by resource extraction and urban/industrial growth. Other environmental impacts include increased use of aquatic resources and degraded water quality caused by concentrated human population (Wang et al., 2001; Stepenuck et al., 2002; Hansen et al., 2005). However, one indirect environmental benefit of this stage is reduction of population density from high NPP areas or agricultural regions (Lobao & Meyer, 2001). This is yet to happen in the Nepal study site as the mainstay of the economy is agriculture and people are still attracted to the fertile floodplains of the valley. However in the USA, improved transportation and industrial technologies resulted in depopulation from high NPP areas that led to abandonment of marginal agricultural lands in places such as southern and northeastern Iowa. As a result, northeastern areas of the USA experienced substantial forest regeneration while in the western USA, impact from grazing was reduced and grassland was re-

established (Licht, 1997; Hall et al., 2002; Foster et al., 2003). Nonetheless, this recovery might be beneficial to the local or regional biodiversity but may be short lived if the population continues to grow and food production becomes less efficient (Huston 1995; Waggoner & Ausubel, 2001).

The third stage, communication or information stage, enabled humanity to be more independent than in the two stages discussed above. As noted, the direct impact was on the low productivity areas, reservoirs of biodiversity that were largely ignored during agrarian and industrial stages. Such areas tend to have higher densities of rare 'endemic' species of plants and animals and these areas are mostly targeted for aesthetic purposes such as views of natural scenery of streams, rocks and vegetation (Hansen et al., 2005). Thus, in third stage, people were able to build houses on once inaccessible but aesthetically valuable hillsides and ridge tops or near lakes as they can electronically transfer wealth generated in urban/industrial areas for use in remote areas (Jacobs, 1984). Consequently, these low productivity areas are being developed regardless of its sensitivity to anthropogenic disturbances such as land clearing and road construction thereby impacting its water availability and higher productivity content that are critical to ecosystem function and biodiversity (Abbott et al., 2001; Hansen et al., 2005). Further impact can be seen on the population of plants and animals as they tend to be smaller in such areas. And if disturbed, it takes longer for the plants and animals to recover and make them more vulnerable to land clearing and invasion by exotic species (Huston, 1994; Huston, 2004). Unfortunately, in developed countries such as the USA, these agriculturally marginal, low-productivity landscapes frequently occur in public lands that are subject of current rapid land-use alterations (Huston, 1993; Scott et al., 2001; Hansen, 2005). Thus, until recently these marginal low-productivity areas have been the primary refuges for biodiversity and are currently

threatened with the third stage of communication development. The three stages discussed here have been potent drivers of forest loss in both developed and developing worlds. As mentioned above, in developed countries, low NPP areas are the current subject of exploitation due to improved communication technologies but developing countries are still going through agrarian and industrial stages.

Biodiversity Hotspots

Jha and Bawa (2006) studied relationships between population growth, human development index (HDI), and deforestation rate in thirty countries in Asia, Africa and Latin America. They made two groups of 11 and 19 countries. Some countries are included in the current list of biodiversity hotspots of the world by Conservation International (explained later in this section). They also examined the Gini coefficient (measurement of income inequality) of some countries. HDI measures income, health and education of a population (Jha & Bawa, 2006). Their results showed that high population growth can increase deforestation but high HDI can mitigate that rate. However, HDI effects can be uneven across countries. In other words, with improved economic status, health and education, deforestation rate can decrease but this is not always the case. Even with HDI values, some countries such as Costa Rica, the Philippines, and Thailand (hotspots) had high deforestation rate and this is attributed to the policies of these countries that favored over logging, land clearing for agriculture, and conversion to ranch land (Bawa & Dayanandan, 1997; Kaimowitz & Angeisen, 1998). However, once the policies were reversed, these countries saw substantial drop in deforestation rate. This shows that besides high HDI, low population growth and low deforestation rate, policies that favor biodiversity conservation are very important.

Many regions of the developing world have been identified as biodiversity hotpots where unique assemblage of species and habitats occur that are experiencing a severe threat of overexploitation (Cincotta et al., 2000; Jha & Bawa, 2006). A biodiversity hotspot is a biogeographic region with 0.5% or more of the world's flora endemic to that place and that has already lost at least 70% or more of its primary vegetation or their original geographic extent (Myers et al., 2002; Brooks et al., 2002). In other words, to qualify as a hotspot the area should contain at least 0.5% or 1,500 of the world's 300,000 plant (vascular) flora species as endemics (Mittermeier et al., 1998; Myers et al., 2000). It is impossible to include all the species of a biotic community and 'surrogate' species are commonly used to represent biodiversity of an area (Sarkar, 2002). However, according to Rozzi et al. (2003), use of surrogate species might under-represent species of an area that contain limited vascular plants. They suggest that use of other abundant species might be feasible in such cases. For example, bryophytes are abundant in Chile and they can be used as one of the hotspot criteria.

Beside plant endemism, four groups of vertebrates (aves, mammal, reptile and amphibia) are very important to consider, although they are not directly used as criteria for hotspot selection (Mittermeier et al., 1998; Myers et al., 2000). The vertebrate data was used as back-up support, to determine congruence, and to facilitate other comparisons among the hotspots. Moreover, the species dimensions were emphasized on vascular plants because of their importance to all forms of animal life and are fairly well known scientifically (Mittermeier et al., 1998; Margules & Pressey, 2000; Myers et al., 2000; Brooks et al., 2002). Thus, endemism and degree of threat of a hotspot makes them both irreplaceable and vulnerable because endemics require and depend on a particular area to survive (Mittermeier et al., 1998; Myers et al., 2000). And this restricted range

can become the target of extinction episodes thus requiring immediate effective conservation action (McNeely et al., 1990; Pimm et al., 1995).

Currently, there are 34 biodiversity hotspots around the world and about half (16) are located in the developing world, where threats are greatest and conservation resources are scarcest (Myers et al., 2000; Conservation International, 2005; Jha & Bawa, 2006) (Figure 1.1). These hotspots contain 50% of the world's vascular plants and 42% of four terrestrial vertebrates in just 2.3% of land area (Myers et al., 2000; Brooks et al., 2002; Conservation International, 2005). Previously hotspots occupied 17.4 million square kilometers or 11.8% of the earth's land surface. According to Cincotta et al. (2000), there were 1.1 billion people living within the hotspots in 1995 and growing at a rate of 1.8%/yr (higher than world's growth rate of 1.3%). They calculated population density in the hotspots and found 73 people per square kilometer, which is well above world's average (42 people per km^2). Their findings indicate substantial human-induced environmental changes are likely to continue in the hotspots and that demographic change will remain an important factor in biodiversity conservation (Cincotta et al., 2000).

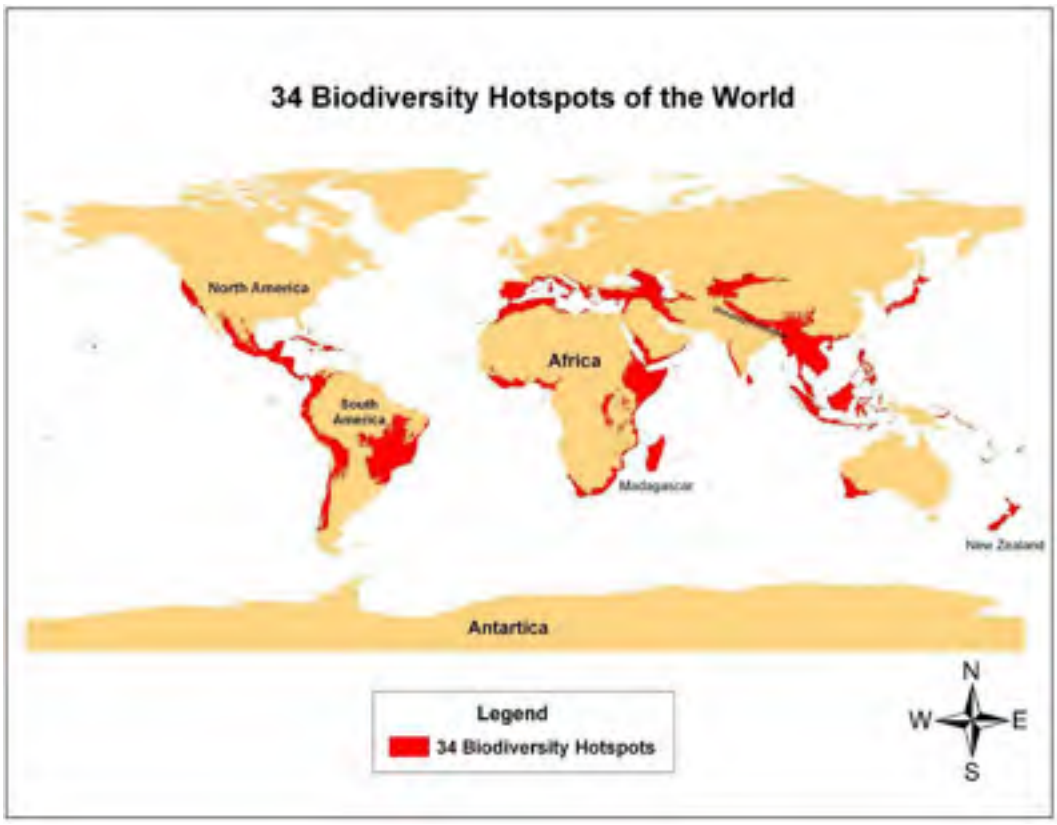

Figure 1.1. Current 34 biodiversity hotspots of the world.

Among 34 biodiversity hotspots, the Himalaya hotspot covers approximately 750,000 km^2 and is divided into two parts; Eastern and Western (Conservation International, 2009) (Figure 1.1). The eastern part extends from Nepal to Bhutan, northeast Indian states of West Bengal, Sikkim, Assam, Arunachal Pradesh, southeast Tibet (China) and northern Myanmar. The Western Himalaya extends from Kumaon-Garhwal, northwest Kashmir to northern Pakistan. The Eastern Himalaya hotspot is home to eight of the world's highest mountains, including Mt. Everest, as well as several of the world's deepest river gorges. It is home to important populations of several large mammals and birds, including vultures, tigers, elephants, rhinos and wild water buffalo. The primary reason for such diverse assemblage of faunal species is due to the unique topography of this region. The mountains rise abruptly from less than 300 meters to more than 8,000 meters in only a couple of hundred kilometers, creating a diversity of

ecosystems from alluvial grasslands (among the tallest in the world) and subtropical broadleaf forests along the foothills to temperate broadleaf forests in the mid hills, mixed conifer and conifer forests in the higher hills, and alpine meadows above the treeline. This eastern hotspot includes one of the study area; Chitwan National Park (CNP).

Even though one of this thesis's study areas, the Big Thicket National Preserve (BTNP), does not qualify as a global biodiversity hotspot in terms of plant endemism, it was recently recognized by UNESCO and is in the list of International Biosphere Reserves (National Parks Service 2009). In addition, the American Bird Conservancy designated BTNP a Globally Important Bird Area in 2001. BTNP is also designated as Biological Crossroads of North America due to its unique congruence of four different ecosystems. The southeastern swamps, Appalachians, eastern forests, central plains and southwest deserts mark the biological crossroads of BTNP. As a result, 85 tree species, more than 60 shrubs, nearly 1000 flowering plants including 20 orchids, 26 ferns and allies, and four of North America's insectivorous plants make their home in BTNP (Callicott et al., 2007). In addition, about 50 species of reptiles and 300 kinds of birds live in BTNP including the vulnerable red-cockaded woodpecker species and many migratory species. Thus, both study areas are important in terms of ecological and biological refuges for above mentioned vulnerable species and co-existence of other wildlife species.

Land Use and Wildlife

Land use practice is often linked to the loss and fragmentation of wildlife habitats and has evolved to become one of the most important factors to increase the current wildlife extinction rate. Even though, loss and fragmentation of habitat are inextricably related or linked, they differ

markedly in the severity of impact they impose upon wildlife. Fragmented habitats may still contain enough of the original features such as sufficient life or habitat requisites to sustain small or viable populations of some species, but loss of habitat has detrimental effects on species survival or may even become the cause for their extinction. Our hotspot study site, CNP (Figure 2.1) is one such area that still contains some original features of the landscape such as mosaic alluvial grasslands and riverine forests that sustain some of the world's largest vertebrates today. However, it has experienced both natural and anthropogenic disturbances. Most significant among natural disturbances is the annual monsoon, which makes three major rivers (Rapti, Narayani and Reu) change their course. As result new grassland pockets are regularly created and some are lost forever. In addition, recent invasion of a rapid growing vine species covering the critically important grassland has increased the threat dramatically. Anthropogenically, the park is surrounded by burgeoning human population that has led to increased pressure on the wildlife and its habitat, accelerated illegal grass cutting and poaching.

In the BTNP, changes in land use patterns are also primarily human-induced by activities such as agriculture, forestry and plantations, oil and gas operations, and urbanization. Before the European settlement, there were 200 million acres of pine forest sprawled across southeastern United States of which 92 million acres were inhabited by red-cockaded woodpecker. Today only 3 million acres remain (almost a 98% decline) of which only 1 percent is in natural condition. Hundreds of years of extensive logging of southern pine forests, suppression of fire in the landscape, change in forest species and recent forestry practices such as clear cutting and short rotation of tree harvest have all been detrimental to red-cockaded woodpeckers. Over the last five decades, the landscape surrounding the BTNP has been converted from contiguous pine forest to a matrix dominated by agriculture, pasture, timber plantations and exurban and

suburban development (Wilcove et al., 1986). As a result, the once intact pine forests have been converted into small patches that are mutually isolated by a matrix of agricultural or other developed lands (Callicott et al., 2007).

Dissertation Structure

The dissertation is divided into four chapters and an appendix as follows: chapter 1, this introduction; chapter 2, One-Horned Rhinoceros Habitat Analysis; chapter 3, Red-Cockaded Woodpecker Habitat Analysis; chapter 4, Development Potential Maps in BTNP; and the appendix, Data Search for Big Thicket Region.

The three chapters after this introduction include manuscripts submitted or being submitted for publication, while the appendix explains how the data were searched that was used to complete the fourth chapter. The chapters are presented as individual papers since they are written for submission to peer-reviewed journals.

Chapters 2 and 3 illustrate how a common methodology based on remote sensing, geographic information systems, and fragmentation analysis can be used for both species. The methodology conducted in chapter 4 is applied only to the BTNP study, where significant NSF-funded research resources were invested in data acquisition, modeling and analysis. In addition, this chapter illustrates how this methodology could eventually be applied to Chitwan and other wildlife conservation areas of the world.

CHAPTER 2

ANALYSIS OF THE HABITAT OF GREATER ONE-HORNED RHINOCEROS AT THE CHITWAN NATIONAL PARK, NEPAL*

Abstract

Remote sensing and geographic information systems (GIS) are widely used for a plethora of applications including habitat analysis. However, prior to this project, use of these tools and techniques to evaluate greater one-horned rhinoceros (*Rhinoceros unicornis*) habitat was lacking. We have employed the aforementioned tools to investigate available habitat area of the rhinoceros at the Chitwan National Park of Nepal during 2004–2005. We used a Landsat image of April 12, 2003 to derive the vegetation types of the park area. The image was classified into eight land-cover types: wetland, sand, water, mixed forest, sal forest, agriculture, settlement, and grassland. This classified image was converted into habitat suitability index (HSI) maps by using a heuristic model based on the abundance of food, water, and cover in a neighborhood around each pixel. The rhinoceros prefers areas with tall grass for food, water for drinking and wallowing, and nearby closed canopy for refuge from floods and for breeding during the monsoon and mating seasons, respectively. We developed an HSI map that categorizes habitat into three types: very unsuitable, unsuitable, and suitable. We then used this map to estimate the amount and fragmentation of each habitat type. Patch and class metrics associated with the habitat types were determined with FRAGSTATS program. These metrics exhibited highly fragmented status for all three habitat types explored. The vegetation and HSI maps derived using remote sensing and GIS combined with metrics resulted in a useful tool to quantify the

* This chapter has been submitted to the *Journal of Wildlife Management* with Miguel Acevedo and Kul Limbu as co-authors.

habitat of the rhinos. Furthermore, our results can be used for management, monitoring, and improvement of the habitat of greater one-horned rhinoceros and other wildlife.

KEYWORDS: Chitwan National Park, Greater one-horned rhinoceros, GIS, Habitat suitability index model, Habitat fragmentation, Remote sensing.

Introduction

The Asian or greater one-horned rhinoceros (*Rhinoceros unicornis*) evolved in the hygrophilous tall grass floodplains of South Asia along with woodlands, tropical moist deciduous and tropical semi-evergreen forests that remain in a state of flux due to recurring flood and succession (Rawat, 2005). The rhinoceroses were once widely distributed throughout the Brahmaputra, Indus, and Ganges plains of South Asia, but indiscriminate poaching and unprecedented habitat loss has nearly pushed them to extinction (Laurie, 1978; Dinerstein & Price, 1991; Jnawali & Wegge, 1993; Dinerstein, 2003). They are now restricted to small isolated populations on the Indian subcontinent, mainly in India and Nepal (Laurie, 1978: Rawat, 2005). The current estimated wild population of the greater one-horned rhinoceros is about 2800, with Kaziranga National Park (KNP) of India harboring the highest population of more than 1900 (Dinerstein & McCracken, 1990; Dinerstein & Price, 1991; Rawat, 2005). A free-ranging population of 1000 rhinoceroses survived in the malaria infested southern lowlands of Nepal until early 1950s. However, with the abatement of malaria in Nepal and Northern India during the same year, the once inaccessible rhino habitats were opened to human settlement followed by subsequent poaching and massive destruction of alluvial floodplains, adjacent swamps, and forests, triggering a drastic decline of the rhinoceros population (Laurie, 1978; Cohn, 1988; Dinerstein, 2003; Harini et al., 2008).

Only small populations of less than 100 individuals were reported to have survived in the floodplains of the major rivers – the Reu, Rapti, and Narayani (Laurie, 1978; Dinerstein & Wemmer, 1988; Dinerstein & Price, 1991; Dinerstein, 2003; Harini et al., 2008). Fortunately, these prime habitats of 932 km^2 of Chitwan valley were declared a national park in 1973 (Chitwan National Park, CNP), and the rhinoceroses became the property of Nepal government. This change reduced poaching and other illegal activities significantly. As a result, the rhinoceros population increased dramatically and nearly 600 rhinoceroses wandered the floodplains during late 1990s, marking this as one of the most successful conservation stories in South Asia (Dinerstein & Price, 1991; Dinerstein, 2003). Around the same decade, Dinerstein and Price (1991) recognized four distinct subpopulations based on their isolation. They used physical barriers such as rivers and low mountains and ecological boundaries such as sal forests and agricultural lands to identify the four subpopulations of the Sauraha (1), the Bandarjhola-Narayani River (2), the west (3) and the south (4) (Figure 2.1). They also reported frequent movement of animals from far-east of the park boundary that was initially thought as separate population by Laurie (1978). They combined this population with the Sauraha, which currently has the highest population of rhinos and is most intensively studied. Simultaneously, the increased population of wildlife, especially of the greater one-horned Rhinoceros, intensified park-people conflicts (Nepal & Weber, 1995). As a consequence, 80 rhinoceroses were translocated to Bardia National Park, Nepal (Jnawali & Wegge, 1993).

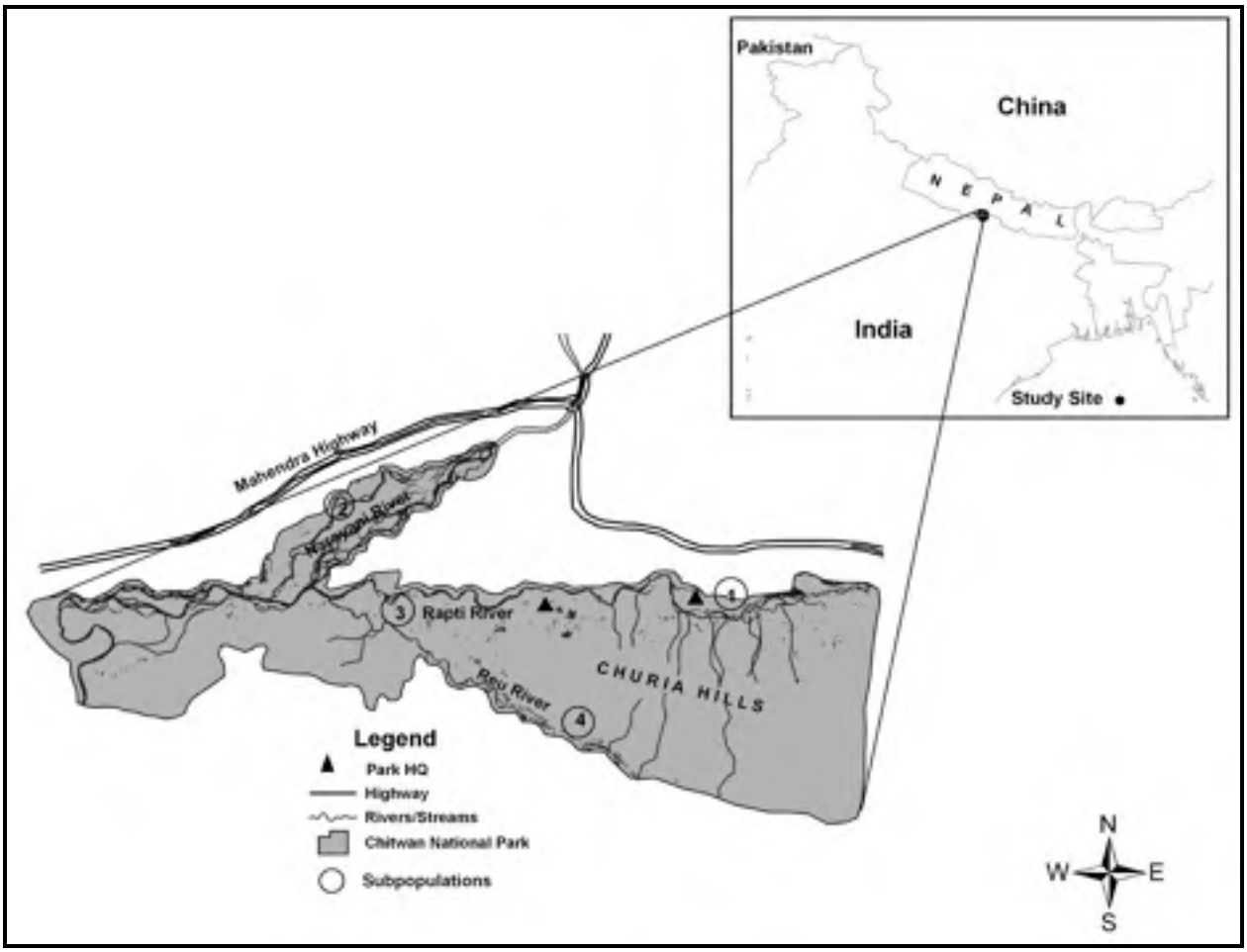

Figure 2.1. Study area showing location of rhino subpopulations and others.

However, the success was short-lived as Nepal plunged into deep political strife due to Maoists insurgency in 1996 that lasted for nearly a decade and cost more than 12,000 lives (Baral & Heinen, 2005). As with other sectors, ongoing conservation efforts were severely impacted and Chitwan valley saw an increase in poaching of rhino and Bengal tigers and other endangered animals. For example, CNP had 32 army posts prior to the insurgency that were reduced to 8 by early 2000 (Dinerstein, 2003; Baral & Heinen, 2005; Sharma, 2005). As a result, rhino numbers plummeted to less than 400 individuals supporting the statement that habitat or species are never safe (Dinerstein, 2003).

Thus, the insurgency interrupted Nepal's tradition of being one of the few countries where national army and civilians patrol and protect national parks and reserves along with

international conservation partners. However, in 2006, once Maoists were included in the Government, conservation efforts resumed. Recent rhino census indicates a gradual increase in the population from ~350 to 408 in CNP (DNPWC, 2008). This success shows that with strict regulations and relative political stability, these mega vertebrates can bounce back from the brink of extinction. However, increase in wildlife population number warrants continuous and effective management of existing habitat pockets, i.e. grasslands in the national park and to ensure sustainability of current viable populations. In addition, a thorough study of biological and ecological behavior of target species is critical for effective habitat management.

Greater one-horned rhinos are usually solitary animals except for females with young (Laurie, 1978). They are primarily grazers but occasionally browse. They inhabit riverine (floodplain) grasslands and seasonally utilize adjacent woodland or mixed forests (Dinerstein & Wemmer, 1988; Dinerstein & Price, 1991; Jnawali & Wegge, 1993; Lott & McCoy, 1995). The animal's frequent mixed forests during the cool season, as availability of nutritious grassland becomes low, and seek refuge in the upland sal forests from annual monsoon floods. They wallow in oxbow lakes to regulate body temperature in the hot season and feed on aquatic plants indicating amphibious ancestry (Dinerstein, 2003) (Figure 2.2). Females reach sexual maturity between 5 to 7 years of age while males at 8 to 10 years of age. The gestation period lasts approximately 15-16 months and the mothers give birth to one calf every 1-3 years (Laurie, 1978; Dinerstein, 2003). Depending on the suitability of habitat (abundance of forage and water) and season (whether it is the cool or hot season), the annual home range of breeding male and female is found to be 4.3 km^2 and 3.5 km^2 respectively (Dinerstein, 2003). In other words, rhinos do travel far if the habitat fails to provide enough food and water (Jnawali & Wegge, 1993).

However, most research reports indicate the importance of grassland habitats for their survival (Figure 2.2).

Figure 2.2. Grassland habitat and its inhabitant (photo by K.P. Limbu and Vivek Thapa).

The existing literature on monitoring rhino habitats of Chitwan valley is scarce since most papers on rhino focus on biological and ecological aspects of the species (Laurie, 1978; Owen-Smith, 1988; Lott & McCoy, 1995; Dinerstein, 2003). Satellite remote sensing and GIS (Geographic Information Systems) offer an opportunity to contribute knowledge about the habitat. These technologies are increasingly used to model spatial information about wildlife habitat (Porwal & Roy, 1996; Sharma et al., 2004). In addition, remote sensing coupled with

field work and GIS has proven effective in deriving much needed data for habitat monitoring, conservation and management and such data is lacking for greater one-horned rhinoceros (Laperriere et al., 1980; Porwal & Roy, 1996; Innes & Koch, 1998; Berlanga-Robles & Ruiz-Luna, 2002; Dinerstein et al., 2003).

Satellite images represent important data sources to develop vegetation maps for large areas. Particularly, Landsat 7 Enhanced Thematic Mapper-Plus (ETM+) images have been proven useful and cost-effective for large-scale habitat analysis (McClain and Porter, 2000). A vegetation map derived from remote sensing can be processed to determine habitat suitability by using habitat evaluation procedures (HEP) leading to development of a map of habitat suitability index (HSI). HEP involves collection of information on behavior, food habits, mating season, taxonomy and the animal's position in the trophic niche of a target species in order to evaluate its habitat (Porwal & Roy, 1996; Sharma et al., 2004). The resulting HSI map can aid in the understanding and management of habitat for this species. It could be used to locate, target and manage areas of suitable habitats and therefore support conservation and restoration program in CNP. In addition, HSI maps can be further analyzed to determine spatial structure, particularly fragmentation, of suitable habitat. The FRAGSTATS program (McGarigal & Marks, 1994) offers capabilities to calculate several metrics related to spatial structure and fragmentation.

The major objective of this paper is to determine the amount and spatial structure of the remaining rhino habitat in CNP. Our research consisted of three major components: 1) developing a land-cover map emphasizing the vegetation of the CNP by using a Landsat ETM+ image, 2) developing HEP to generate a HSI map, and 3) determining the spatial distribution of the current suitable habitat area for rhinoceroses via fragmentation metrics.

Methods

Study Area

CNP was located in the lowlands of Nepal along the northern border of India (Figure 2.3) at an elevation of 120 to 200 m above sea level and covers an area of 932 km^2 in the Chitwan district. Although the area was almost flat, the terrain contains some depressions. Geographically, the park lies from 83º 41' to 83 º 49' E longitudes and from 27º 1' to 27º 41' N latitude. CNP was bordered to the northeast, northwest and west by privately owned land used primarily for agriculture and on the southeast by another wildlife reserve, Bardia National Park, which was regarded as ideal habitat for wild elephants. The climate was subtropical, with temperatures rising to approximately 37 ^oC on a typical summer day. The mean annual precipitation was 2400 mm with 90% of it falling during the period from May to September.

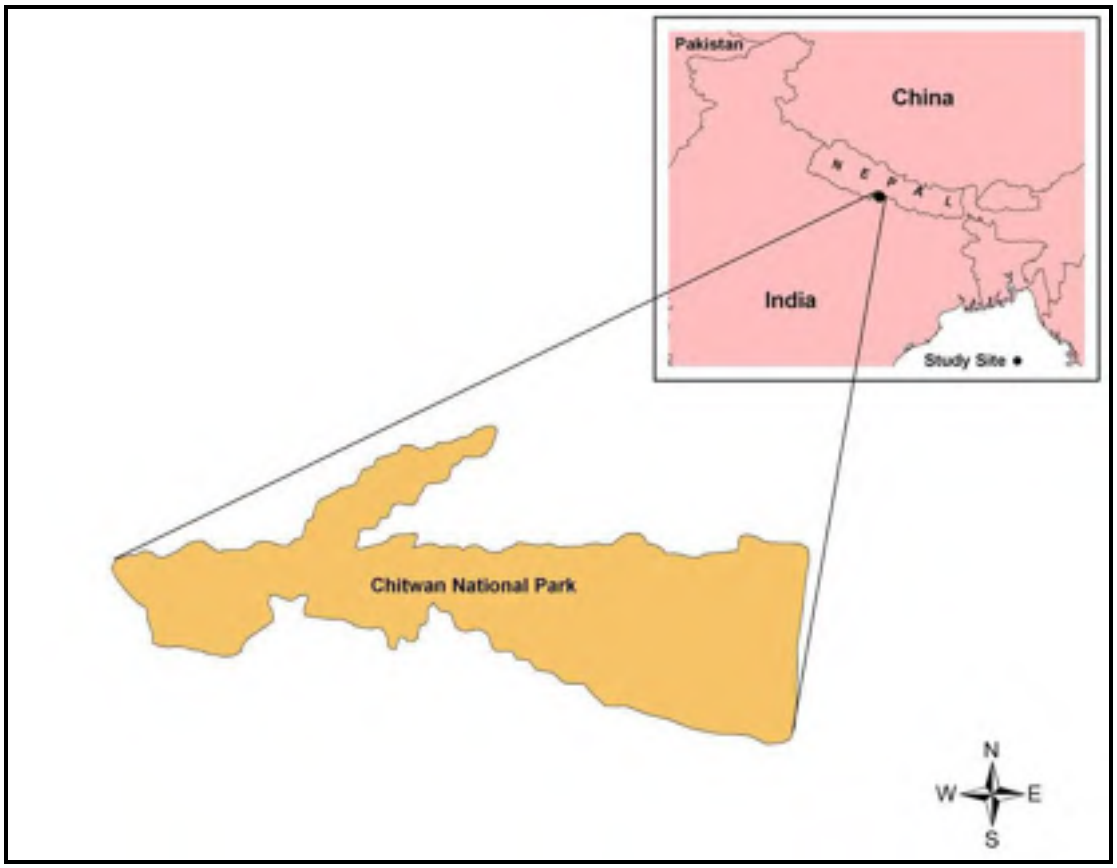

Figure 2.3. Study area in the Himalaya hotspot.

The vegetation consists of deciduous, mixed, and riverine forests punctuated by grassland communities. Sal forests are a prominent forest type, covering 70% of the park area dominated by trees of *Shorea robusta* and occur on upland, well-drained slopes rarely used by the rhinoceroses (Laurie, 1978). The riverine forest association is composed of *Trewia nudiflora*, *Bombax ceiba*, *Acacia catechu*, and *Dalbergia sisoo* frequently used by the rhinoceros. Mixed forest was mostly composed of *T. nudiflora* and *B. ceiba* and the rhinoceroses ate the fruits of *T.nudiflora* during the summer (Dinerstein & Price, 1991; Jnawali & Wegge, 1993; Dinerstein, 2003; Rawat, 2005).

The grassland habitat associations included either monospecific stands of tall grass species of *Saccharum spontaneum* (4-6m); *S. benghalensis, Narenga porphyrocoma*, and *Themeda arundinacae* (5-7m) or mixed with short grass species of *Imperata cylindrica, Chrysopogon aciculatus*, *Eragrostis* spp and several others (Lekhmul, 1988; Dinerstein, 1989; Dinerstein and Price, 1991; Dinerstein, 2003). The short grasses usually occurred within tall grasslands and were intensively grazed by the rhinos. The physiographic distribution of tall grasslands was also noteworthy. According to Dinerstein (2003), the tall grass species occupied approximately 15% of the total park area and occurred on higher terraces of the floodplain. The rhinoceros grazed on the young shoots of these grasses but largely avoided them once they grew past shoot stage.

Another tall grass species, *S.spontaneum,* was the first to colonize the major river banks after the retreat of annual monsoon floods. It often occurred in pure stands and its thickness range from less than 100 m to more than 1 km in width. This type of grassland accounts for only 5% of the total park area (Dinerstein, 2003). Among the grassland types, the rhinoceros seeks out

S.spontaneum as it is the most nutritious of available tall grass species of Chitwan valley (Laurie, 1989; Lekhmul, 1988; Dinerstein & price, 1991; Dinerstein, 2003) (Figure 2.4).

Figure 2.4. Saccharum spontaneum grass along the major rivers.

Satellite Data Selection and Processing

We selected one ETM+ image for analysis based on criteria of desired geographic coverage, cloud-free conditions, and date (for seasonal considerations). Single-date scene (path 142/ row 41, collected in April 12, 2003) from early summer or pre-monsoon (mid-February to mid-June) was considered optimal because the deciduous trees are leafless enhancing the chances of discriminating deciduous from evergreen forests (Harini & Gadgil, 1999). The ETM+ images provide multispectral coverage for seven spectral bands in the visible (TM1, TM2, TM3), near-infrared (NIR TM4), mid infrared (MIR TM5, TM7) and thermal portions (TM 6) of the

electromagnetic spectrum. Vegetation pixels are pronounced in TM4 (0.7 – 0.9 μm). The spatial resolution of these bands is 30 m except for the thermal which is 60 m. Because of this coarse resolution, we excluded thermal resolution from the analysis. The image also provides a panchromatic spectral band with better spatial resolution (15 m), which is commonly used for producing quality fusion imagery to obtain richer information in the spatial and spectral domain (Choi et al., 2005).

The image of the study area was geo-referenced using ground control points (GCPs) collected from topographic maps of 1:25000. We used locations of park headquarters, small towns, hotels, army posts and naturally visible features such as lakes to collect GCPs in order to reduce geometric and location distortion in the image (Hardison, 2003). We used the image as a guide map during our field work in 2004 and 2005. In 2004, we collected more than 800 ground truth reference points using global positioning systems (GPS). Although there is no standard minimum distance between ground truth points, we separated points by at least 150 m in order to avoid overlap. In 2005, we made another trip to collect additional GPS points (20) of confused pixels (to be explained with detail in the results section). Each point was accompanied with notes of vegetation and soil type, moisture regime and elevation. We used half of the points to conduct supervised classification of eight land cover types, by employing the maximum likelihood algorithm (Harini & Gadgil, 1999). The eight land cover types were water, sand, grassland, agriculture, wetland, settlements, mixed and sal forest (Figure 2.5). Our clipped image contained some agricultural lands and settlements adjacent to CNP. Therefore, we defined a separate class as agriculture and settlement as rhinos do venture out to nearby fields especially during night and sometimes become a source of wildlife-people conflict (Nepal & Weber, 1995; Studsrod & Wegge, 1995).

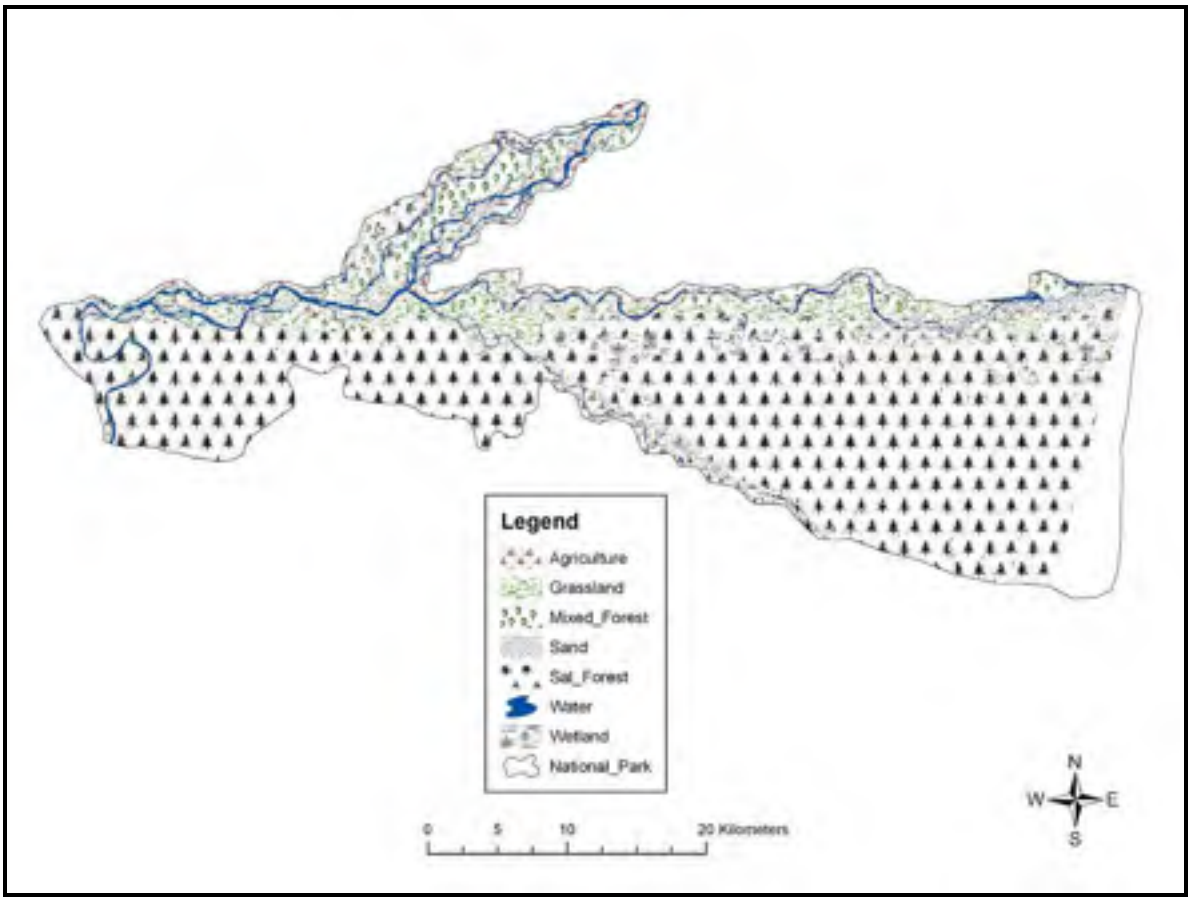

Figure 2.5. Symbolized classes derived from supervised classification.

We used the other half of the ground-truth points to assess classification accuracy. Generally, random points are used as a reference class to assess accuracy. However, in our case, we used a set of the ground-truth points as a reference class and compared with classified image class values to evaluate accuracy. This set of ground-truth points employed for evaluation was different from the set employed for classification.

Habitat Suitability Index (HSI)

According to Dettki et al. (2003), two approaches are used to assess wildlife habitat relationships: process and empirical oriented approaches. Process-oriented models assess plausible causal relationships or functional processes underlying habitat use and provide a more

general conceptual framework. In contrast, empirical models analyze data on habitat use and habitat characteristics collected at specific sites.

Process-oriented HSI models use habitat requisites or parameters such as food, cover, and proximity to water as input variables to a function providing a dimensionless 0.0 – 1.0 index, where 0 and 1 indicates unsuitable and optimum habitat conditions respectively (Dettki et al., 2003). This function is determined by assumptions on how each one of the habitat requisites and their combination affect suitability and evaluate aptness of a habitat (Porwal et al., 1996; Dettki et al., 2003). We adopted a process-oriented approach to develop a heuristic HSI model for the greater one-horned rhinoceros inspired by moose habitat analysis of Dettki et al. (2003). Even though both species differ in habitat use, the model is applicable to any wildlife as it simply requires specific habitat use parameters. To estimate these parameters, we derived detailed rhino habitat use information from several published papers and field observations (Laurie, 1978; Dinerstein & Wemmer, 1988; Lekhmul, 1988; Owen – Smith, 1988; Dinerstein & Price, 1991; Jnawali & Wegge, 1993; Dinerstein, 2003).

We made two major assumptions while constructing the HSI model for the rhino. First, we assumed that existing information on habitat use by the animal can be translated to data related to model parameter values. Second, we assumed that the uncertainty associated with these parameter estimates can be evaluated by sensitivity analysis. We used presence of grass, and forest in a neighborhood of 70x70 grid of a target pixel as input variables to calculate the HSI value for that pixel. The neighborhood size was determined according to the animal's average mean annual home range, which is ~4km^2 = 400 ha = 70x70 pixels x 900 m^2 = 4410000/10000 = 441 ha. We selected focal over block statistics to calculate the HSI value of each pixel. Focal functions assign a value for each processing cell and allow overlap while block

statistics do not allow overlap (all cells within the block receive identical value). We extracted food (grass and agriculture) and cover (sal forest and mixed forest) from the land cover map and ran focal statistics to calculate proportion of food and cover in a neighborhood, denoted by *xf* and *xc* respectively. These were then used in the following way.

We define the suitability Sf and Sc for food and cover as

$$Sf = \begin{cases} xf / Tf & \text{when } xf < Tf \\ 1 & \text{when } xf \geq Tf \end{cases}$$

and

$$Sc = \begin{cases} xc / Tc & \text{when } xc < Tc \\ 1 & \text{when } xc \geq Tc \end{cases}$$

where *Tf* and *Tc* are parameters that define thresholds for each factor to obtain maximum suitability. These threshold parameters are determined in the following manner.

For food, a large rhino eats between 60-80 kg a day fresh weight and spends most of its time browsing or grazing (Dinerstein, 2003). In addition, the food primarily consists of wild sugarcane *Saccharum* species. According to Coombs and Vlitos (1978) estimation, the standing biomass of sugarcane is 100 MT/ha fresh weight or 35 MT/ha dry weight, which gives a fresh/dry ratio of 100/35. So, one rhino eats approximately 21-28 kg/day of dry weight. Assuming the mid value of this range, 24.5 kg/day, the annual food requirement of one animal is 24.5 kg/day x 365 day/year = 8.9 Tons/year.

Furthermore, Dinerstein (2003) calculated 0.34 kg/ m^2 dry weight of *Saccharum* in Chitwan. Thus in the home range 400 ha, we would have a total of 3400 kg/ha x 400 ha = 1,360 Tons of dry food if it is covered entirely by grass. According to Dinerstein and Price (1991) about 39 animals have been reported to use 3.2 km^2 (320 ha) area of prime habitats mostly composed of *Saccharum* and riverine forests. Therefore, we assume 40 animals would use the

400 ha of home range area. Then, 8.9 Tons/year per animal x 40 animals = 356 Tons of food per year which represents a fraction *Tf* = 356 /1360 = 0.26. However, there are no data available to estimate parameter *Tc*. We assumed that 12 ha out of 400 ha would be sufficient cover, and therefore *Tc*=12/400= 0.03. Because of its uncertainty we will use sensitivity analysis as described later.

The impact of cover on habitat suitability must take into account its seasonal importance. During monsoon season (4 months), we factor in the need for cover by using a geometric mean of food *Sf* and cover *Sc* suitability with a weight factor *a*. However, during the rest of the year (8 months), the animals do not need cover and food suitability accounts for HSI. The final HSI model is then a weighted arithmetic mean of the monsoon and off-monsoon suitability

$$HSI = \frac{4}{12}\left(Sf^{a} \times Sc^{(1-a)}\right) + \frac{8}{12}Sf$$

For parameter *a*, we estimated that food is much more important than cover and assigned a value of *a* = 0.8 (4 times more important). In order to study the potential error that the arbitrary selections of *a* and *Tc* may produce, we conducted sensitivity analysis by varying *a* and *Tc* by ±20% around their nominal values (*a* = 0.8, *Tc* = 0.03).

Figure 2.6 shows the effect of varying parameter *a*. As expected, for values of *xf*, *xc* around or exceeding the corresponding threshold values the HSI is insensitive to changes in *a*. Only for very low values of fraction of food the HSI is more sensitive to *a*, reaching values of up to 25-30% change in HSI. Figure 2.7 show the effect of varying parameter *Tc*. As before, for values of *xf*, *xc* exceeding the corresponding threshold the HSI is insensitive to changes in *Tc*. Only for very low values of fraction of cover the HSI is more sensitive to *Tc* and represents less than 1-2% change. Therefore, the uncertainty with respect to *Tc* is very small.

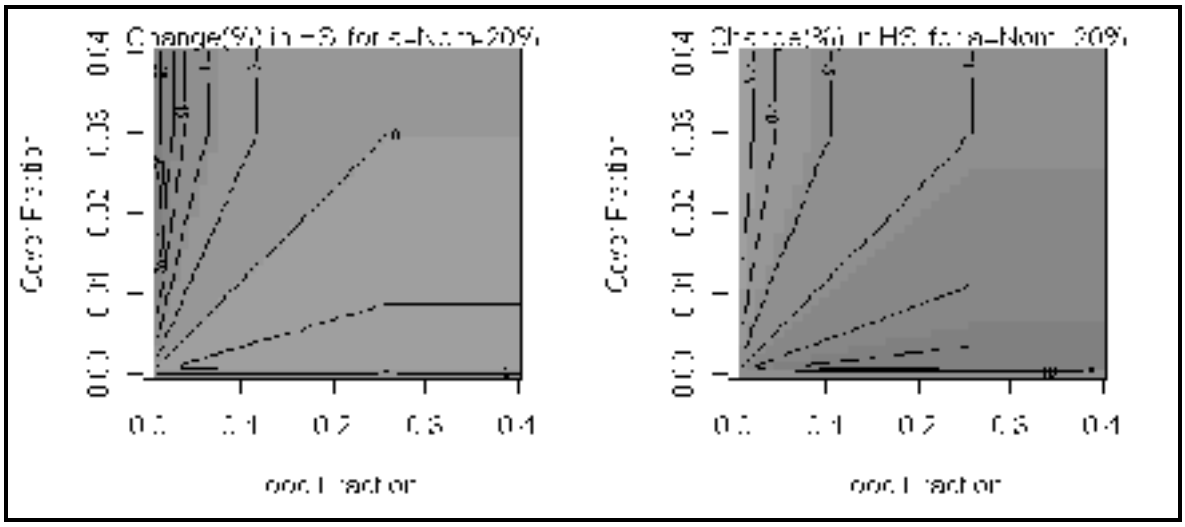

Figure 2.6. Effects of varying parameter a.

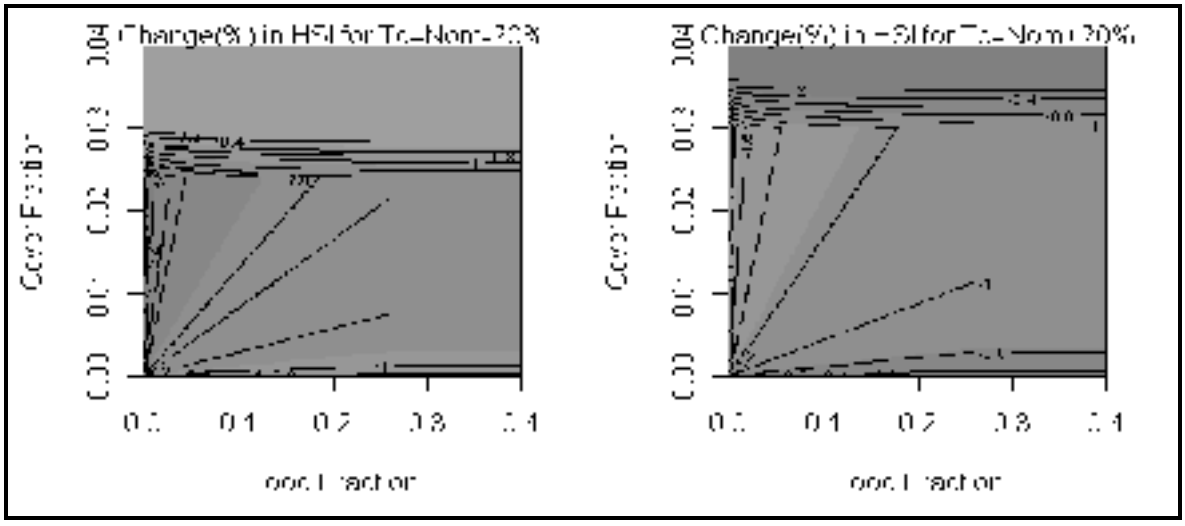

Figure 2.7. Effects of varying parameter Tc.

From this sensitivity analysis we conclude that the HSI value of a pixel could change with uncertainty in parameter *a* for very low values of fraction of food. Moreover, it will not vary due to uncertainty in this parameter as long as the neighborhood around that pixel has fractions of food larger than the threshold *Tf* = 0.26 or 10 ha in 400 ha. Therefore, the HSI map will only be relatively uncertain for outside or edge grassland patches. This uncertainty is further reduced by the following classification of pixels into four classes (as explained below) - highly unsuitable, unsuitable suitable, moderately suitable and suitable habitat types, since all areas of

low HSI values (which are relatively uncertain values) will be classified as either highly unsuitable , unsuitable or moderately suitable. The resultant HSI map pixels had values ranging from 0 to 1 (Figure 2.8).

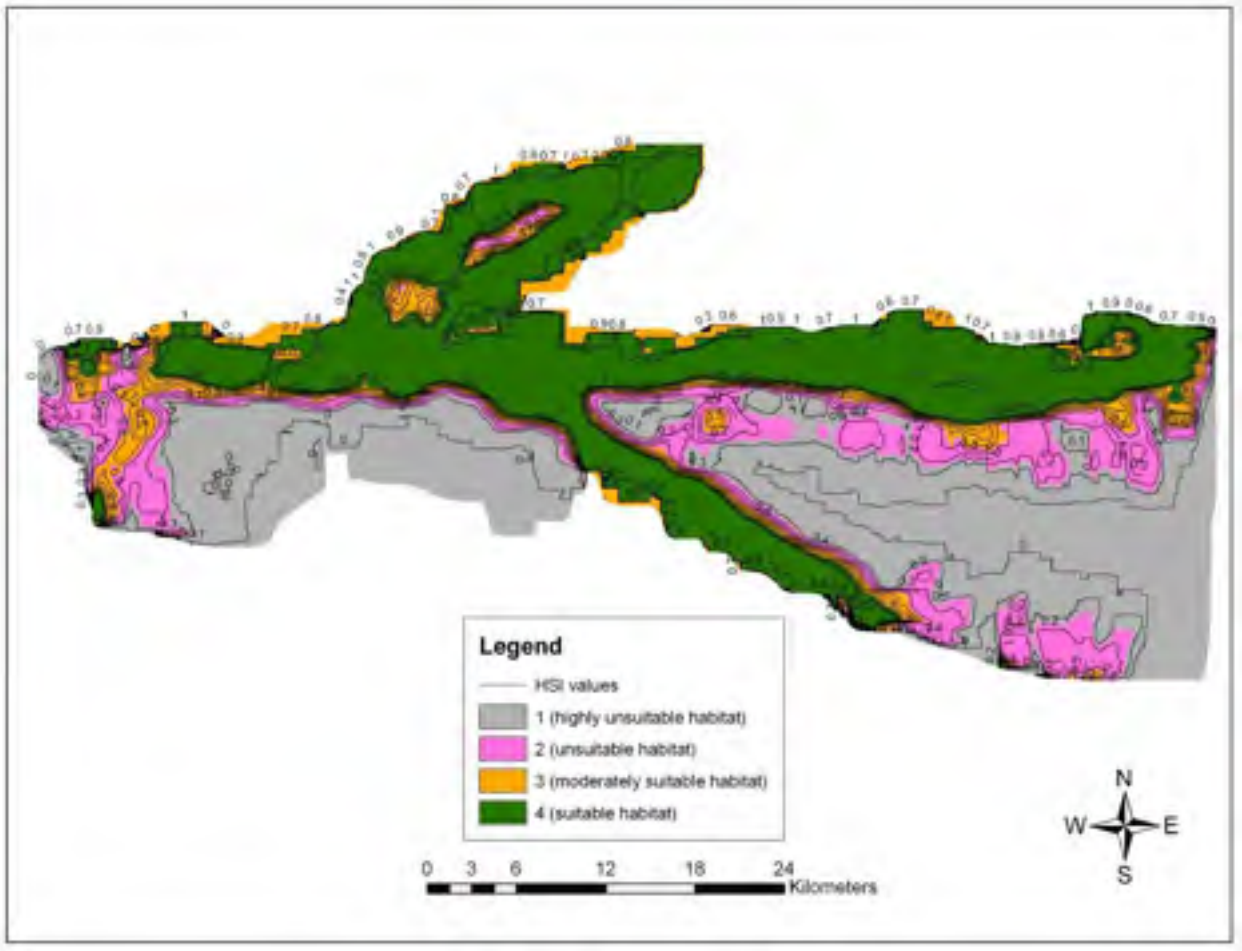

Figure 2.8. Habitat suitability map.

We needed to group the values between 0 and 1 into different classes that represented different habitat types and that in turn reflected habitat conditions. For example, pixels with low values such as 0.01, 0.0, 0.14, 0.23 etc reflected poor habitat conditions (these pixels either had less cover or food or vice versa) as compared to pixel values of 0.5, 0.8 and so on. Thus, higher pixel values indicated favorable habitat conditions. And to assign the pixels into different habitat types, we selected natural breaks (Jenks) as classification method in ArcMap and derived four

classes as shown in Figure 2.8. We selected this method primarily because we wanted to find the breaks (high jumps) in the pixel data values of 0 and 1. The break serves as a boundary while delineating classes. For example, pixels with values from 0 - 0.14 were grouped in one class and pixels with values from 0.14 – 0.44 were grouped in another class and so forth. In this case, the boundary lies at pixels with 0.14 values. In order to use these classes in FRAGSTATS (decimals are not accepted), we further assigned integer values of 1, 2, 3 and 4 to represent the four habitat categories (1= highly unsuitable, 2 = unsuitable, 3 = moderately suitable and 4 = suitable habitat pixels) (Figure 2.8). We converted HSI map into ASCII text file and calculated metrics. We carefully selected metrics relevant to the habitat requirements of the rhinoceros and that met our objectives (Table 2.1).

Table 2.1

FRAGSTATS Metrics at Patch and Class Levels

Metric	**Designation**
Patch Level	
Area/Density/Edge:	
Patch Area	AREA
Class Level	
Area/Density/Edge:	
Class Area	CA/TA
Percentage of class	PLAND
Number of patches	NP
Connectivity	
Cohesion	

Note. Landscape level metrics were not analyzed because of their little interpretive value and identical behavior at class level.

Our primary interests were 1) to find the size of individual patch 2) to find the amount and distribution of particular patch type and 3) to find whether particular patch types are contiguous or fragmented. And to meet our first objective, we selected AREA metric at patch level. This is useful metric as many vertebrates including rhino require suitable habitat patches larger than some minimum size. For example, the average home range of a rhino is ~400 ha. We selected CA/TA (Total Area), PLAND (Percentage of Landscape) and NP (Number of Patches) at class level to satisfy second objective. These metrics quantify composition of the patches. And to meet third objective, we selected COHESION (Patch Cohesion Index) to find physical connectedness of particular patch type. This metric measure configuration of a patch to it its neighbors in the landscape.

Results

Vegetation Classification

The overall accuracy was about 70 % with more than 80% of water, sand, sal forest and mixed forest pixels accurately classified (Table 2.2). KHAT index for water and sand exhibited more than 90% agreement between reference and classified pixels. Whereas it was less than 40% for agriculture indicating 60% of the pixels were incorrectly classified. The classification of sand, sal, and mixed forest was satisfactory. It was easy to create area of interest (AOI) for sal and sand pixels as 70% of the park area is covered by sal forest and sand pixels were easy to select based on the location and spectral profile. The three major rivers had sandy banks of relative thickness running parallel to them that made easier to create AOI. Once a group of pixels belonging to same class is identified, ERDAS automatically select areas with similar pixels under the supervision of the user – a tool commonly employed during supervised classification.

On the other hand, wetland, grassland and agriculture were classified with 75% and 50% accuracy. The reason for low accuracy of grassland category may have resulted from confusion of agriculture and grass pixels, a typical situation in such studies. The growth stage or the height of the crops and the grass could have been similar when this image was taken.

The agricultural land contains some of the settlement and grassland pixels. Similarly, wetland pixels could be confused with other water bodies. The largest wetland area is actually the outlet of one of the major lake, Tamar Tal (Tamar Lake). It is located closer to the confluence of the three rivers; and when the lake is inundated during monsoon season, water overflows to this area. The purpose of the second visit to the field was to confirm vegetation and location of this area. The fieldwork revealed a secondary succession of grassland in the outlet. While one side of the outlet was covered with marshy vegetation, the other side flourished with grassland. The marshy vegetation would eventually convert into grassland that would serve as additional habitat for the greater one-horned rhinoceros. The area or the lake could have overflowed when this image was taken in 2003. The spectral profiles of these pixels also exhibit the nature of vegetation that is submerged in water. New classification routines are needed that can tease apart detailed reflectance patterns that are essential to distinguish agriculture, grassland, and settlement pixels. This increases need in field identification of these classes, and the use of higher-resolution imagery is another promising alternative.

Table 2.2

Errors of Commission (User's Accuracy), Errors of Omission (Producer's Accuracy), and Kappa Statistics for Classification of 2003 Landsat ETM Image (Overall Accuracy was 69.90%)

Serial No.	**Classes**	**Producer's Accuracy (%)**	**User's Accuracy (%)**	**Kappa Statistics**
1	Water	55.17	94.12	0.9365
2	Wetland	100.00	75.00	0.7441
3	Agriculture	96.05	50.34	0.3840
4	Settlement	0.00	0.00	0.0000
5	Sand	52.38	91.67	0.9119
6	Sal Forest	87.65	84.52	0.8049
7	Mixed Forest	52.54	81.58	0.7832
8	Grassland	61.76	75.00	0.6621

HSI and Habitat Fragmentation

For one-horned rhinoceros, food is considered to be the most important factor of their habitat components with some seasonal cover. Thus, we assigned a value of 0.8 for parameter *a*. We calculated threshold values for food to be *Tf*=0.26. And for cover threshold, we assumed 12 ha out of 400 ha (mean annual home range) would be sufficient to hold one animal and *Tc* = 0.03. We performed sensitivity analysis by varying the nominal values of *a* and *Tc* by ± 20%. Interestingly, we found HSI is only sensitive to a with low values of fractions of food (*xf*) and cover (*xc*). In other words, the uncertainty of parameter *a* is minimum if food and cover availability is more than their respective thresholds. The small uncertainty of parameter *Tc* suggested that forests are used less frequently or used seasonally but it is critical component of

habitat requisites. The HSI map showed distinct spatial pattern, with high values of HSI along the areas near water bodies and adjacent grasslands and edges of sal forests with low values in the inland areas (Figure 2.8).

The metric result showed presence of 476 patches that belong to four different habitat types (Table 2.3 and Table 2.4). AREA metric revealed the largest patch (51,065.73 ha) belonged to suitable habitat type (Table 2.3). The total area of suitable habitat is 51,781.95 ha or 517.82 km^2 that include some buffer zone and agricultural areas outside the park boundary. Our results correlate to the recent findings of Hemanta et al. (2009). They reported presence of 614 km^2 of potential suitable habitat in CNP and suggests increase of artificial oxbow lakes to achieve this extent of habitat. Moreover, the lowest number of patches (NP = 18) and highest value of connectivity metrics (99.84) for suitable habitat support its homogeneity across the landscape especially along the river boundaries (Table 2.4).

Table 2.3

Patch Metric Results

PID	TYPE	AREA	PID	TYPE	AREA	PID	TYPE	AREA	PID	TYPE	AREA
4	1	0.09	247	2	0.09	332	3	0.09	82	4	0.09
455	1	0.09	367	2	0.18	96	3	0.18	28	4	0.18
459	1	0.09	445	2	0.27	423	3	0.27	132	4	0.27
6	1	0.18	152	2	0.36	411	3	0.36	252	4	0.72
16	1	0.18	299	2	0.45	88	3	0.45	23	4	1.08
385	1	0.18	319	2	0.54	366	3	0.54	63	4	1.35
392	1	0.18	440	2	0.63	413	3	0.63	52	4	1.53
399	1	0.18	144	2	0.72	433	3	0.72	131	4	1.98
402	1	0.18	182	2	0.9	86	3	0.81	166	4	2.07

43	1	0.27	258	2	0.99	119	3	0.9	371	4	14.22
224	1	0.27	95	2	1.26	127	3	0.99	425	4	25.29
355	1	0.27	133	2	1.35	246	3	1.08	475	4	178.2
469	1	0.27	222	2	1.53	393	3	1.17	135	4	488.7
36	1	0.36	309	2	1.62	287	3	1.26	328	4	51065.73

Table 2.4

Class Metric Results

LID	**CA (ha)**	**PLAND (%)**	**NP**	**COHESION**
1	56647.26	39.275	176	99.84
2	21441.96	14.8661	98	99.67
3	14362.92	9.9581	184	99.25
4	51781.95	35.9013	18	99.94
			476	

This last result indicates rhinos inhabiting habitats near three major rivers can travel undeterred using river banks as migrating route. This is corroborated by the findings of Dinerstein and Price (1991) that discovered frequent rhino movement from far-east to the Sauraha subpopulation. However, resident rhinos of Reu and Rapti may be permanently separated by contiguous blocks of highly unsuitable habitat of sal forest and so are the subpopulation of the Bandarjhola-Narayani River and the Sauraha by extensive blocks of agriculture and settlements. The rhinos can use river banks but previous works has indicated that they do not travel far if prime habitats are nearby i.e. abundant productive floodplains. Other metrics such as PLAND indicated highly unsuitable habitat (mostly sal forests) occupied the largest percentage of the landscape (39%)

followed by suitable habitat patches (36%). Moderately suitable habitat patches are the most fragmented and the least in numbers as indicated by NP and COHESION metrics and occurred adjacent to the suitable habitat patches (Table 2.4).

Discussion

Vegetation Classification

The most valuable data – land-cover types, soil profile, plant composition, and density of canopy cover – were determined by the field study. Field verification of land cover types proved to be the most effective method and best suited to using a GPS unit as the device of choice. Ground-truth data along with pictures of field activities compensated the paucity of previously tested data such as aerial photos and assisted in classifying the vegetation types represented in CNP. We used supervised method to classify the image into eight land cover classes – water, sand, settlement, wetland, grassland, agriculture, mixed and sal forest. We employed a new technique to assess classification accuracy. Generally, random points created in ERDAS or aerial photos or previous data are used to assess accuracy of a thematic map (Anderson et al., 1976; Congalton and Green, 1999; Salovaara et al., 2005). For this project, we used ground-truth points to classify, test and enhance accuracy. The overall classification accuracy was 70%. Most categories including water, sand, sal and mixed forest, and wetland were classified with more than 80% accuracy. The low accuracy value for grassland and agriculture could be attributed to the confusion of their pixels. Depending on growth stage and season, agricultural pixels are easily mistaken for grass and it is a common and persisting problem in remote sensing. Moreover, grasslands near Tamar Lake are classified as mixed or sal forest; this classification may be due to the tall nature of these grasslands. With a height ranging from 6 to 8 m, sometimes

they grow with small trees and shrubs and can completely overshadow them. To achieve more accuracy for the grassland, we recommend the use of higher-resolution imagery.

HSI Model and Habitat Fragmentation

We constructed two maps (food and cover) from the land cover map. We used two land cover categories i.e. agriculture and grassland to make food map and used sal forest cover type to make cover map. And we ran focal neighborhood statistics to calculate the proportion of food and cover in 70x70 cell neighborhood that represented mean annual home range of an adult rhino. In this way, we developed a heuristic HSI model for the greater one-horned rhinoceros based on a process-oriented approach. In other words, we merely attempted to develop HSI using habitat use parameters that were collected from extensive literature reviews of spacing behavior, biology, and daily routine of a rhino (Laurie, 1978; Dinerstein & Wemmer, 1988; Lekhmul, 1988; Dinerstein, 1989; Dinerstein & McCracken, 1990; Dinerstein & Price, 1991; Jnawali & Wegge, 1993; Dinerstein, 2003). We used this information to conduct neighborhood analysis, to select, construct and build HSI and to assign threshold to the parameters. Our sensitivity analysis confirmed about 0.03 cover and 0.26 of food in ~ 400 ha is sufficient to sustain a rhino crash (a group of rhinos). As noted above, this research applied habitat use to generate an HSI model in an attempt to examine whether such HSIs can be developed for the mega herbivore; and after conducting these procedures, we determined that the development of the indices was feasible. However, validation of the results of any HSIs require rigorous field study involving home range, telemetric studies for years, and habitat use (Dettki et al., 2003). We think this method will be effective and useful if used with data that are acquired in the manner explained above and

if such data are available we can apply these procedures to study the habitat suitability of other large ungulates in the study region or elsewhere.

We demonstrated careful selection of FRAGSTATS metrics yields interesting and useful results. We quantified the four habitat patches with respect to patch size, number of patches and connectivity of corresponding patch types. This would provide much needed data on the habitat of the rhinoceros (especially on the remaining suitable habitat patches). COHESION metrics revealed contiguous nature of suitable habitat patches that is vital to the survival of rhinos and other sympatric species. In case of rhinos, this means CNP landscape facilitates ecological flows i.e. there is constant movement of animals among habitat patches thus reducing the threat of extinction threshold. As noted above, the rhinos seek out the most nutritious of all grass species (*Saccharum*) that are available year around. These grass species thrive on the floodplains and are maintained by periodic monsoon floods. It would be interesting to find core habitats, number of core habitats, edge density, diversity and several others and FRAGSTATS produces several metrics to study these aspects of a landscape. However, lack of fine scale data such as edge effect on rhino population or individual or how a rhino perceive its habitat and the actual size of the habitat etc limited our study. We relied heavily on the studies that were conducted mostly on ecological and biological aspects of a group of rhinoceros not on individual. Laurie (1978) and Dinerstein and Price (1991) did use conventional radio-telemetry to study habitat use but they focused mainly in finding mean annual home range, seasonal distribution and feeding habits. Thus, study of effect of edge on a rhino movement is still lacking and such studies could provide vital information about distribution and movement of a rhino within its suitable habitat and influence on its behavior due to adjoining unsuitable habitat – an open area for future study.

Management Implications

We examined process-oriented approach to model the rhino habitat and found it can be ecologically meaningful if selection of the used environmental variables is based on the habitat requirements of the target species. And if the variables are correctly identified, they enable us to understand the effects of changes in the landscape on the model outcome. The wildlife managers of Chitwan can find the results of this study valuable for managing the remaining and available habitats as such habitats need constant monitoring to ensure prolonged management. The vegetation and HSI maps would facilitate future conservation and management of the suitable habitats and aid in further ecological researches. Presently, Nepal is undergoing political transition whose end does not appear to be in sight anytime soon. The imminent impact is on the wildlife of Chitwan valley because it is located on *Terai* or plain and is more accessible than other Himalayan parks and wildlife reserves. Rhino deaths continue to make headlines. In 2009, 15 rhinos died in the hands of poachers and recently in April and May of 2010, 7 rhinos have perished (Himalayan Times, 2010). Not to mention, current invasive vine spread have added to the worsening situation. All these factors contribute to the bleak future of the *Rhinoceros unicornis* in the Chitwan valley of Nepal. However, we hope with the return of relative peace (Maoists gave up arms in 2006) and the tools developed and the results obtained in this project could help in managing the remaining habitat and improve the deteriorating condition of this mega herbivore and its habitat.

CHAPTER 3

HABITAT QUANTITY OF RED-COCKADED WOODPECKER IN A HUMAN-DOMINATED LANDSCAPE NEAR THE BIG THICKET NATIONAL PRESERVE, TEXAS*

Abstract

The goal of this study was to quantify the pine habitat of red-cockaded woodpecker (*Picoides borealis*). These birds require extensive patches of pine-forest with little mid-story vegetation for successful breeding and foraging. Natural and human-induced fires controlled the overgrowth of mid-story vegetation for decades. Red-cockaded woodpeckers evolved in the low intensity, fire-dominated pine ecosystems of the Southeastern United States. Consumptive land-use practices contributed greatly to the loss of pine forests, which reduced the red-cockaded woodpecker's nesting and foraging habitat and altered their spatial distribution. We used a remotely sensed image and geographic information systems (GIS) to create a land-use/land cover map and to evaluate the potential habitat for the bird. We calculated a habitat suitability index (HSI) from the proportion of pixels in a selected neighborhood that met habitat requirements; i.e., adequate coverage of pine trees for breeding and foraging. Then, this index was used to produce a HSI map with three habitat types – very unsuitable, unsuitable, and potentially suitable. We used FRAGSTATS to compute patch, class, and landscape metrics for each habitat type. The metrics provided area, perimeter, percentage, size and fragmentation of each habitat type at patch, class, and landscape levels. Our results show the study area is heavily fragmented owing to mixed anthropogenic use. We suggest that once a potentially suitable habitat is

* This chapter has been submitted to the *Texas Journal of Science* with Miguel Acevedo and J. Baird Callicott as co-authors.

identified, the under and mid-stories may be managed for suitable foraging habitat by prescribed burning.

KEYWORDS: Habitat suitability, Landsat image, Accuracy assessment, Global positioning system, Habitat fragmentation, Patches, Metrics, Big Thicket National Preserve.

Introduction

Red-cockaded woodpeckers are habitat specialists. They require large, old and living pine species of longleaf (*Pinus palustris*), shortleaf (*P. echinata*), loblolly (*P. taeda*), pond (*P. serotina*) and slash (*P. elliotii*) pine, but prefer longleaf for nesting and foraging habitat (Conner et al., 2004; Hedrick et al., 1998; Hopper et al., 1980; Jackson, 1994). The tree age varies for species i.e. 80-100 years for loblolly and shortleaf and 100-120 years for longleaf with enough heartwood space to support cavity chamber and little or no midstory hardwood vegetation (Conner et al., 1994; Hedrick et al., 1998; Hooper et al., 1980). Natural or prescribed fires controlled the midstory overgrowth for decades and the result was open, park-like mature pine woodlands and savannahs with abundant herbaceous ground cover that provided an ideal habitat for these birds. Besides age, the potential cavity tree has high rates of red heart fungal (*Phellinus pini*) infection that softens the heartwood and facilitates cavity excavation (Conner & Locke, 1982; Conner et al., 1976; Conner et al., 1994; Conner et al., 2004). In other words, they depend on open, park-like, mature pine stands for foraging and red heart fungus infected trees for nesting and roosting. A colony or cluster is a collection of two to more than 12 cavity trees on a 5 to 10 acres (2-4 ha) of land and the cavity trees are normally located within one mile radius or less from each other (Hopper, 1988). A single colony is used by only one clan or group that has two to nine birds but contains only one breeding pair and the rest are helpers. A suitable foraging

habitat or territory surrounds a colony and covers an area of 30 to 81 contiguous hectares (75 to 200 acres) of park-like mature pine stands (Jackson, 1994). Thus, contiguous open stands of mature longleaf pine and other pine species with an herbaceous ground cover offers a high quality habitat or potentially suitable habitat for a clan of red-cockaded woodpeckers (Conner & Rudolph, 1991).

Few studies exist on the use of geographic information systems (GIS) and remote sensing to study the habitat of red-cockaded woodpeckers. Thomlinson (1993) used GIS, remote sensing and landscape ecology to study ecological characters of suitable pine stands in southeast Texas. Cox et al. (2001) evaluated GIS methods that were used to assess red-cockaded woodpecker habitat and cluster characteristics. Ertep and Lee (1994) used GRASS to facilitate red-cockaded woodpecker management at Fort Benning Military Reservation. Another recent study by Santos et al. (2010) reports the use of remote sensing based on hyperspectral imagery to study tree senescence in red-cockaded woodpecker habitat. They used reflectance properties of the bands to detect senesced pine trees and found red-cockaded woodpeckers did not inhabit such trees. In contrast, most study focuses on biological and ecological interaction of the birds with its special habitat (Baker, 1971; Conner, 1981; Conner et al., 1975; Conner et al., 2004).

We utilized GIS and remote sensing techniques to study spatial distribution of pine forest in one of the former historic range of red-cockaded woodpeckers i.e. southeast Texas and assess suitable habitat and its fragmentation. Furthermore, we used habitat suitability index (HSI) models and FRASGSTATS to evaluate or quantify species-habitat relationships. HSI models provide a quantitative measure of the quality of wildlife habitats, and can integrate our understanding of wildlife-habitat relationships especially at landscape scales (Larson et. al., 2003). In addition, process-oriented and empirical HSI models are commonly used to assess

wildlife-habitat relationships (Dettki et al., 2003). Process-oriented models assess plausible causal relationships to provide a general conceptual framework; whereas empirical models analyze data on habitat characteristics collected at specific sites for a long period of time (Thapa, 2005).

For this paper, we adopted a process-oriented approach for developing a heuristic HSI model for the red-cockaded woodpecker. This approach is based on a literature review (U.S. Fish and Wildlife Service's HSI models), field observations (ground-truth), and geographic data obtained from topographic maps (scale 1:24000, USGS). An HSI is based on a set of functional relationships between habitat suitability (expressed as a dimensionless index or score) and habitat requirements (variables). These variables are selected according to their relevance to the organism; for example, herbaceous canopy cover, tree canopy cover, tree height, tree age and proximity to water. There is a partial suitability for each variable, which scales from 0 (unsuitable habitat) to 1 (optimum habitat).

The overall HSI, which also scales from 0 to 1, is calculated with a formula that represents hypothetical relationships between partial suitability indices. GIS provide a tool to synthesize habitat data derived from remotely sensed sources together with databases of elevation, soil types, land use, and land cover. Thus, GIS can be coupled with remote sensing to calculate HSI over relatively large geographic areas, and incorporate landscape variables at multiple spatial scales. We also demonstrate the use of GIS and remote sensing to collect or prepare data for habitat fragmentation study by using software called FRAGSTATS, which is a computational program designed to compute a wide array of landscape metrics for categorical map patterns (McGarigal, 2002). Some of the metrics are commonly used to measure and quantify spatial patchiness in terms of composition (patch types and abundance) and

configuration (shape and juxtaposition). These metrics represent the percentage of fragmented habitats, area of largest patch, and — most importantly — the area of remaining potentially suitable habitat.

In this paper, we used aforementioned habitat characteristics and applied remote sensing, GIS and FRAGSTATS techniques to examine abundance, distribution and fragmentation of available pine forest and provide a possible scenario of re-colonization of red-cockaded woodpeckers. We have four scientific objectives: (1) to use a Landsat Enhanced Thematic Mapper Plus (ETM+) image to develop a land-use/land-cover map; (2) to develop a heuristic GIS-based habitat suitability index model and a map for the woodpecker; (3) to determine the spatial distribution of current potentially suitable habitats and (4), to illustrate a general methodology for conservation cartography and spatial analysis that can be adapted to other interior-forest-dwelling avifauna of conservation interest. In addition, we have two policy-oriented objectives: (1) to provide a map of potentially suitable red-cockaded woodpecker habitat that may be preserved for (a) existing populations in the region or (b) that may serve as sites for establishing new populations in the region: and (2) to indicate the most important habitat characteristics, such as shape, size, habitat composition, etc., for purposes of proactive red-cockaded woodpecker habitat management in the region.

Methods

Study Area

The study area is located near the Gulf coastal plains of southeast Texas between the Trinity River to the west and the Neches River to the east, around the small towns of Kountze, Silsbee, Lumberton and suburbs north of Beaumont that adjoin the 39,338-ha Big Thicket

National Preserve (BTNP) (30^{o} to 31^{o} N to 94^{o} to 95^{o} W) (Figure 3.1). Over the last five decades, the landscape surrounding the BTNP has been converted from continuous pine forest to a matrix dominated by agriculture, pasture, timber plantations and exurban and suburban development (Wilcove et al., 1986). As a result, the once intact pine forests were converted into small patches that are mutually isolated by a matrix of agricultural or other developed lands (Callicott et al., 2007). The study area was further subjected to intense oil and gas exploration that continues today, although such activities seem to have minimal effects on the breeding but proximity to roads and vehicular movement does affect and reduce foraging activities of red-cockaded woodpeckers (Charles & Howard, 1996). Annual precipitation averages 1350 mm (Marks & Harcombe, 1981; Callicott et al., 2007) and is uniformly distributed throughout the year, but because of its proximity to the Gulf of Mexico, the Big Thicket study area experiences a high frequency of devastating tropical storms and hurricanes. Since 1900, 40 tropical storms and hurricanes have struck the Gulf coast, with Rita in 2005 and Ike in 2008 being the most recent big storms to hit Texas. However, these hurricanes did not cause damage in the study area as they did in the surrounding counties and areas especially near Angelina, Harris, and Galveston Bay (NOAA).

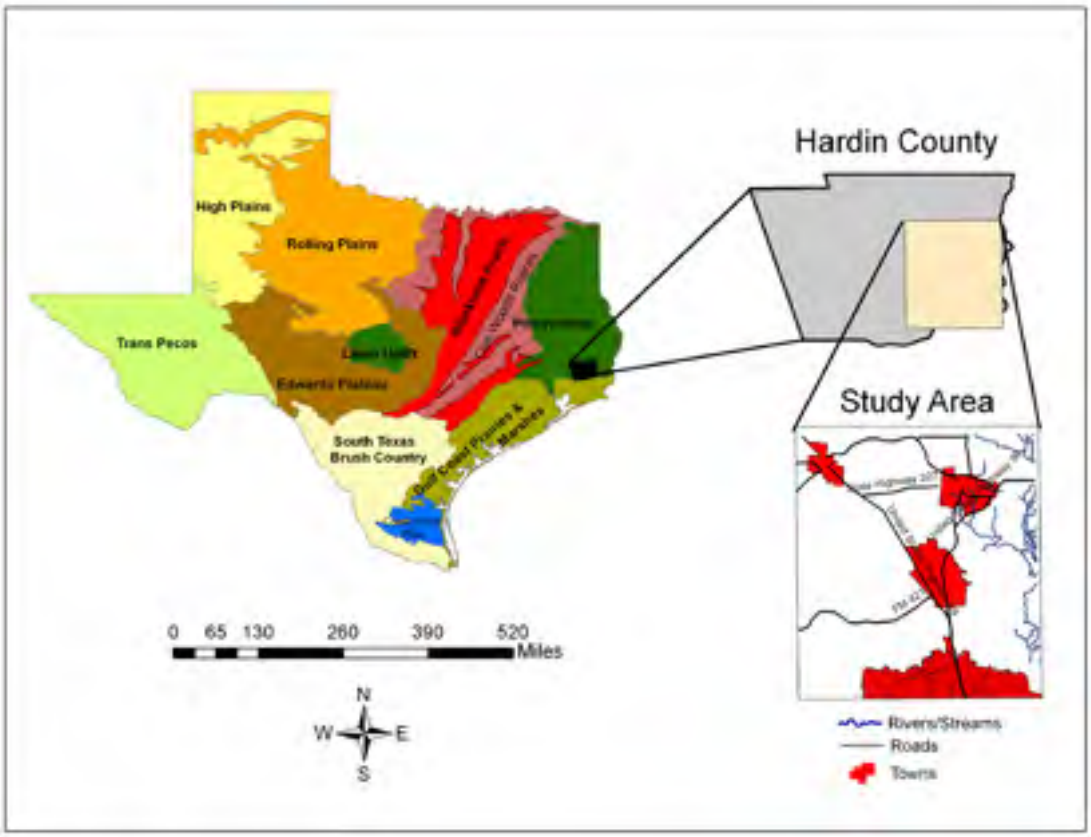

Figure 3.1. Vegetation types and map of the study site that is located in the Pineywoods region of southeast Texas, USA.

Nevertheless, hurricanes and other extreme natural disturbances such as severe winters can damage large portions of cavity and foraging trees, thereby affecting breeding populations of red-cockaded woodpeckers, which in turn leads to loss of genetic diversity (Reed et al., 1988).

The vegetation types of the study area can be characterized by both community physiognomy and physiographic position. Forests, savannas, and shrub thickets are normally combined with important trees such as pine, oak, and other hardwoods to characterize community physiognomy while upland, slope, floodplain and flatland indicate the physiographic position of the vegetation (Marks & Harcombe, 1981). Thus, according to community physiognomy and physiographic position, four broad types of vegetation characterize the Big Thicket region. The upland forest community consists of dominant longleaf pine forest or mixed

with a small-tree layer of Bluejack oak (*Quercus incana*). The slope community includes dominant species of shortleaf and loblolly pines with overstory hardwoods of Southern red oak (*Q. falcata*), White oak (*Q. alba*), Magnolia (*Magnolia grandiflora*), and American beech (*Fagus grandifolia*). The floodplain vegetation consists of hardwood forests of European hornbeams (*Caprinus spp*), Sweetgum (*Liquidambar styraciflua*) and Water oak (*Q. nigra*) mixed with Bald cypress (*Taxodium distichum*) and Water tupelo (*Nyssa aquatica*) and very few loblolly pines. And the flatlands include dominant species of Basket oak (*Q. michauxii*), Willow oak (*Q. phellos*), Laurel oak (*Q. lauriflora*), *P. taeda* and Red ash (*Fraxinus pensylvanica*).

Data Acquisition and Image Processing

We selected a cloud-free Landsat ETM+ scene of March 2003 for analysis because the spring season was considered optimal for achieving the highest reflectance for floodplain hardwood forests and pine trees (Thomlinson, 1993). The image was geographically referenced using ground control points (GCPs) created in ERDAS IMAGINE (a suite of software tools by Leica Geosystems Geospatial Imaging). The GCPs should be uniformly distributed over the image with good coverage near the edges. At least, 16 GCPs are considered reasonable if each GCP can be located with an accuracy of one-third of a pixel size (Bernstein, 1983). This number may not be sufficient, however, if the GCPs are poorly distributed or if the nature of the landscape prevents accurate placement (Campbell, 1996). Following these guidelines, we extracted 19 GCPs from topographic maps to georectify the image. In addition, the coordinate system was modified into the Universal Transverse Mercator coordinate system (zone 15) and newly revised datum of the 1984 world geodetic system to correlate with the image. Landsat TM data were acquired from six spectral bands: TM1 (0.45 to 0.52 μm), TM 2 (0.52 to 0.60 μm), TM3 (0.63 to 0.69 μm), TM4 (0.7 6 to .90 μm), TM5 (1.55 to 1.75 μm) and TM7 (2.08 to 2.35

μm) (Luiz & Garcia, 1997). Other data include topographic maps at a scale of 1:24,000; GIS files of roads and streets; polygons of towns; and aerial reconnaissance of 41 sections of the study area. More detailed data on vegetation were obtained by ground-truth (GPS points) visits to 287 sites. Individual global positioning system (GPS) points were accompanied with notes of soil texture, soil moisture regime, land use, plant composition, and elevation data. Digital cameras were used to take photographs of each site visited. ArcMap, a suite of GIS tools by Environmental Research Systems Inc. (ESRI), was used for GIS processing. A file with GPS points was imported to ArcMap as a shape file.

Vegetation Classification

We used supervised classification procedure to derive final land use and land cover (LU/LC) categories. Supervised methods require the user to define the spectral characteristics of known areas of land-use types and develop training sites (Thapa, 2005). The training sites or signature is employed to verify and define distinct classes (Jenson, 1996). This is achieved either by user's prior knowledge of the geographic features of an area of interest such as identification of distinct, homogenous regions that represent each class (e.g. water or grass) or by ground-truth data such as GPS points, which refers to the acquisition of knowledge about the study area from field work, analysis of aerial photography, personal experience etc (Conner et al., 1975). Ground-truth data are considered to be the most accurate (true) data available about the area of study. They should be collected at the same time as the remotely sensed data, so the data corresponds as much as possible (Stars & Estes, 1990). We used March landsat image of 2003 for the study and collected GPS points in May of 2007.

Furthermore, elements of visual interpretations such as color, shape, texture and pattern on aerial photos are commonly used that provides valuable clue during supervised classification. For example, we employed texture and pattern analysis technique on aerial photos and selected pixels in such areas. With texture and pattern, it is easy to differentiate naturally growing trees and human managed plantations e.g. coconut and pine plantation. We derived seven LU/LC categories (water, urban areas, pine forest, pine plantation, mixed forest, grass, and cypress forest on floodplain) from the landsat image (Figure 3.2). We classified entire pixels into their designated classes according to the vegetation categories found in the study area. For example, areas with tall pine trees were classified as 'pine trees', areas with mixed pine and oak trees were labeled as 'Mixed Forest', areas of floodplain were labeled as 'Cypress trees on sloughs' and so on. GPS locations of each category accompanied with aerial and field photos were extensively used during classification process.

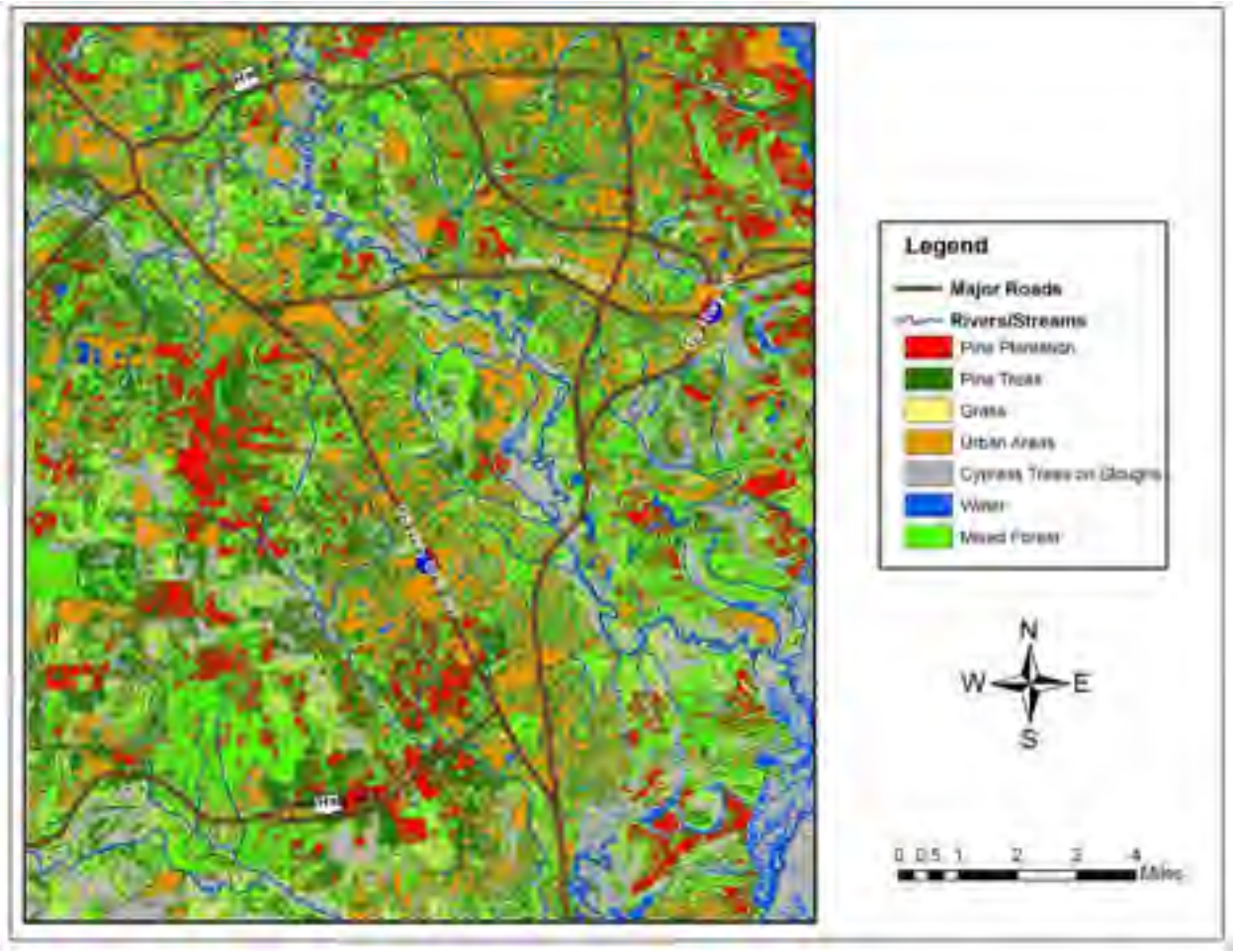

Figure 3.2. Seven land-use categories derived from supervised classification.

Accuracy Assessment

It is necessary to assess the accuracy of any thematic classification to evaluate its intended application and high accuracy assures consistency and reliability of derived landscape metrics (Xulong et al., 2005; Shao & Wu, 2008). Several factors, related to the sensors as well as to the classification process, contribute to classification errors (Lunetta et al., 1991). Furthermore, it is critical to measure quality and accuracy of the data utilized for the classification (Congalton & Green, 1999). The classification or errors are analyzed by a confusion or error matrix, which is also called as accuracy assessment (Congalton & Green, 1999). An error matrix or accuracy assessment cell array is a table with entries representing the

number of sample units; i.e., pixels, clusters of pixels, or polygons that are assigned to a specified class relative to the actual class found on the ground (Congalton, 1991). Rows contain a list of class values for the pixels in the classified image file. And column represent class values for the corresponding reference pixels that are input by the user and are generally collected from sources such as aerial photographs, GPS points, previously tested maps, or other data. The reference class values are compared with the classified image class values to assess the accuracy of an image classification. And according to Anderson et al. (1976), classification accuracy closer to 85% for LU/LC study is acceptable.

Several statistical measures of a classified LU/LC map can be derived from an error matrix including overall classification accuracy (sum of the diagonal elements divided by the total number of sample points), categorical omission and commission errors, and the KHAT coefficient (an index that measures the agreement between reference and classified data). A minimum of 204 reference points are required to achieve 85% accuracy with an allowable error of 5% (Jensen, 1996). First, we generated about 300 random (reference) points and with the help of aerial photos and with prior knowledge of geographic features we assigned values for each random point. Then, we compared these reference class values with the classified image class values, which gave us an overall accuracy of 77.33% with KHAT = 0.7277. Second, we used GPS locations as reference points and compared with the class values of image file, which produced an overall accuracy of 81.48% with KHAT = 0.7449 (Table 3.1). The latter accuracy was deemed acceptable for this study because it was within the five-percent allowable margin of error and was closer to 85%.

Table 3.1

Combination of GPS and Random Points to Assess Classification Accuracy

Class Name	Reference Totals	Classified Totals	Number Correct	Producer's Accuracy, %	User's Accuracy, %
1. Grass	5	4	3	60.00	75.00
2. Pine plantation	13	11	10	76.92	90.91
3. Pine trees	53	59	44	83.02	74.58
4. Urban area	59	58	52	88.14	89.66
5. Cypress trees on sloughs	12	13	10	83.33	76.92
6. Water	1	1	1	100.00	100
7. Mixed forest	19	17	13	68.42	76.47
Totals	**162**	**163**	**133**		
Overall Kappa Statistics					**0.7449**
Overall Accuracy, %					**81.48**

Habitat Suitability Index Models

We computed HSI value for each pixel of the resultant classified image. We selected pine trees class only because adequate acreage of pine trees of specified species is required for successful breeding and foraging as explained in the beginning of this chapter. We assigned 1 to pine trees class value and the rest to 0. In this way, we had a binary map of pine trees only. We ran neighborhood analysis in ArcGIS, which is a statistic that uses surrounding pixels in a defined neighborhood to assign a value to a target pixel. It is commonly used to find the most dominant land-cover category in a neighborhood or to find the number of certain LU/LC categories within a specified neighborhood. We selected neighborhood size based on the annual

home range size of the red-cockaded woodpeckers as reported by several studies and determined using a variety of methodologies including 100%, 95%, 50% minimum convex polygons and 95% fixed kernel estimator (DeLotelle et al., 1987; Doster & James, 1998; Engstrom & Sanders, 1997; Walters et al., 2002).

According to Franzreb (2006), the minimum convex polygon estimator includes outliers or areas that are not even used by the animals (birds in this case) and provide overestimate of the home-range size making it less suitable as a descriptive statistic in terms of the biology of the species. On the other hand, the fixed kernel estimator is relatively insensitive to the presence of outliers and is less biased and produced more consistent results. Thus, we selected the home-range size that was produced by fixed kernel estimator i.e. ~ 50 ha. To implement this, we selected a neighborhood size of 23 × 23 pixels, i.e., 529 pixels of 900 m^2each (30 m × 30 m) which yields a slightly lower value of 476,100 m^2 or 47.61 ha or 117.6 acres. A suitability index *S* for a pixel was determined as the proportion of pixels in pine tree cover in the neighborhood around the target pixel. Once all pixels are evaluated, we have a HSI map (Figure 3.3).

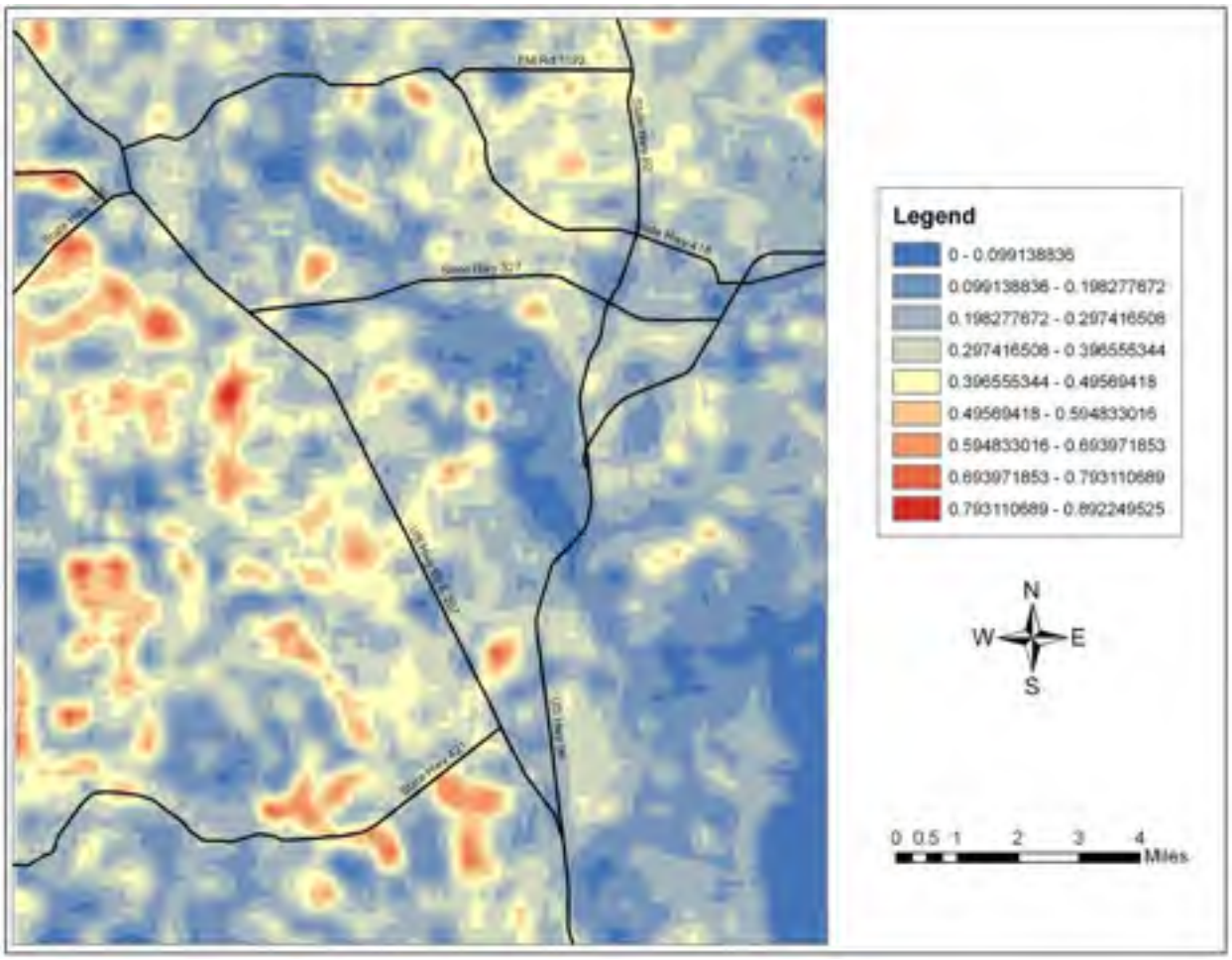

Figure 3.3. HSI map showing suitability values in nine levels.

For simplification we reclassified the HSI map to three classes only: 1, very unsuitable habitat (HSI, 0 - 0.333); 2, unsuitable habitat (HSI, 0.333 - 0.666); and 3, potentially suitable habitat (HSI, 0.666 – 1). The reclassified map is shown in Figure 3.4. These nominal break points were selected arbitrarily to provide equal intervals and will be varied later for sensitivity analysis.

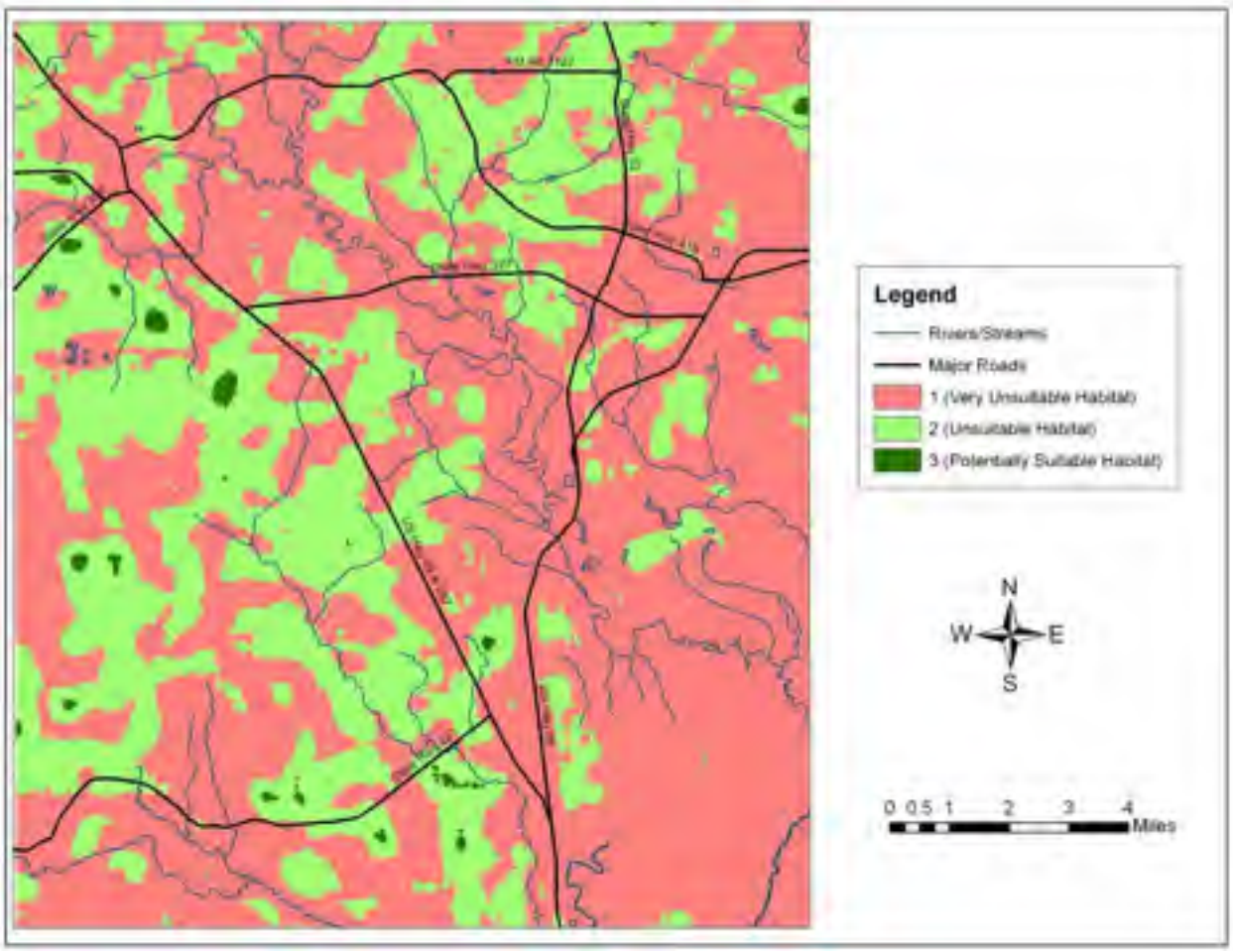

Figure 3.4. Habitat suitability index (HSI) map with three habitat types – very unsuitable, unsuitable, and potentially suitable.

Then we converted the resulting HSI raster map to polygon features to calculate areas in hectares of each patch (Figure 3.5).

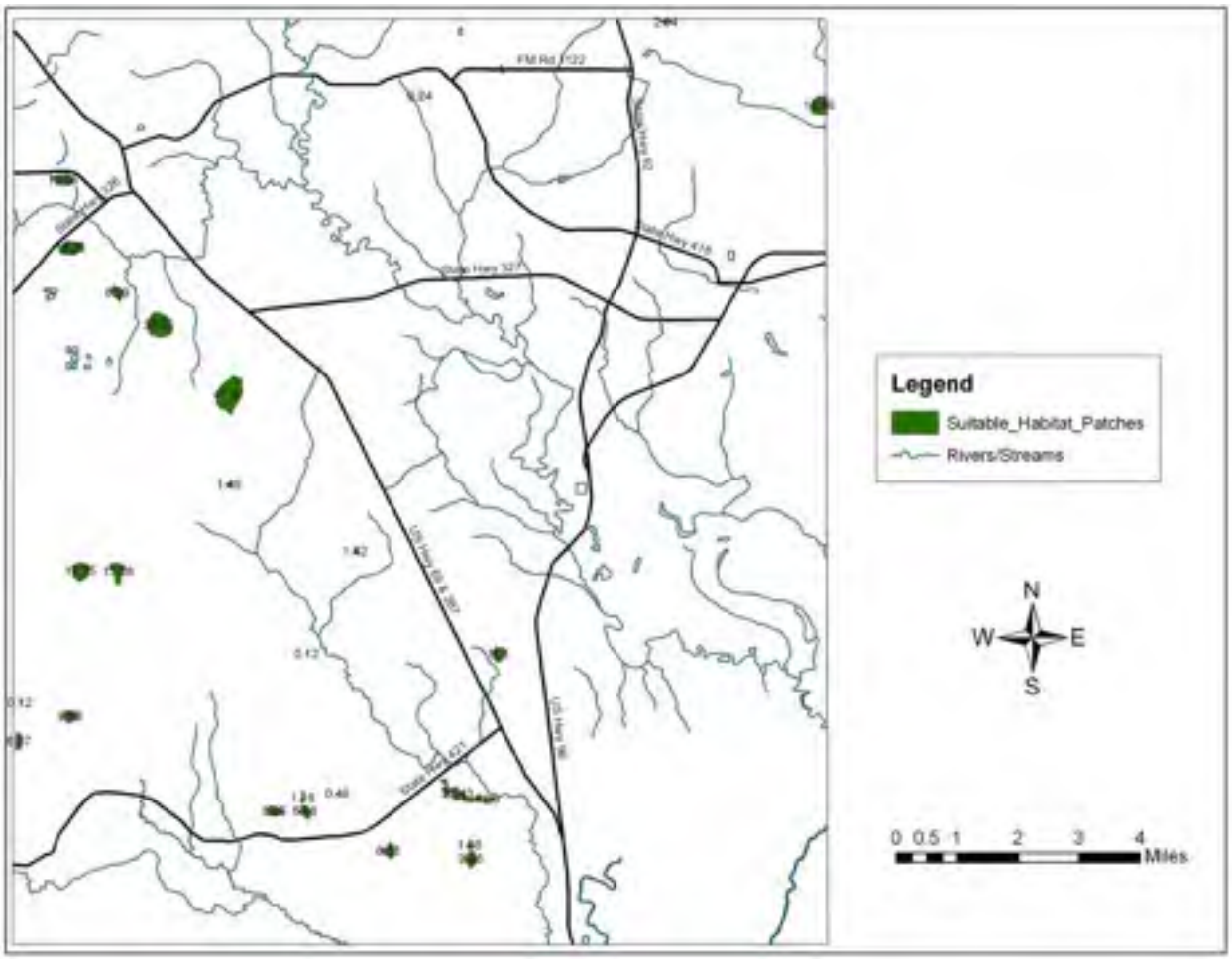

Figure 3.5. Potentially suitable habitat patches and their areas in ha.

Habitat Fragmentation and FRAGSTATS

FRAGSTATS accepts Arc/Info (a GIS ESRI tool) polygon files (vector) or "raster" (a matrix or grid of pixels) images in a variety of formats (McGarigal & Marks, 1994). For our study, we adopted the raster version of FRAGSTATS and used the HSI map as input data. Prior to this, the HSI map was reclassified into three discrete classes using equal interval method, one of the several classification methods available in ArcMap. We selected this method because it groups the pixels according to their values and allowed us to maximize the difference amongst classes. Recall from the previous section that a pixel was assigned a value of 1, 2, or 3, according to the interval break values (0.000 to 0.333 for class 1, 0.333 to 0.666 for class 2, and 0.666 to 1

for class 3). These three classes represent very unsuitable (1), unsuitable (2), and (3) potentially suitable habitat. A suite of metrics was selected and computed at patch, class, and landscape levels (Table 3.2). The resultant metrics reflected various configurations and compositions of a landscape (Thapa, 2005).

Table 3.2

Selected Metrics

Area/Density/Edge Metrics	Connectivity Metrics
CA/TA = Total Class Area (ha)	COHESION = Patch Cohesion Index
PLAND = Percentage of Landscape (%)	
NP = Number of patches	
LPI = Largest Patch Index (%)	

Results

Image Processing

From a total of 287 GPS points, we used 162 points for classification accuracy. The rest (125) were used during image classification. Use of GPS points and visual interpretation of aerial photos proved effective in Landsat ETM+ classification and facilitated the process. Our results show pine trees and grass have the lowest classification accuracy with 74.58% and 75% respectively. For pine trees, it might be due to insufficient GPS points because we could not gather data from private lands and such lands contained pure stands of old pine trees. For grass, it is possible to classify agricultural lands as grass and a common problem with Landsat image of 30 m resolution. In addition, short-grass areas (grazed pastures or manicured lawns) and dirt

roads had overlapping values with other urban areas such as patches of bare soil and asphalt roads. We classified pine plantation with 90.91% accuracy because they were easily identified based on texture and pattern on aerial photos and GPS data collected from well within the plantation areas. Similarly, we classified urban areas with 89.66% accuracy as they are also easily identifiable on aerial photos.

Water pixels were classified with 100% accuracy. And it is one of the geographic features that a user can accurately classify in remote sensing applications as water pixels exhibits the lowest reflectance property when examined in a spectral profile. Profile Tools of ERDAS allow the users to examine spectral behavior of pixels of different features. Cypress trees on sloughs class was classified with 76.92% accuracy. Cypress trees occur mostly in sloughs of floodplains mixed with oak species and several factors such as topographic shadows and deep water contributed to the low accuracy of this class. Similar to water, wet sandy banks of creeks, streams, rivers, and sloughs have a lower reflectance in most bands and they became a source of confusion. Statistical analysis of spectral responses or profile from training samples, as well as ellipse and dendrogram plots, showed a similar reflectance with dark pixels (wet soils, black soil, and topographic shadows). Furthermore, vegetated (forest, urban, grass) and non-vegetated (water) were spectrally distinct. In order to redefine, refine and improve accuracy, we constantly reduced, merged and masked the confused classes.

Sensitivity Analysis

Since the selection of nominal class break values of 0 - 0.333, 0.333 - 0.666 and 0.666 – 1 was arbitrary, we performed sensitivity analysis by perturbing these break values by 10% to examine the effect on the resultant habitat suitability indices (Table 3.3). We perturbed two break

values of 0.333 and 0.666 as the minimum of 0 and maximum of 1 will remain constant. These two breaks represent unsuitable (UB) and suitable breaks (SB). We multiplied each value of UB to the individual value (three) of SB to get nine break values shown in Table 3.4.

Table 3.3

Perturbation Above and Below the Nominal Break Values

Breaks	-10%	Nominal	+10%
Unsuitable Breaks (UB)	0.3	0.333	0.366
Suitable Breaks (SB)	0.599	0.666	0.733

Table 3.4

Nine Break Selections

Breaks Selection	Habitat Type		
	1	2	3
1	0-0.3	0.3-0.599	0.599-1
2	0-0.333	0.333-0.599	0.599-1
3	0-0.366	0.366-0.599	0.599-1
4	0-0.3	0.3-0.666	0.666-1
5	0-0.333	0.333-0.666	0.666-1
6	0-0.366	0.366-0.666	0.666-1
7	0-0.3	0.3-0.733	0.733-1
8	0-0.333	0.333-0.733	0.733-1
9	0-0.366	0.366-0.733	0.733-1

The maps are presented in Figure 3.6, Figure 3.7 and Figure 3.8. Each figure is organized in a row of maps that represents change in UB while SB remains constant. In the first row of maps (Figure 3.6), with increasing range in the UB values, there is decrease in the unsuitable habitat and increase in the highly unsuitable habitat areas. As expected the suitable habitat areas remain unchanged. Similarly, in the second row of maps (Figure 3.7), the areas of very unsuitable habitat increases dramatically while the amount of unsuitable habitat decreases and the potentially suitable habitat areas remain unchanged. And the last row of the maps (Figure 3.8) represents the final group of break values. With this break selection, the potentially suitable habitat decreases and the very unsuitable habitat area increases with more fragmentation of unsuitable habitats.

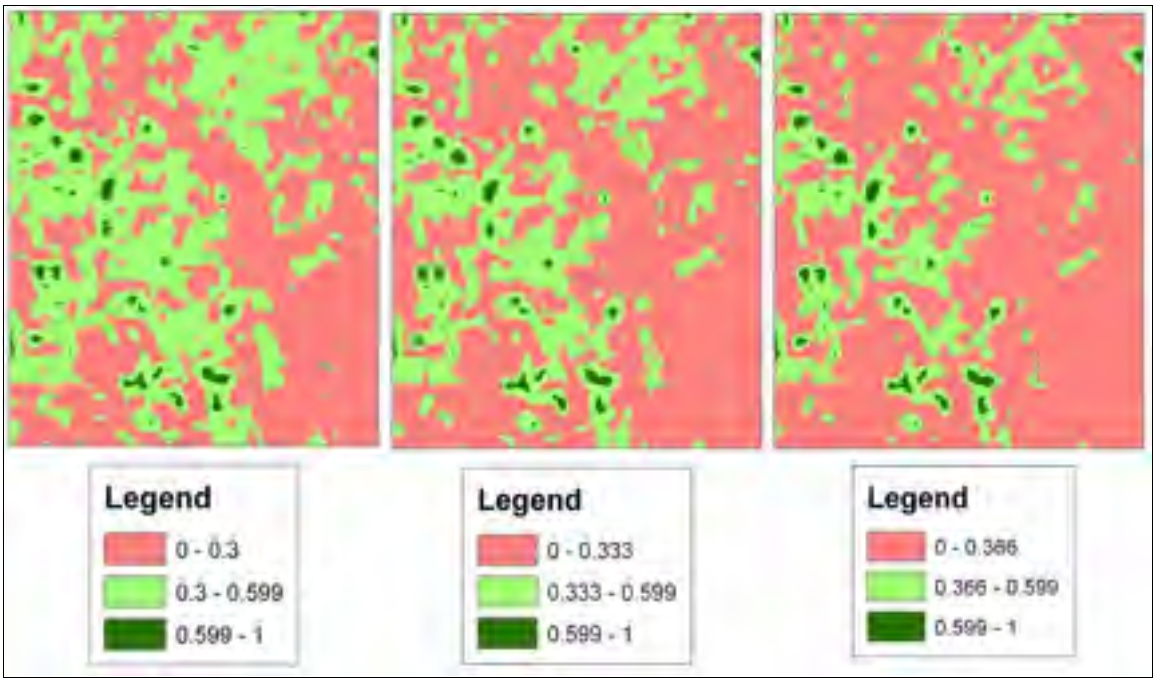

Figure 3.6. Maps of first set of three break value selections.

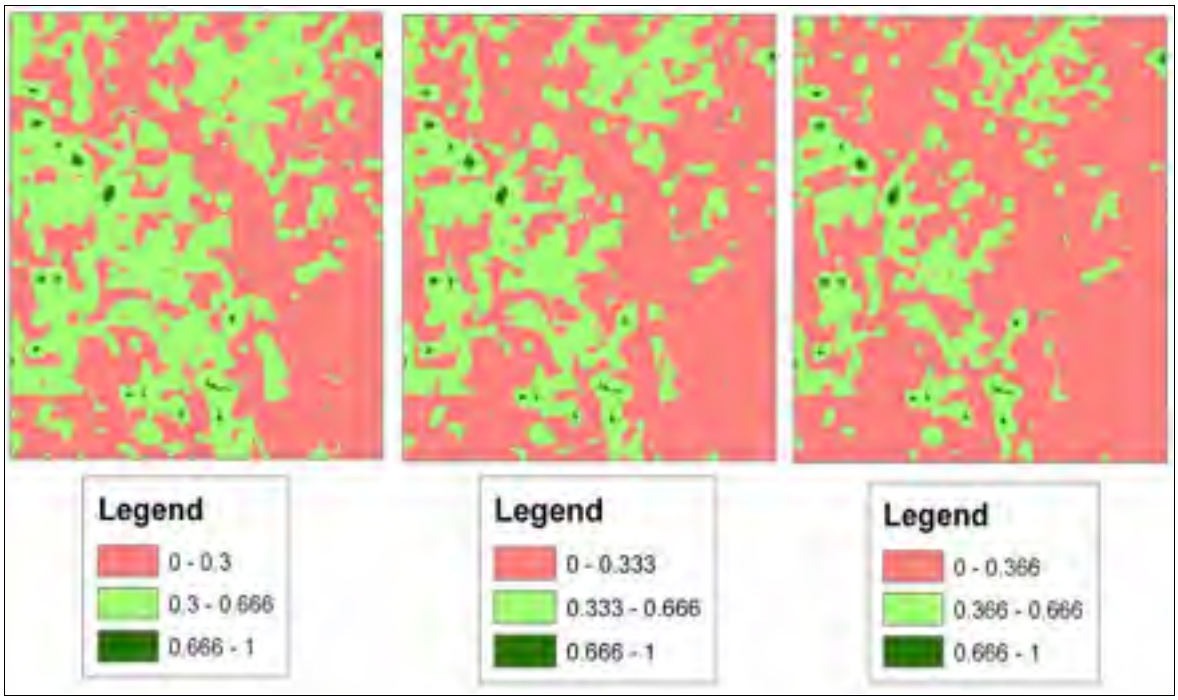

Figure 3.7. Maps of second set of three break value selections.

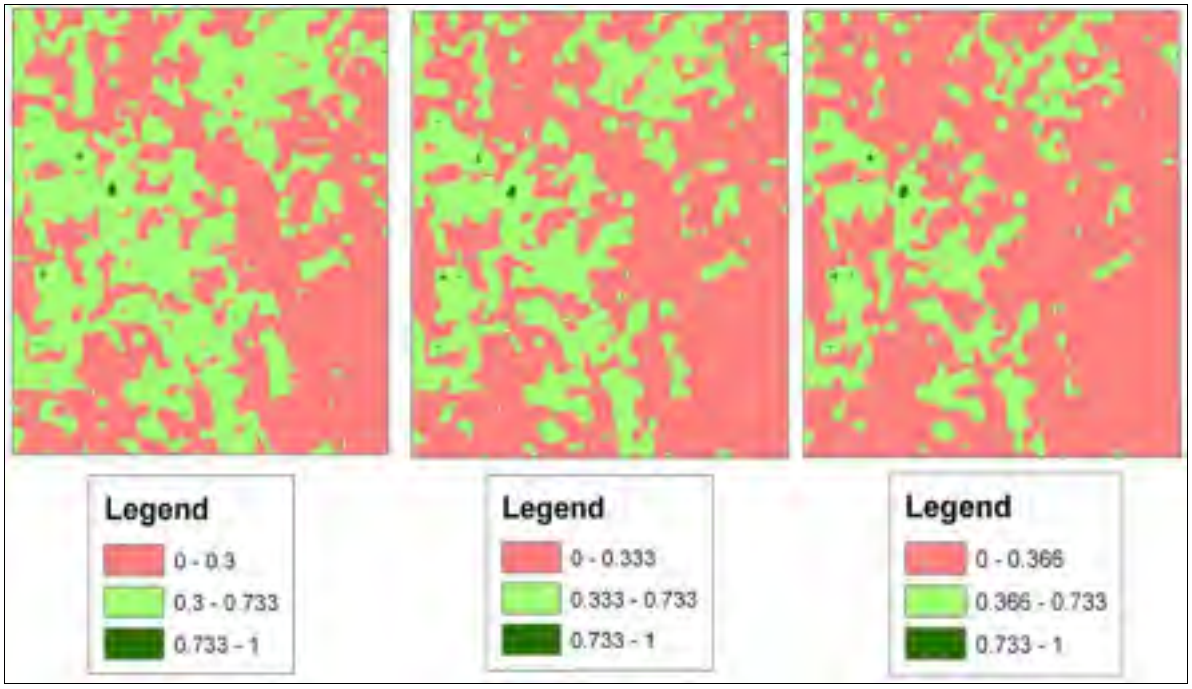

Figure 3.8. Maps of third set of three break value selections.

Metrics at Patch, Class, and Landscape Levels

We used nine selection break values to compute landscape metrics (Table 3.4). We calculated two metrics i.e. area/density/edge and connectivity of three different patch types (class) or habitat types i.e. very unsuitable, unsuitable and suitable. These metrics were used to examine composition and configuration of patches in the study area (McGarigal et al., 2002). Even though, FRAGSTATS provide individual patch property at three levels i.e. patch, class and landscape, we quantified patch properties at class level only because most metrics are redundant and provide similar values at patch and landscape levels. For example, total core area (TCA) at class and landscape levels is defined the same as core area at patch level except the core area is aggregated over all patches of the corresponding patch type at the class and landscape levels. Total (Class) Area (CA/TA) and Percentage of landscape (PLAND) metrics measure landscape composition (Table 3.5). CA measures how much of the landscape is occupied by a particular patch type. For potentially suitable habitat, the value of CA/TA decreases with increasing value of the break point for that class. For example, potentially suitable habitats reach 878.76 ha when the break is 0.599, decreases to 264.96 ha when the break is 0.666, and further decreases to 62.46 ha when the break is 0.733 (Table 3.5). PLAND quantifies the proportional abundance of patch type in a landscape. PLAND approaches 0 when a landscape consists of single patch type. PLAND metrics largely mirror the patterns of CA. The PLAND metric revealed that potentially suitable habitat occupies 1.7% when the break is 0.599, decreases to 0.5% when the break is 0.666, and further decreases to 0.12% when the break is 0.733. Thus, the amount of potentially suitable habitat area decreases with increasing break value. Number of Patches (NP) is a simple measure of the extent of subdivision or fragmentation of a patch type. NP = 1 when the landscape contains only a single patch type and NP > 1 indicates degree of fragmentation.

Table 3.5

Class Metric Results

Breaks Selection	CA/TA (ha)			PLAND (%)			NP			LPI			COHESION		
	Habitat Type			Habitat Type			Habitat Type			Habitat Type			Habitat Type		
	1	2	3	1	2	3	1	2	3	1	2	3	1	2	3
1	28964.43	22528.71	878.76	55.30	43.02	1.7	192	220	62	39.02	24.6	0.17	99.8	99.70	94.21
2	34562.97	16930.17	878.76	65.99	32.33	1.7	153	233	62	59.32	17.21	0.17	99.92	99.56	94.21
3	39151.34	12341.34	878.76	74.76	23.56	1.7	99	220	62	72.79	9	0.17	99.96	99.25	94.21
4	28964.43	23142.51	264.96	55.30	44.19	0.5	192	219	27	39.03	25.63	0.09	99.80	99.70	92.03
5	34562.97	17543.97	264.96	65.99	33.5	0.5	153	232	27	59.32	18.02	0.09	99.92	99.55	92.03
6	39151.80	12955.14	264.96	74.76	24.74	0.5	99	219	27	72.79	9.4	0.09	99.96	99.25	92.03
7	28964.43	23345.01	62.46	55.30	44.57	0.12	192	218	14	39.03	25.96	0.05	99.8	99.69	89.29
8	34562.97	17746.47	62.46	65.99	33.88	0.12	153	231	14	59.32	18.29	0.05	99.92	99.55	89.29
9	39151.80	13157.64	62.46	74.76	25.12	0.12	99	218	14	72.79	9.55	0.05	99.96	99.25	89.29

NP for potentially suitable habitat varies from 62, to 27, and 14 as the break value changes from 0.599, 0.666, and 0.733 indicating that this habitat type is more fragmented than the unsuitable and very unsuitable types (Table 3.5).

Largest patch index (LPI) is a simple measure of dominance as it quantifies the percentage of total landscape occupied by the largest patch. LPI = 0 when the largest patch of the corresponding patch type is small and 100 when the largest patch occupies the entire landscape. The largest patch of potentially suitable habitat occupies only 0.05 – 0.17 % of the landscape as compared to 9 - 26% and 39 – 73% for unsuitable and very unsuitable habitat types respectively. This corroborates the results of CA/TA and PLAND that showed presence of small amount of potentially habitat types as compared to the other two. Connectivity is considered a vital element of landscape structure and we used a single connectivity metric, i.e. COHESION to observe physical connection between patches. COHESION = 0 when patches are less connected and approaches 100 when they are more connected. Our analysis showed that the potential suitable habitat patch type is physically disconnected as indicated by 89 – 94 as compared to the other two habitat types with sometimes approaching almost 100 showing they are more connected and contiguous.

Discussion

Overall, the LU/LC map derived from satellite imagery was satisfactory because categories were adequately mapped, and resulted only in minor misclassifications. The resultant map was refined with spatial masking and recoding to achieve acceptable accuracy. Use of aerial photographs and GPS points proved effective in improving classification accuracy. The contrasting reflectance of bare areas and vegetation in the visible and infrared bands facilitated

accurate identification. However, accurate delineation of grass from crops and shrubs represented a challenge (as in many remote sensing studies). Visual examination of the satellite imagery of the study area and field work revealed numerous dirt roads crisscrossing the entire landscape. Our study area once contained booming oil towns and clearly shows signs of human-induced fragmentation. Several pipelines, power lines, railroads cut through the study area thus dissecting the entire landscape into smaller fragments.

GPS locations of different categories or classes proved to be the most critical data during LU/LC classification of the landsat image in facilitating and enhancing classification accuracy. Composition metrics such as CA/TA, NP and PLAND revealed heterogeneous structure of the landscape especially the number of patches. NP ranged from 14-233 patches depending on the break selections. For example, the NP for first break value is 192 patches for very unsuitable, 220 for unsuitable and 62 for potentially suitable habitats. Therefore, the total NP for first break value is 192 + 220 + 62 = 474. The NP for potentially suitable habitat patches decreases with decreasing pixel values from 0.733 to 1 for which NP is only 14 (Table 3.5). Similarly, CA/TA and PLAND indicated low amount of land occupied by potentially suitable habitat patches (PLAND = 0.12 to 1.7%) as compared to 55-75% for very unsuitable and 24-45% for unsuitable habitat respectively. On the other hand, configuration metrics such as LPI and COHESION produced expected results. LPI for potentially suitable habitat ranged from 0.09 to 0.17% for the nine break values indicating even the largest patch occupies only 878.76 ha of the total 52,371.90 ha landscape (for first break value).

The composition metrics showed that about 9-73% of the study area is composed of very unsuitable and unsuitable habitats combined. This includes floodplain areas near major rivers and streams, pine plantations, areas around small towns and mixed forests. The metrics further

indicated only about 0.05-0.17% of the study area is composed of potentially suitable habitat and included areas located away from urban areas and major roads. For three break values of potentially suitable habitats, NP ranged from 14-62 for 62.46-878.76 ha of land and COHESION metrics ranged from 89.29-94.21 exhibited severe fragmentation (Figure 3.4). This suggests that the isolation and size of smaller fragments might be the cause of decline of clans from those patches if there were any because for a territorial avian species such as red-cockaded woodpeckers with very restrictive habitat requirements and limited gap-crossing ability will likely be the most sensitive to isolation effects (Conner & Rudolph, 1991; Dale et al., 1994; Pearson et al., 1996; With & Christ, 1995).

The connectivity metrics (COHESION) provided vital information about the structure of landscape i.e. the patches of potentially suitable habitat patches are more physically disconnected than the other two unsuitable habitat patches. Thus, we were able to show composition, configuration and connectedness of the three habitat patches that formed a heterogeneous habitat across the study area. In addition, for this study, we used maps as means to study effects of changes in parameters. In our case, the parameters were the pixel value ranges. We showed with change in each break values, there was obvious impact on the three habitat types. And the most dramatic effect was observed on two habitat types especially on the unsuitable and potentially suitable habitat patches. This result is also corroborated by the findings of landscape metrics (Table 3.5).

Conclusion

We presented a method of quantifying composition and configuration of possible habitats for the red-cockaded woodpecker by using GIS, remote sensing and FRAGSTATS. We did not

include other variables which may impact habitat such as tree age, tree diameter and tree species because these are difficult to assess from a Landsat image. Hyperspectral images can provide these variables as reported in a recent study by Santos et al. (2010). Thus, our methods could be coupled with variables obtained from hyperspectral images for better understanding of the current potential suitable habitat available in the study region. By using sensitivity analysis, we were able to show that only few areas contain adequate amount of pine trees that could sustain a group of woodpeckers. However, to assess the full quality of the habitat, we would require inclusion of other variables as noted above.

The results revealed a highly fragmented nature of available habitats in public and private rural lands especially near the towns of Kountze, Silsbee, and Lumberton. Most of the potentially suitable habitats were found well away from the towns, especially on the west side of the study area near Highways 69, 326, 421 and public lands (Figure 3.4). FRAGSTAT analysis revealed 62.46 to 878.76 ha of available potentially suitable habitat; visual inspection of the habitat suitability map shows that these habitats are highly fragmented and mostly occur on the west side of HW 69 & 287 and FM 421. There is one in the V-notch of highways 69 and 96 and another bigger patch on the north east side of HW 96.

We assume that red-cockaded woodpeckers are absent near towns due to small fragments of possible habitats and lack of foraging habitat, traffic activity and patch isolation. There was row of patches located on public lands near the town of Kountze (Figure 3.5). The patch sizes were 47, 33, 9, 18 and 13 hectares respectively. Four of the patches are located within a mile while the fifth and the largest one are located within 1.5 miles from the nearest one. The other large patches are located near FM 421and are less than 1.5 miles apart from each other. Our field activity revealed presence of massive pockets of pure pine stands in these areas. And if these

patches contains some clans of red-cockaded woodpecker, they can travel to and fro within these patches as they are located within a mile (foraging radius is ~1 mile). However, this is unlikely to happen owing to the bird's fidelity to their cavities. We determined that areas larger than 50 ha are able to sustain a group of red-cockaded woodpeckers given that they contain old, red heart fungus infected cavity trees with few or no midstory. Landowners who have a red-cockaded woodpecker group or groups can do much to enhance survival, regardless of the size of their property by controlling midstories and building artificial cavities. USFWS assists landowners to manage habitat and even provides incentives and grants to promote red-cockaded woodpecker conservation.

This study is confined to determining the quantity of potentially suitable red-cockaded woodpecker habitat in the current landscape near and around the Big Thicket National Preserve. We conclude that there are no large patches (more than 50 ha) that can sustain a clan or populations of red-cockaded woodpeckers under ideal habitat conditions. Most of the large patches are located within a distance of one mile and isolation might not be a cause of decline if there were any clans living in those habitats. Other factors such as encroaching midstory and suppressed fire might have contributed to the loss. To assess quality of these patches; a thorough study of midstory vegetation, pine tree age, diameter and species is strongly warranted. In addition, our study reveals that a woodpecker census in the region might be fruitful and that with proper management practices to preserve red-cockaded-woodpecker habitat both in private and federal lands, existing populations (if any) might be conserved and new populations might be established there.

CHAPTER 4

POTENTIAL DEVELOPMENT MAPS AND HABITAT SUITABILITY INDEX MAP TO QUANTIFY SUITABLE HABITATS OF THE RED-COCKADED WOODPECKER IN A REGION NEAR THE BIG THICKET NATIONAL PRESERVE, TEXAS

Abstract

We combine land-use (LU) change models and habitat suitability index (HSI) models to quantify the amount of potentially suitable habitats of red-cockaded woodpecker for various scenarios of hypothetical development. LU models are increasingly used to forecast conversion of vegetated land parcels to urban land cover. These models require varied information that range from physical structures, population density, to information on current land cover. In this paper, we describe the processes involved in creating variables that drive a LU model such as proximity to roads, population density and several land cover types. Geographic Information Systems (GIS) and remote sensing are useful tools in the construction of these variables. We combined these variables to find potential development probabilities for residential, commercial, industrial, as well as total probability of LU change. Then, we used HSI models to calculate the amount of suitable habitats available before and after the hypothetical developments have occurred. Our results indicate this method is useful to evaluate the effects of urbanization on wildlife habitat. This method could be even more effective when more data are available through the use of high resolution images and field work and when functions are validated empirically.

KEYWORDS: Land-use change, Simulation models, Potential development maps, Southeast Texas, Habitat suitability, Habitat fragmentation, Big Thicket National Preserve.

Introduction

Even though a variety of factors including economics, culture, and land management policies play vital roles in shaping LU pattern in a region, population growth is undoubtedly the most potent driving force (Dale et al., 1993; Houghton, 1994; Lambin, 2001; Ramankutty et al., 2002; Shoshany et al., 2002; Ningal et al., 2007; Silveira & Dentinho, 2010). The need to feed growing populations has caused increased conversion of forests and grasslands into cropland (Ningal et al., 2007). Resultant LU change from the aforementioned activities can have direct impact on the world's biotic diversity (Wilson, 1988; Sala et al., 2000), on soil quality (Buschbacher et al., 1988; Tolba et al., 1992), on local, regional and global climate conditions (Chase et al., 1999; Houghton et al., 1999) and may alter ecosystem services that humans require to survive (Vitousek et al., 1997).

Locally, in north central Texas (Denton County), human population nearly doubled from 1990 to 2003 i.e. from 273,775 to 504,750 (Callicott et al., 2006; Monticino et al., 2007). In the city of Denton, the population grew from 66,270 in 1990 to 106,050 in 2008 (62% increase in 18 years, NCTCOG 2008). Simultaneously, percentage of developed land also doubled from 13% to 26.8% from 1995 to 2000 and the number of housing units also increased by over 10% (NCTCOG, 2003) and by over 26% from 2000 to 2005 (NCTCOG, 2005). About 39,000 new single-family units were completed in 2007 which was 9000 fewer than in 2006. However, 11,600 multi-family units were added in the same year showing a sizeable increase, up from 8,300 in 2006 (NCTCOG, 2008). The housing trend indicates that even though the single-family unit's construction slowed and a high number of them remained vacant at the end of 2007, they are likely to become occupied as long as the region continues to experience job growth and might experience increase in single-family construction. On the other hand, the multi-family

construction is expected to continue at the current rate pace (NCTCOG, 2008). The additional housing units certainly increased the percentage of developed lands and impervious surface. These development and human population growth trends are likely to increase the impact on the Greenbelt corridor – a protected part that covers ~ 20 km^2 of the Cross Timbers and Prairies biogeographic province of Texas (Acevedo et al., 2008).

In southeast Texas, potent drivers of LU change are operations by timber companies along with gas and oil companies. Such extractive industries often lead to deforested land cover as LU activity associated with logging results in denuded lands (Lambin, 1997). In addition, recent restructure in the timber industry led to increased demand for residential properties. The restructure prompted big real estate companies to acquire large tracts of land set aside for residential development and sell it to big timber companies (Callicott et al., 2006). In addition, proximity to refineries in Port Arthur and city of Beaumont with a population of more than 100,000 (NCTCOG, 2008), has resulted in steady increase in residential development making this another potent driver of LU/land-cover change.

Besides timber, gas and oil companies, this region is comprised of matrix of privately owned timberland, small farms and a few small towns – a clear sign of fragmentation. Such rapid development and increased demand for land is threatening one of the most biologically diverse regions of Texas called the Big Thicket National Preserve (BTNP) that lie adjacent to the matrix of above lumbered, farmed, and mined lands (Gunter, 1993). The preserve is composed of legally preserved areas that are small and tenuously connected by riparian corridors (Cozine, 2004).

According to landscape ecological theory, the extent of development and its impact is determined by location of development relative to spatial pattern of ecological features (Turner

et al., 2001) with agents or entities such as humans actively participating in the landscape (Brandt et al., 2002; Lundberg, 2002; Zube, 1987). Several approaches have been proposed to reduce the ecological impacts of development and to prevent or minimize urban sprawl (Brown et al., 2004). An array of spatial modeling techniques are being employed to understand the drivers of urban development and their future impacts and to develop scenarios that can be used to test alternative approaches to minimize these impacts. Simulation models based on discrete choice statistics focus are used to estimate likely locations of development (Landis, 1994). And artificial neural networks are used to identify non-linear interactions between predictor variables and possible locations of development (Pijanowski et al., 2002). Percolation theory is used to develop mathematical models that correlate physical arrangement, configuration, population and size distribution of towns and cities (Makse et al., 1998). This theory applies statistical physics to urban growth phenomena and yields valuable information on how cities grow and change; these results in turn can be used for future planning and management. Such models have proven effective in evaluating the impacts of variables and processes that lead to change in LU.

In this paper, we have the following objectives: a) to assess the fate of rural or undeveloped land parcels by using a potential development model that is based on discrete choice statistics (Acevedo et al., 2008); b) to calculate the amount of remaining potentially suitable habitat for red-cockaded woodpecker after the hypothetical development has occurred; c) to evaluate fragmentation of such remaining habitat.

Methodology

Study Site

Our study site includes areas near Big Thicket National Preserve (BTNP) in southeast

Texas (Figure 3.1). The study site includes some portion of protected areas: state parks and areas near the Neches River adjacent to BTNPs. It has a temperate climate with relatively flat relief and precipitation range of approximately 1100-1600 mm annually (Callicott et al., 2007). As for vegetation, piney woods dominate. This region is located near large growing cities (with population over 100,000), threats to natural systems, LU change resulting in deforestation, ecological processes, biodiversity, water (quantity and quality), and habitat fragmentation. Prior to the establishment of the national preserve, the Big Thicket was haven to runaway slaves, draft dodgers, conscientious objectors of Civil War, outlaws and fugitives and to the inroads of timber and oil industries (Cozine, 2004). And now, BTNP is a fragmented group of small conservation units in a rapidly urbanizing rural matrix (Callicott et al., 2006).

Development Potential Functions

The development potential model uses a collection of simple functions, derived from hypothesized mechanisms. These functions were incorporated in routines written in the C programming language to score the suitability or potential for development of a parcel. The potential development model selects the potential development category of a parcel i.e. residential, commercial, or industrial based on factors such as proximity to highways and streets, population density, and proportion of already developed land around the target cell (Callicott et al., 2006). Available or undeveloped land can be agricultural, natural vegetated parcels, denuded lands, a part of floodplain, and a segment in a fragmented landscape.

As mentioned above, several spatial modeling techniques have been used to study urban development patterns: discrete choice statistics to estimate likely locations of development, artificial neural networks are to identify non-linear interactions between predictor variables and

possible locations of development, percolation theory to predict how cities grow and change. We have opted to employ a combination of functions based on hypothetical mechanisms of spatial location choice and discrete choice models.

For our model, we perform the following procedure on the basis of a grid of cells or raster map (in GIS terminology). To calculate the expected utility of converting LU of a cell, we assume that an undeveloped land cell can transform into three development categories: residential, commercial, and industrial. The potential LU change of a cell to one of these three types is a function of five factors:

- Minimum distance to major roads (based on chessboard distance). Major roads are highways, and collector roads. Normalized after dividing by the maximum.
- Minimum distance to all roads (based on chessboard distance). Normalized after dividing by the maximum.
- Proportion of residential or commercial developed land around the target cell. Normalized after dividing by maximum which is the size of neighborhood used for analysis.
- Proportion of industrial developed land around target cell. Normalized after dividing by maximum which is the size of neighborhood used for analysis.
- Population density calculated as population in a circle of given radius centered on the target cell. The search radius operates on raster map produced from census data. Normalized after dividing by maximum.

In addition we consider natural impediment (e.g., floodplain) or legal impediment (e.g., federal or state protected land) to development. In this case the potential change assumes a value of 0.

The factors are denoted by *X*i, *i*=1, 5 and are summarized in Table 4.1. To calculate these factors we wrote routines in the C programming language.

Table 4.1

Input Factors for Potential Development Model that are Used to Create Potential Development Maps

Input Factors	**Description**
*X*1	Chessboard distance to major roads
*X*2	Chessboard distance to all roads
*X*3	Proportion of residential/commercial developed land around a target cell
*X*4	Proportion of industrial developed land around a target cell
*X*5	Population density within a specified radius around the parcel

Define the potential utility *Yi* to change LU to one of the three development types (*i*=1, residential, *i*=2 commercial, and *i*=3 industrial).The potential LU change functions were designed as follows

$$Yi = \sum_{j=1}^{5} w_{ij} \times f_{ij}(Xj)$$

i = 1..., 3 to reflect potential change as a function of all five factors *j*=1,…,5. This is a weighted average of five single variable functions (one for each of the five input factors) with coefficients w_{ij}. We assume that all five functions are equally important and therefore the weights w_{ij} were all set to 1/5=0.2. The Y_i values are viewed as the market's evaluation of the potential utility of the land for the respective type of development. The development utilities – *Y1*, *Y2*, and *Y3* are the first step to determine that a cell will become a residential, commercial or industrial. Later we

will describe how they combine into development potential probabilities, but first let's define the functions f_{ij}.

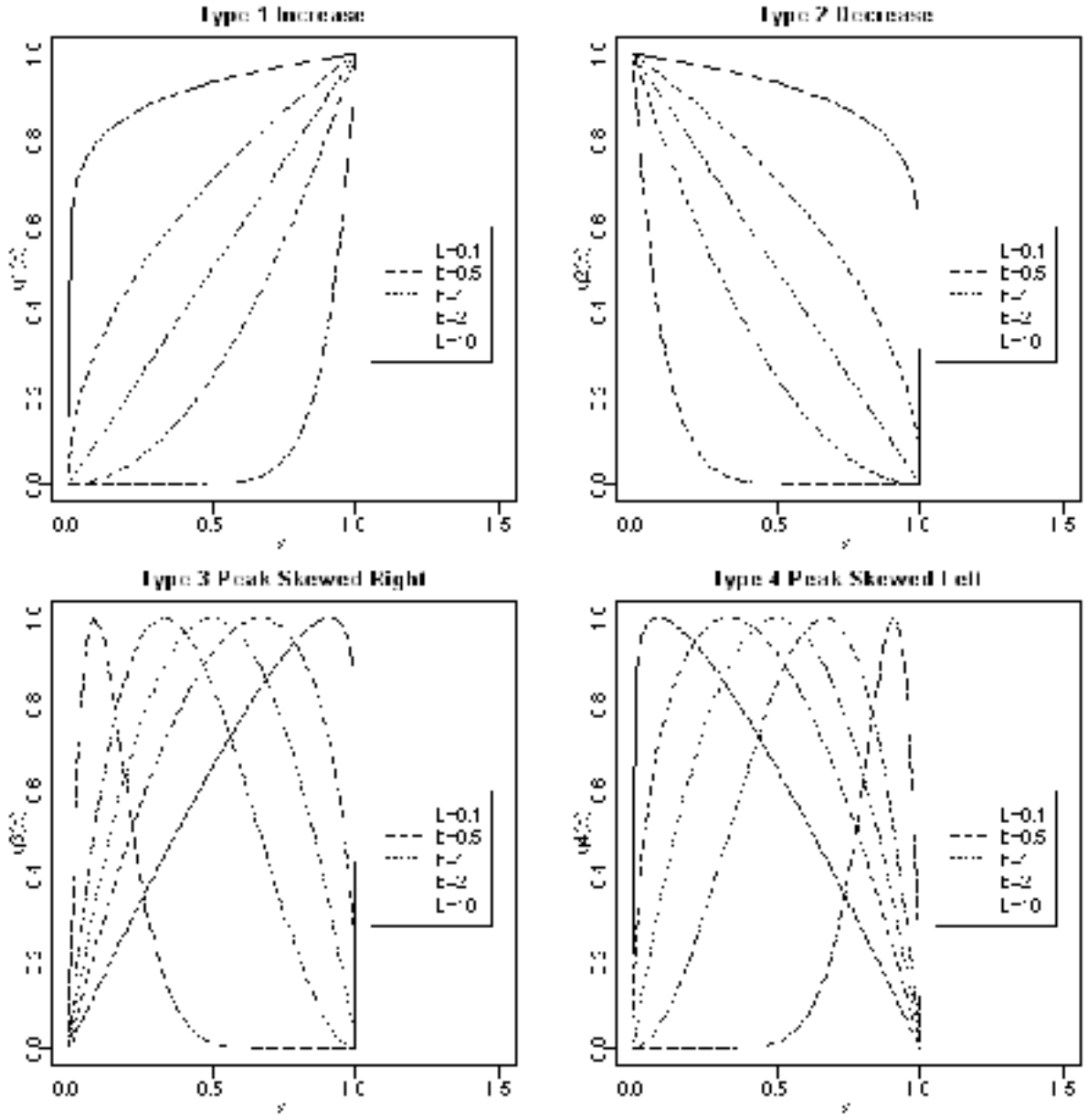

Figure 4.1. Function repertoire.

We need a set of $3\times5 = 15$ f_{ij} functions. Each one was selected from a repertoire of four functions with only one parameter b that were properly scaled. These are: an increasing function $g_1(x) = x^b$, a decreasing function $g_2(x) = (1-x)^b$, a peak skewed to the right, s is height

of peak for scaling $g_3(x) = x(1-x)^b / s$, a peak skewed to the left, where s is height of peak for scaling $g_4(x) = x^b(1-x)/s$. For example, with the set of values 0.1, 0.5, 1.0, 2.0, and 10.00, for parameter b we obtained the function behavior shown in Figure 4.1. Here we used the maximum value $s = b^b/(1+b)^{(1+b)}$ for scaling of g_3 and g_4.

We selected a set of b values and g type for each development type potential utility function *fij* as shown in Table 4.2.

Table 4.2

Functions and Parameters Selected

	g type function, and b value				
*Y*1	g_3, b=0.5	g_2, b=2.0	g_1, b=2.0	g_2, b=10	g_3, b=0.5
*Y*2	g_2, b=2.0	g_2, b=2.0	g_1, b=10	g_2, b=1.0	g_1, b=0.2
*Y*3	g_2, b=2.0	g_2, b=1.0	g_2, b=10	g_1, b=0.5	g_2, b=2.0

The thought processes behind this model are illustrated by Figures 4.2-4.3. Figure 4.2 exhibits the effect of five factors on residential development using these functions and parameter values. The first graph shows higher potential to change to residential areas when cells are mid-distant from the major roads (*X*1) and lower for both small and large distances. The second graph expresses the concept that potential to change to residential areas decreases with increasing distance to all roads (*X*2). The third graph shows higher potential to change to residential areas for areas with higher density of residential and commercial areas (*X*3). In the fourth graph, potential to change to residential areas decreases sharply with increase in proportion of industrial areas. In the fifth graph, potential to change to residential areas increases with population (*X*5) but decreases if the population continues to grow above 0.6%.

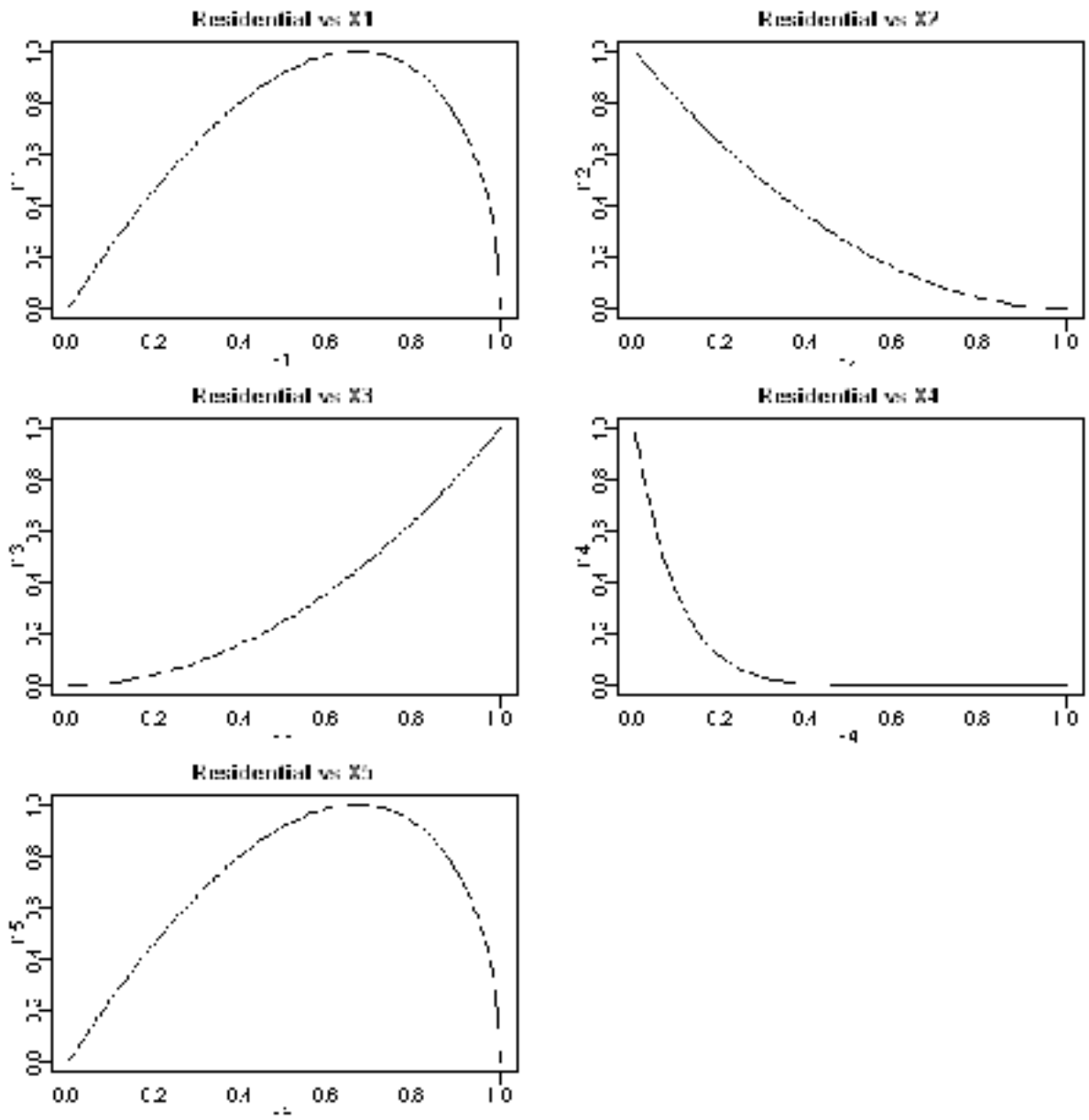

Figure 4.2. Effects on residential.

Potential to develop to commercial areas is shown in Figure 4.3. The first and second graph show a decrease with increasing distance to major roads (*X*1) as well as distance to all roads (*X*2). However, this potential will increase sharply for larger proportion of residential areas (*X*3, third graph) but decreases linearly with proportion of industrial developments (*X*4). Potential to develop to commercial areas increases rapidly with population density (*X*5).

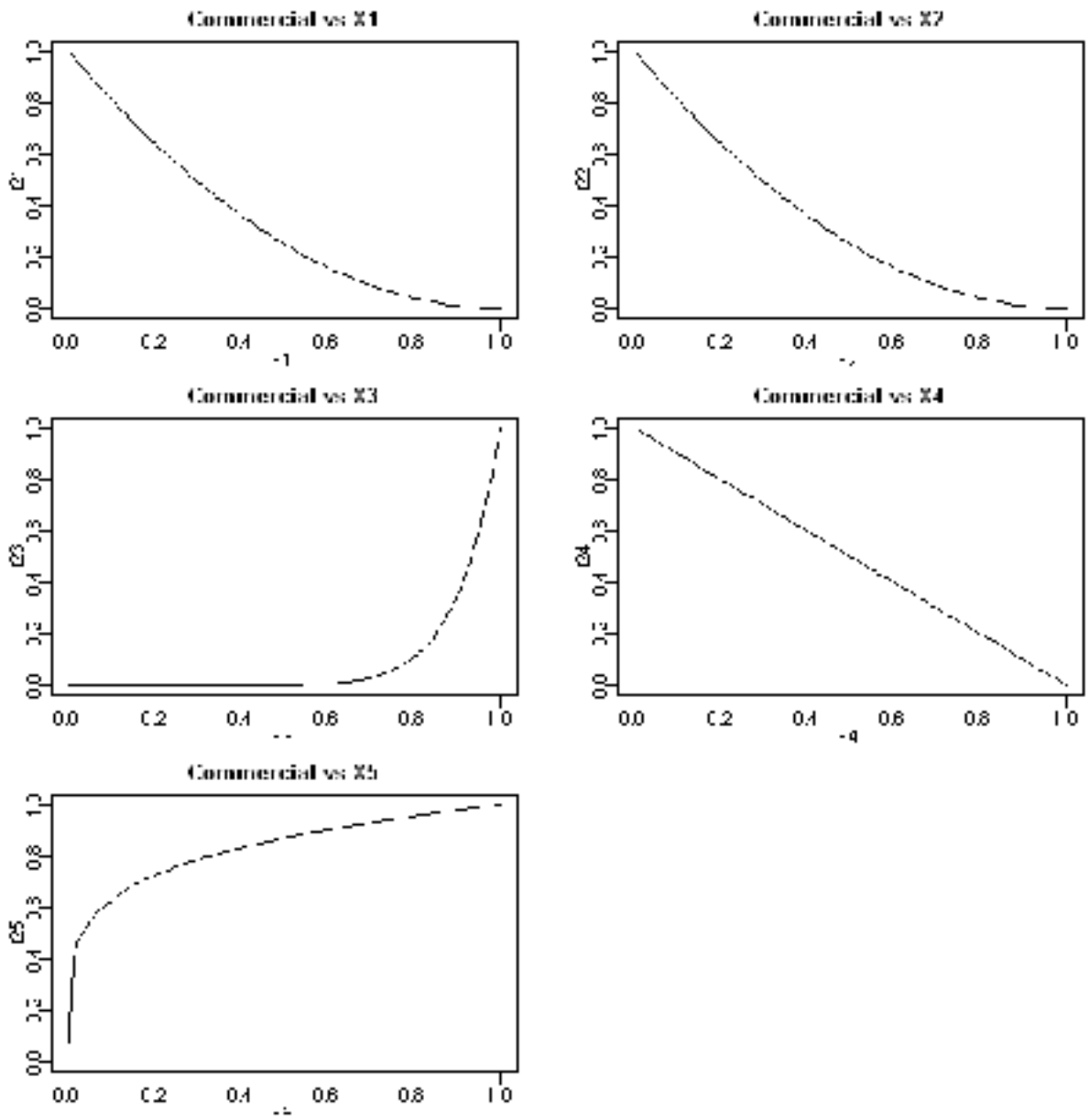

Figure 4.3. Effect on commercial.

Potential to develop to industrial areas is shown in Figure 4.4. The first and second graph show a decrease with increasing distance to major roads (*X*1) as well as distance to all roads (*X*2). But, the decrease with respect to *X*2 is linear. This potential will decrease sharply for smaller proportion of residential areas (*X*3, third graph) but increases with proportion of

industrial developments (*X*4). Potential to develop to commercial areas decreases with increase in population density (*X*5).

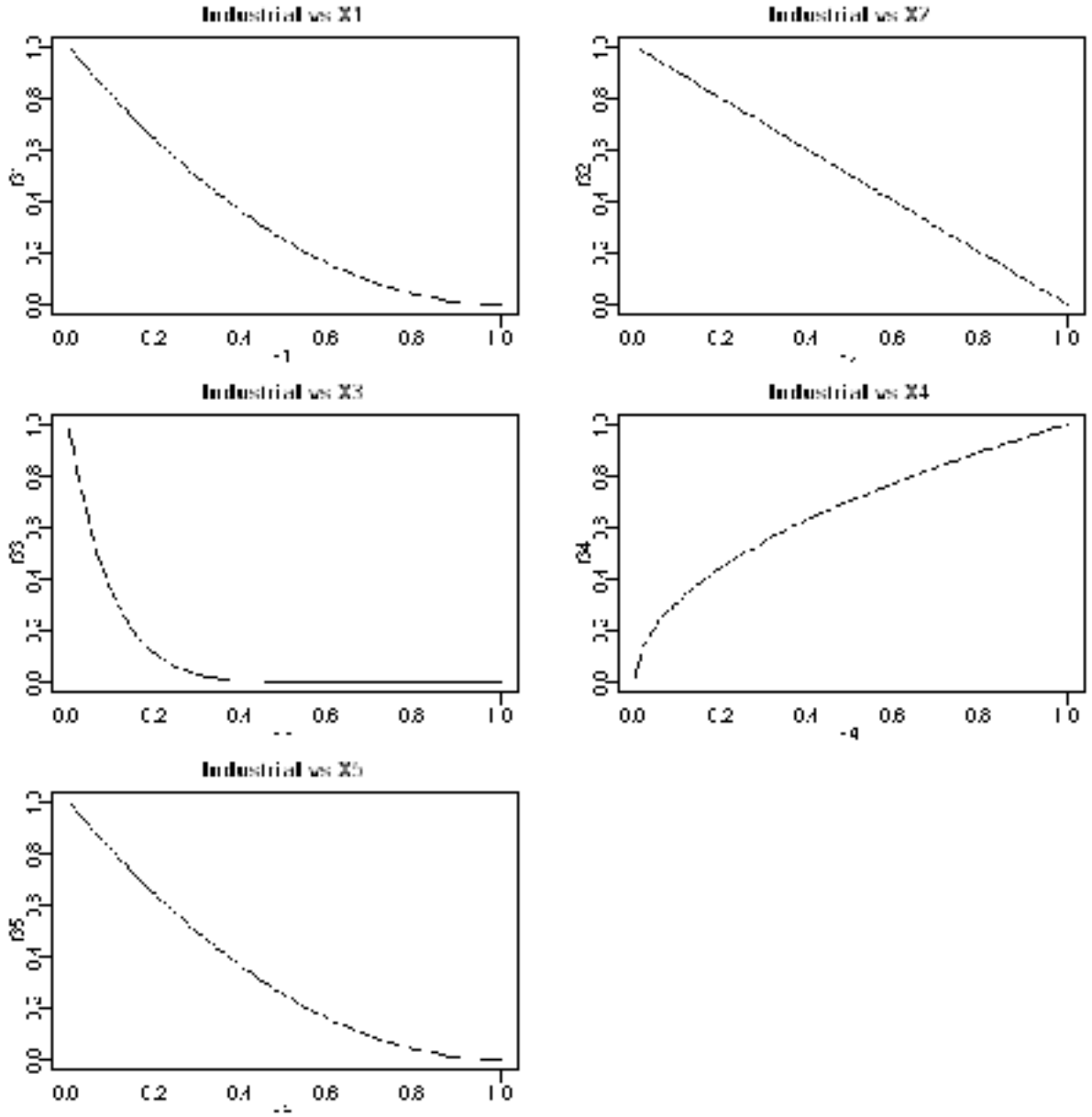

Figure 4.4. Effects on industrial.

The potentials *Y*1, *Y*2, *Y*3 were combined into development potential probabilities or development utilities based on notions from discrete choice theory. We denoted the probability that some type of development will occur on the cell as *P*(*D*). It is set to 0 if there is a natural

(e.g., floodplain) or legal (e.g., federal or state protected land) impediment. Otherwise $P(D)$ is given by

$$P(D) = 1 - \exp(-\delta Y_M)$$

where $Y_M = \max\{Y_1, Y_2, Y_3\}$. Y_M gives the highest utility for the cell's development, and the parameter δ represent the overall desirability of developing land in the region as a whole. Low values of δ produce low probabilities for development even with favorable physical properties of the land. Thus, low δ values represent a region with low economic growth. While high δ values provide higher probabilities of development, even for moderate utility values. It also suggests or represents regions experiencing strong economic growth. The δ value around 2 produced reasonable results for the range of *Y*i values used ($0 \le Y_i \le 1$, for each *i*).

Now, we define the probabilities of development for each LU type as

$$P(R) = P(R \cap D) = P(R \mid D) \times P(D)$$

$$P(C) = P(C \cap D) = P(C \mid D) \times P(D)$$

$$P(I) = P(I \cap D) = P(I \mid D) \times P(D)$$

for residential, commercial, and industrial, respectively. Here, the conditional probabilities for each development type are given by

$$P(R \mid D) = \frac{\exp(\beta Y_1)}{\exp(\beta Y_1) + \exp(\beta Y_2) + \exp(\beta Y_3)}$$

$$P(C \mid D) = \frac{\exp(\beta Y_2)}{\exp(\beta Y_1) + \exp(\beta Y_2) + \exp(\beta Y_3)}$$

$$P(I \mid D) = \frac{\exp(\beta Y_3)}{\exp(\beta Y_1) + \exp(\beta Y_2) + \exp(\beta Y_3)}$$

The parameter β is the developer market's ability to distinguish the relative suitability or utility of the different types of development given that the parcel will develop. Parameter β increases when the probability of development type with the largest utility increase to 1. Parameter β decreases when the development probabilities tend to be equally likely i.e. the market makes little distinction between the suitability of different development types. A value of β around 2 to 3 produced reasonable results for the range of *Yi* values used ($0 \le Y_i \le 1$, for each i).

Data Acquisition for Constructing Input Factors

In this section we describe our methods of data acquisition required for the input factors. To apply the model just described we created maps for the five *X*i factors (Table 4.1) using and several data sources (Table 4.3), Geographic Information Systems (GIS), and the routines written in the C programming language. Model input files were ESRI ASCII grid text files which were generated from raster data or from vector data after conversion to raster. The model also produces ESRI ASCII grid text files that are converted to raster for map display using ESRI's ArcMap.

Table 4.3

Data Acquisition Sources

Raw Data	Source	Data Type
Roads/Streets	www.tnris.state.tx.us	Vector (ESRI shapefiles)
Population	www.census.gov	Tables and vector (ESRI shapefiles)
NLCD 1992	www.mrlc.gov/ http://seamless.usgs.gov/website/seamless/viewer.php	Land cover map (raster)
Parcel data	Hardin County Appraisal District	CAD drawings

Roads and Streets Data ($X1$ and $X2$ Factors)

We downloaded road data from the website mentioned in Table 4.3. The data contained both major highways and residential streets (minor roads). In order to calculate chessboard distance to the major roads, we need a separate file containing major roads. To do this, we used 'Select by Attribute' function from ArcGIS to tease out major roads from the road data. We selected major roads such as interstates, freeways and highways and created a separate shapefile and converted the shapefile to raster. We used a conditional statement to select roads only and made the road cells bigger to ensure only the roads are selected. We applied the same procedure for minor roads.

Then we converted both road rasters to ASCII text files to be used for the C program **roaddist.c** to calculate $X1$ and $X2$ factors using the command

roaddist.exe <input_ASCII_grid> <output_ASCII_grid>

The function was based on chessboard distance. It assumes that one moves on the pixel grid as if a king were making moves in chess, i.e. a diagonal move counts the same as a horizontal move. The metric is given by: D = max (|x2-x1|, |y2-y1|. For our application where speed is more important than accuracy, chessboard distance has an advantage over Euclidean distance. The output is ASCII files of $X1$and $X2$ factors that represented chessboard distance to major roads and combined (major and minor) roads respectively and are converted to raster for visual display (Figure 4.5). On the raster maps, the value of 1 indicated areas further away from roads that are highly suitable for development and areas closer to the both roads are less suitable and are indicated by lower values.

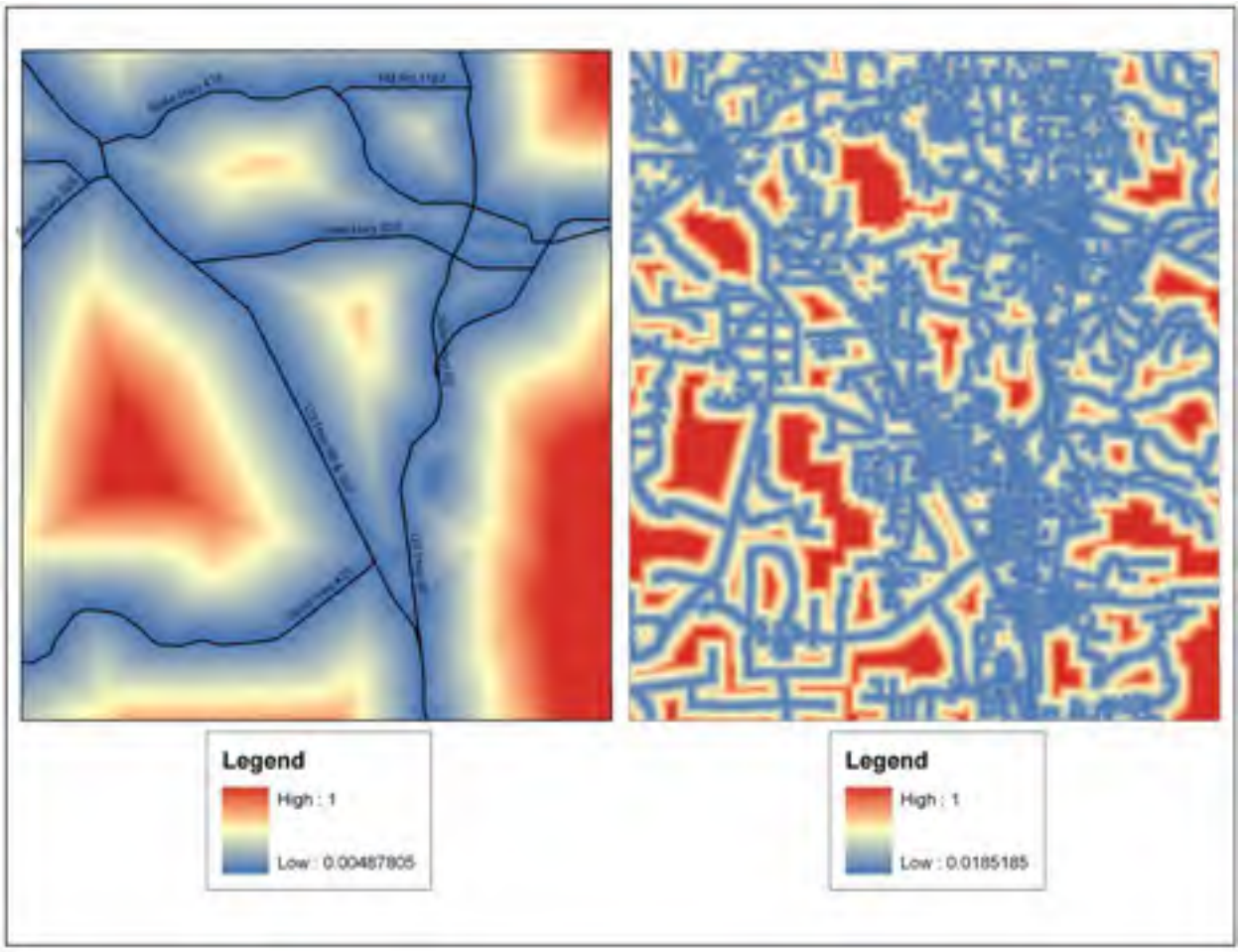

Figure 4.5. X1 and X2 factors.

National Land Cover Dataset (NLCD, 1992/2001) (*X*3 and *X*4 Factors)

The National Land Cover Data (NLCD) is produced by the U.S. Geological Survey (USGS) in collaboration with U.S. Environmental Protection Agency. The NLCD is a component of USGS Land Cover Characterization Program and is produced from 1992 Landsat Thematic Mapper imagery. The seamless NLCD contains 21 categories of land cover information suitable for a variety of State and regional applications, including landscape analysis, land management, and modeling nutrient and pesticide runoff. The data classification system key is given in Table 4.4. Among the categories, 21, 22 and 23 indicate already

developed areas where occurrence of future development is minimal. These areas were selected to produce *X*3 and *X*4 factors. Recall that *X*3 represent proportion of residentially developed lands and *X*4 represent proportion of industrially and commercially developed lands.

Table 4.4

NLCD Classification Schemes (Level II)

Land Cover Description	**Value**	**Land Cover Description**	**Value**
Open water	11	Grassland/Herbaceous	71
Low Intensity Residential	21	Pasture/Hay	81
High Intensity Residential	22	Row Crops	82
Commercial/Industrial/Transportation	23	Small Grains	83
Bare Rock/Sand/Clay	31	Urban/Recreational Grasses	85
Deciduous Forest	41	Woody Wetlands	91
Evergreen Forest	42	Emergent Herb Wetlands	92
Mixed Forest	43	Shrubland	51

First, we reclassified the land cover map to residential and commercial/industrial maps. Areas that contained existing developed lands received a value of 1 and the rest 0. This was done to ensure the exclusion of developed raster cells in the final calculation. However, the development potential model designates *X*3 and *X*4 as proportion of residential or commercial development and the proportion of industrial development respectively. And we followed NLCD classification system to extract already developed areas. Second, we converted the classified maps to ASCII text file and the C program **useprop.c** was ran with each file using the command

useprops.exe <input_ASCII_grid> <output_ASCII_grid> <window size>

The above program calculates proportions of developed land around a target cell using a moving window of given size. In our case, we selected a 7 x7 window. For example, for a total of 49 pixels in the neighborhood size of 7 x 7, if we have 40 pixels that are already developed then 40/49 = 0.81 or 81%. In other words, 81% of the neighborhood is already developed making it less desirable for future development. On the other hand, if 5/49 is developed i.e. only 10% of the neighborhood is developed making it highly desirable for future development. This way, the procedure produced two maps that contained proportion of developed lands from commercial, industrial and residential activities as shown in Figure 4.6.

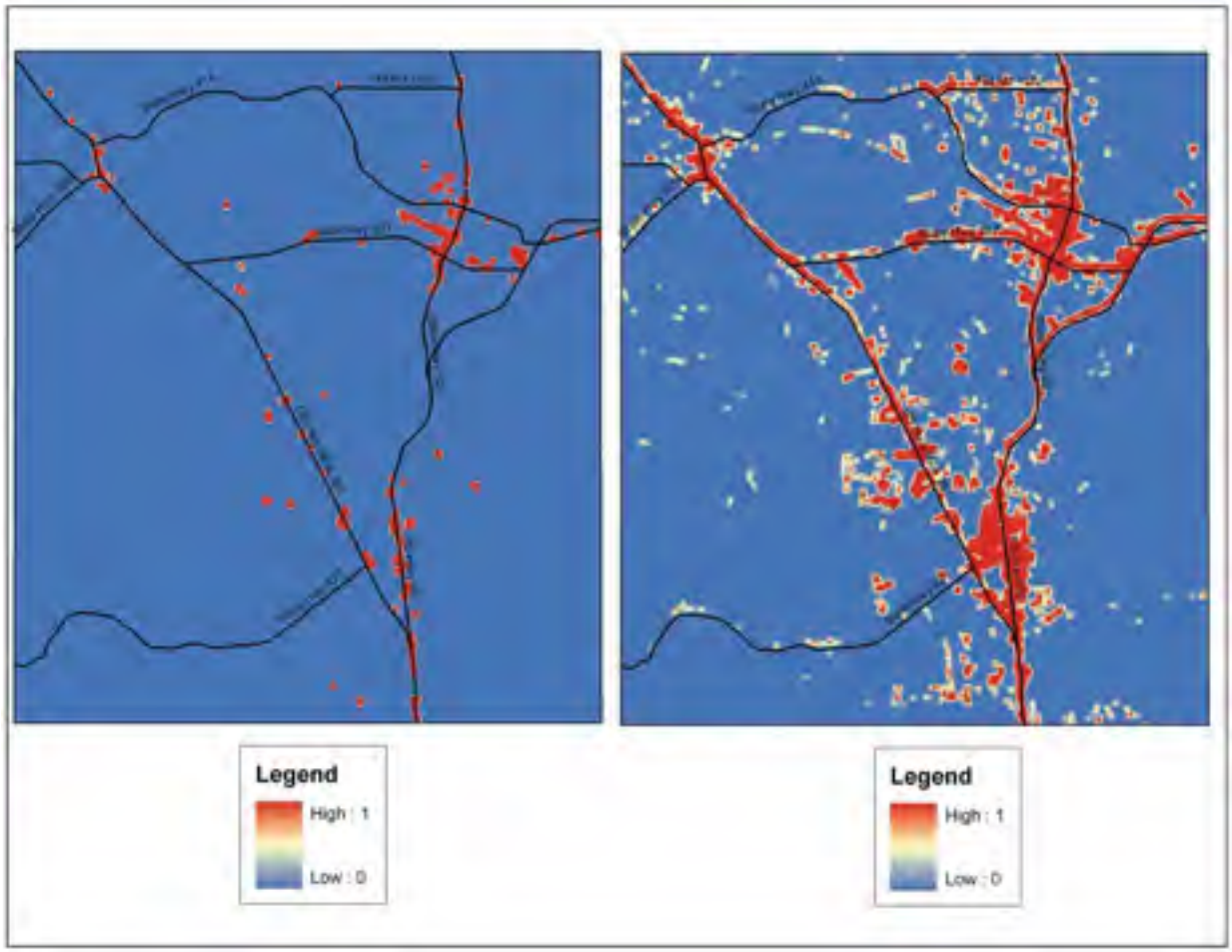

Figure 4.6. X3 and X4 factor.

Population Data (*X*5 Factor)

We downloaded the census data that contains demographic information collected by United States Census Bureau (USCB). However, the data is selected according to the requirement of the study, i.e. whether we are trying to find the population density of a block, block group or a tract. A block is the smallest geographical unit used by USCB for a population density followed by a block group and tract. For our study, we selected block unit to meet our objectives because we were interested in knowing the population density in each parcel polygon. We imported census block data to excel and saved in database format so it can be imported to ArcMap for further analysis. We also downloaded census block shapefiles that contains information of a block such as streets etc. However, in order to join census block shapefiles and census block data; we needed a column with similar field type. A field is a column in a table that stores the values for a single attribute. And field data type is the attribute of a variable. The field or column in a table determines the kind of data it can store and common data types include text, character, integer, decimal, single, double and string. The attribute table of census block shapefile had a column named 'BLOCK' that contained four numbers and we needed a column in census block data table with similar field types and numbers. We created a new field with text field type in the census block .dbf table and named it 'NEW_BLOCK' to match the column 'BLOCK' of the census block shapefile table. This field was used to join the tables and we created two additional fields to hold values of area and population density (population/area) for each polygon in the census attribute table. We selected float and double field types for population density and area columns respectively, square miles as units for area to calculate population density for individual polygons, and population density column to convert the polygon shapefile. This raster was then converted to ASCII text file that in turn was used in the

popdense.c routine of the potential development model. We calculated the population density factor (*X*5) as a population in a circle of given radius of 2.5 km to 3 km or using a moving window of 7 x 7. The search radius operates on a raster map produced from census block data.

popdense.exe <input_ASCII_grid> <output_ASCII_grid> <window size>

The output population density factor was converted to raster for display as shown in Figure 4.7.

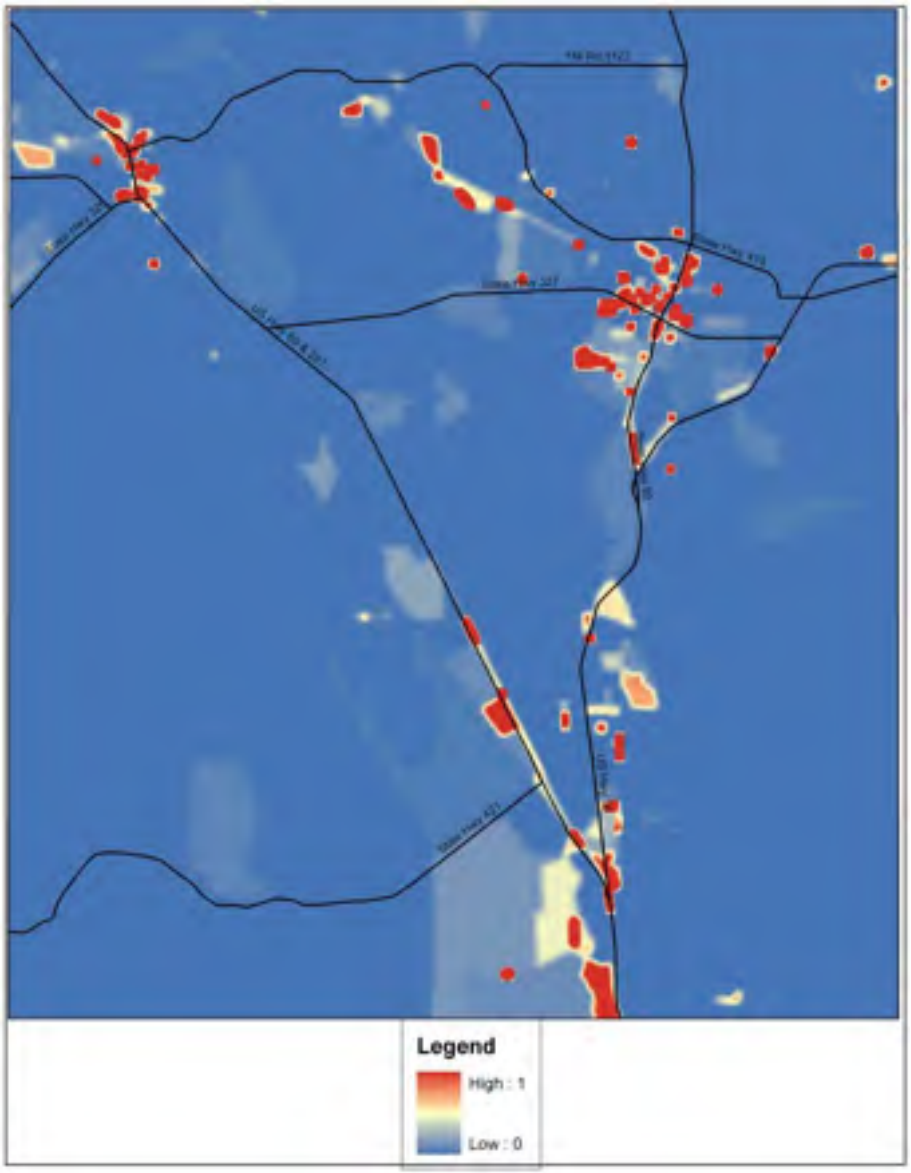

Figure 4.7. X5 factor.

Potential Development Probabilities

Each factor *X*i is normalized by dividing into its maximum to ensure a common scale of 0 to 1. In addition, it was necessary to ensure the five ASCII files contained equal amount of rows and columns. In order to do this, we worked with a larger dataset from the start and after constructing the factor files; we clipped the five ASCII files using the study area polygon. This procedure yielded ASCII files with equal number of rows and columns. Then we executed the development model **devpot.c** to derive maps of four development probabilities, P(R), P(C), P(I), and P(D), i.e. residential, commercial, industrial, and total. The model was executed with the command

devpot.exe <X1> <X2> <X3> <X4> <X5> <o1> <o2> <o3> <o4>

The output is four ASCII grid text files that are denoted by o1, o2, o3, o4 that represents residential, commercial, industrial and total potential development probabilities respectively and are converted to raster for visual display (Figure 4.8). The total potential development map indicates areas for all the three types of development i.e. residential, commercial and industrial development.

Potential Development at the Parcel Level

Visually, the potential development maps provided an effective method to find areas of particular developments i.e. commercial, residential, industrial and total. However, in our case, we wanted to know the probability of individual parcels, i.e. which parcel will likely develop into a particular development type? In order to achieve this, we needed parcel data of the study region to overlay with the potential development maps. As stated above, a typical parcel data contains information such as parcel id, owner id and other attributes.

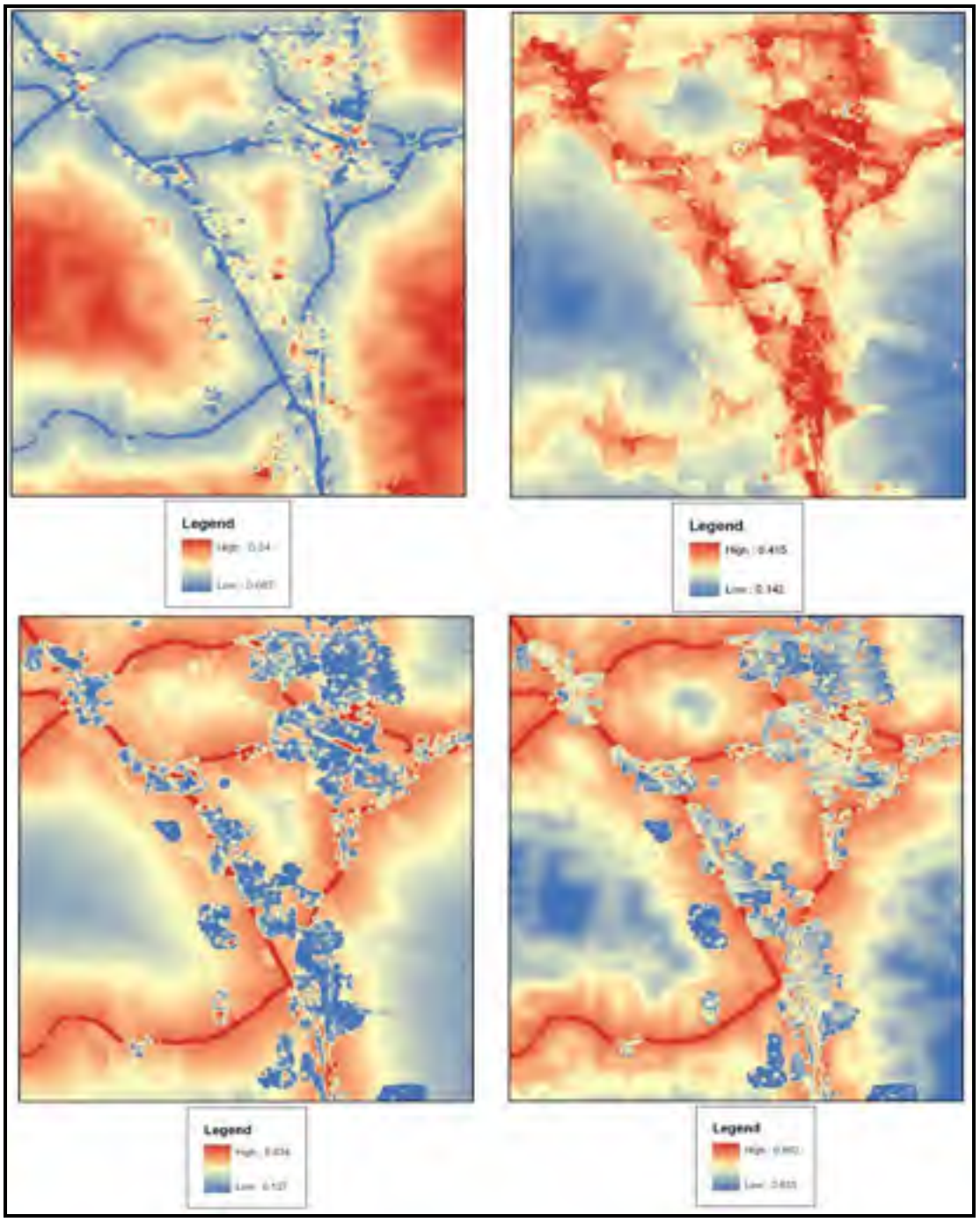

Figure 4.8. Potential development probabilities: a) residential b) commercial c) industrial, and d) total.

However, for Hardin County, there were no such data available. We used CAD polyline to create parcel polygons in GIS instead. This procedure provided a skeleton of parcel polygons suitable for our intended objectives. We examined the attribute table of these parcel polygons – it had

three columns: ‘FID’, ‘shape’ and ‘id’. FID contains numerical number of the parcels, polygons for the shape and the id column was filled with 0s.

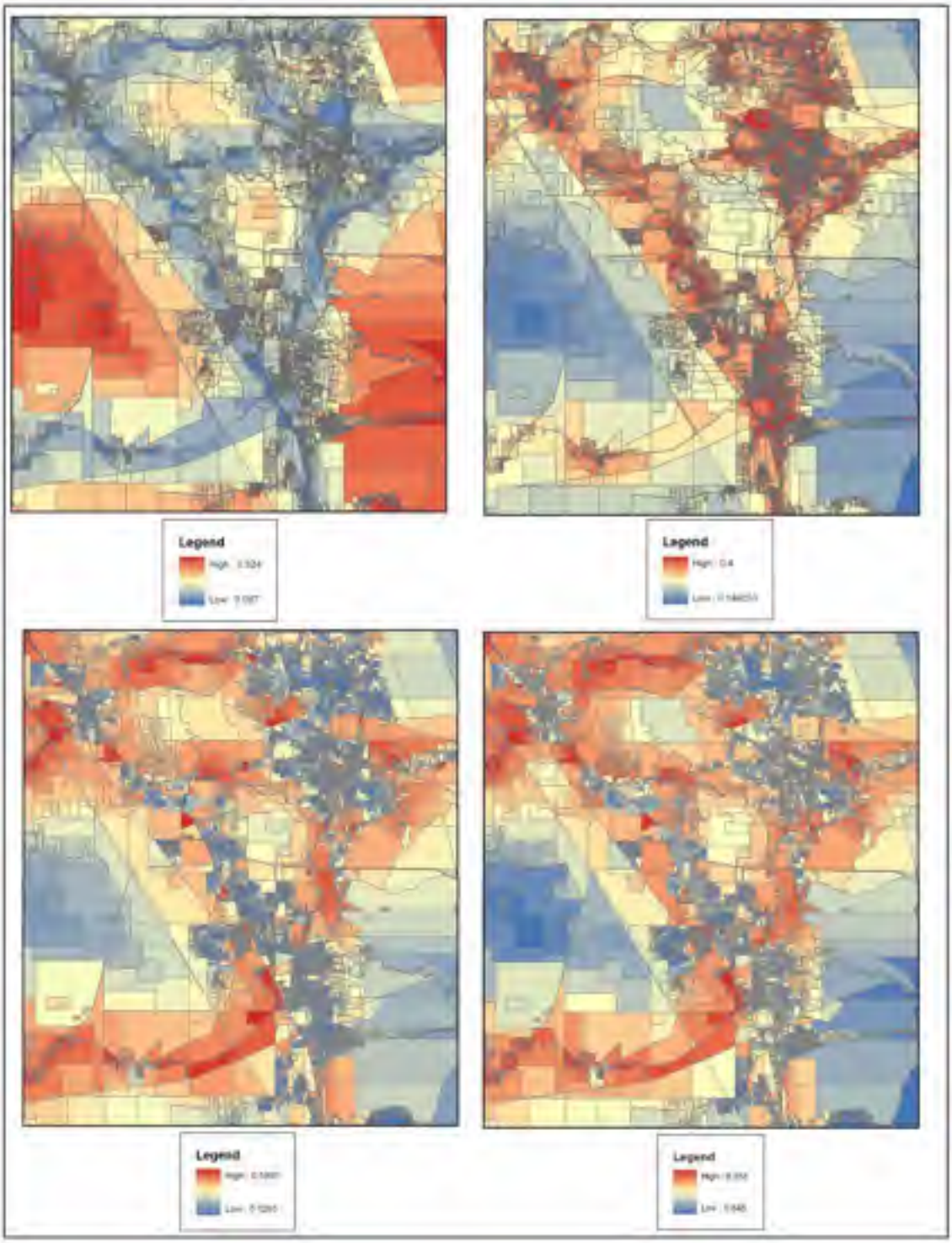

Figure 4.9. Potential development probabilities at parcel level a) residential b) commercial c) industrial and d) total.

We cannot use FID for overlay since it is linked to the shapefile geometry and is automatically created or updated when a new feature is added. Therefore, we used data from FID column to populate 'id' column by using the field calculator from the attribute table. Then we used the newly populated id column as a zone and the potential development rasters as input values. Each cell in the raster contains values from 0 to 1. The zonal statistic function calculates the mean of the pixel values for individual zones i.e. parcel. We overlaid the parcel polygons with the four types of development maps. This way, we calculated mean value for individual parcel that range from 0 – 1. Values closer to 1 indicate higher probability for the parcels to become developed. The resultant map showed the probability of each parcel for a particular type of development at the parcel level (Figure 4.9).

Development in the Red-Cockaded Woodpecker Habitat

After the LU change predictions are made, the habitat for red-cockaded woodpecker is analyzed as in Chapter 3 with a conjunction of remote sensing and FRAGSTATS. We used our previously classified image, neighborhood statistics and landscape metrics to calculate amount of potentially suitable red-cockaded woodpecker habitat in the study region (the calculation of neighborhood and landscape metrics is explained in detail in Chapter 3). The classified image contained seven categories of land cover including pine trees. We reclassified this image to derive a binary image. The pine tree category received a value of 1 and the rest of the land cover classes got 0. As before, we conducted neighborhood analysis in a 23x23 set. This way, a habitat suitability index map was obtained that indicated areas of potential suitable habitat areas along with two other habitat types (highly unsuitable and suitable habitat types) before any sort of

development – this is our first map. In other words, this first map contained the original extent of three habitat types prior to potential development.

Then we created maps of what the habitat would be like after the hypothetical development. For this we generated scenarios at different levels of likelihood of development. In order to create these maps, we employed the following steps: 1) selected thresholds of total probability of development, $P(D)$, to define the scenarios, 2) for each scenario, selected areas above the threshold in the total potential development maps and gave these cells the value 0, and 3) multiplied these new maps with the binary pine tree map to derive areas of pine trees that were left undeveloped.

We selected threshold values of 0.70, 0.75 and 0.80 because the total potential development map had values ranging from 0.55 to 0.86 (Figure 4.8). We used a conditional statement to assign 0 to areas above the designated threshold. As a result of Step 2 of the above procedure, we obtained three maps (one for each scenario) that had areas removed from the habitat due to development and contained remaining undeveloped areas. Once we multiplied each one of these maps with the binary pine tree map, we obtained three maps that showed areas of either remaining pine trees or no trees. In other words, the resulting maps contained areas from which we could calculate remnants of three habitat types after development. Next, we conducted neighborhood statistics on this new map and calculated landscape metrics. Then we calculated differences between the original and the remaining habitat areas but we focused mainly on the amount of potentially suitable habitat.

The resultant maps had different maximum values. For example, the maximum values for the original binary and 80% threshold maps were 0.89 while it was 0.82 for 70 and 75% threshold maps. The results for 80% development probability indicate that most development

occurs near the highways and does not affect the maximum value of habitat suitability (Figure 4.8). For 70 and 75% thresholds, pixels that had high values are removed and pixels with 0.82 become the highest. In Chapter 3, we used nominal breaks of 0-0.333, 0.333-0.666 and 0.666-1 to reclassify the 9 classes to three using equal interval classification method (please refer to Chapter 3 for full details).

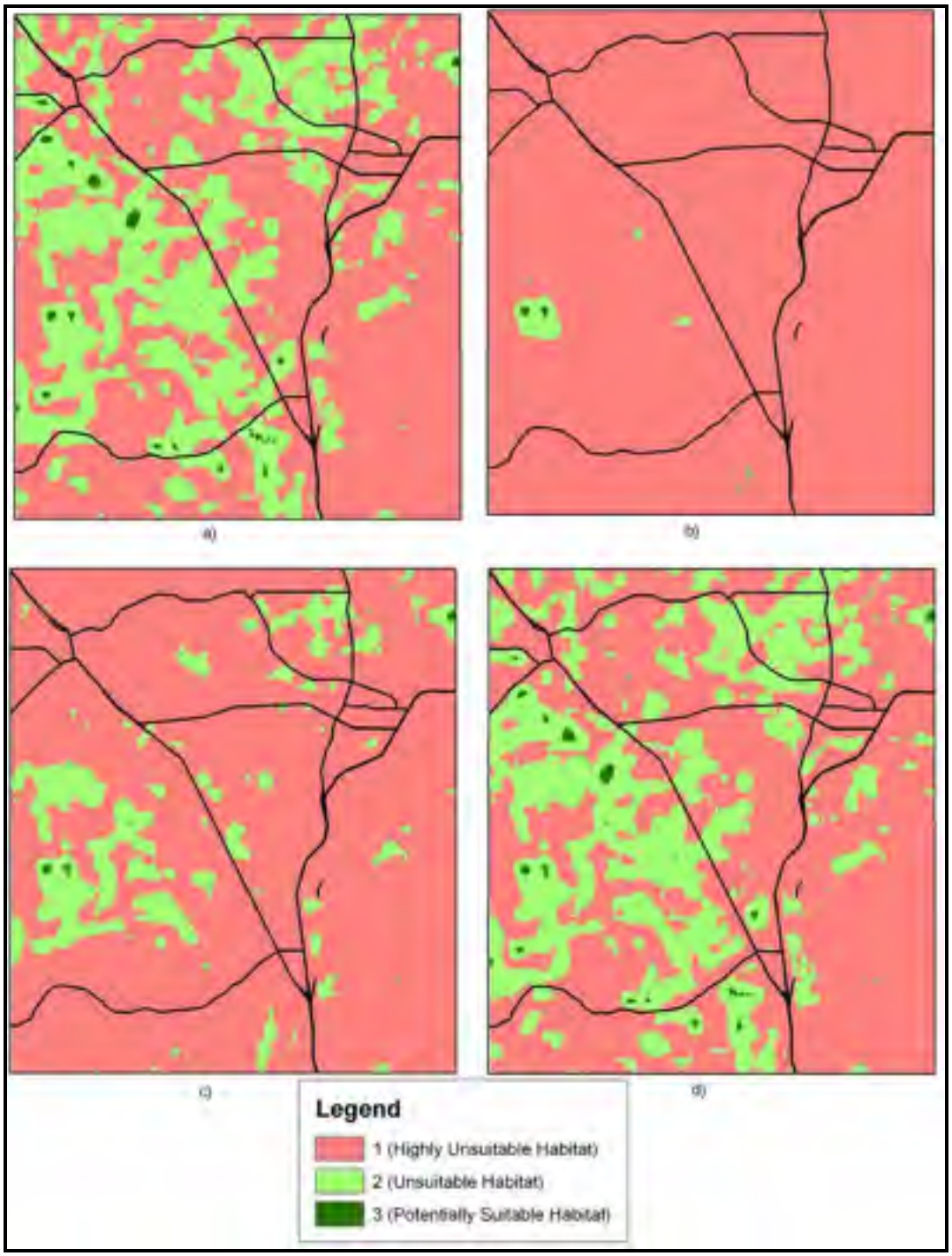

Figure 4.10. Four scenarios of potentially suitable habitat change (a) Before development (b) Probability of development≥70% c) Probability of development ≥75% and d) Probability of development≥ 80 %.

To maintain consistency, we used similar breaks for the four maps and reclassified the nine classes of the four resultant neighborhood maps to derive three classes that represented: 1) very

unsuitable, 2) unsuitable, and 3) potentially suitable habitat. We labeled the reclassified classes obtained from the four maps to 1, 2, and 3 habitat types for comparison (Figure 4.10). Then we conducted FRAGSTATS analysis on all four maps and calculated the difference in the amount of habitat (Table 4.5 to Table 4.6).

Table 4.5

Number of Pixels that Belonged to the Three Habitat Types for Each Threshold

Description	Habitat type	Number of pixels
Neighborhood analysis of current extent of habitat	Very unsuitable	384033
	Unsuitable	194933
	Potentially suitable	2944
Neighborhood analysis for more than 70% development	Very unsuitable	576990
	Unsuitable	4588
	Potentially suitable	332
Neighborhood analysis for more than 75% development	Very unsuitable	518731
	Unsuitable	62611
	Potentially suitable	568
Neighborhood analysis for more than 80% development	Very unsuitable	393441
	Unsuitable	185769
	Potentially suitable	2700

Table 4.6

Class Metric Results for Current Situation – Before Any Further Development

TYPE	CA/TA	PLAND	NP	LPI	COHESION
1	34562.97	65.99	153	59.32	99.92
2	17543.97	33.5	232	18.02	99.55
3	264.96	0.5	27	0.09	92.04

In addition, we used the map of total potential development probabilities at parcel level to calculate the habitat amounts for the four scenarios mentioned above (Figure 4.11). Interestingly, the results or the habitat amounts looked similar with minute changes in the shape of the patches. We did observe rough edges of the parcels when we first removed the pixels with different thresholds and disappeared when we ran the neighborhood statistics.

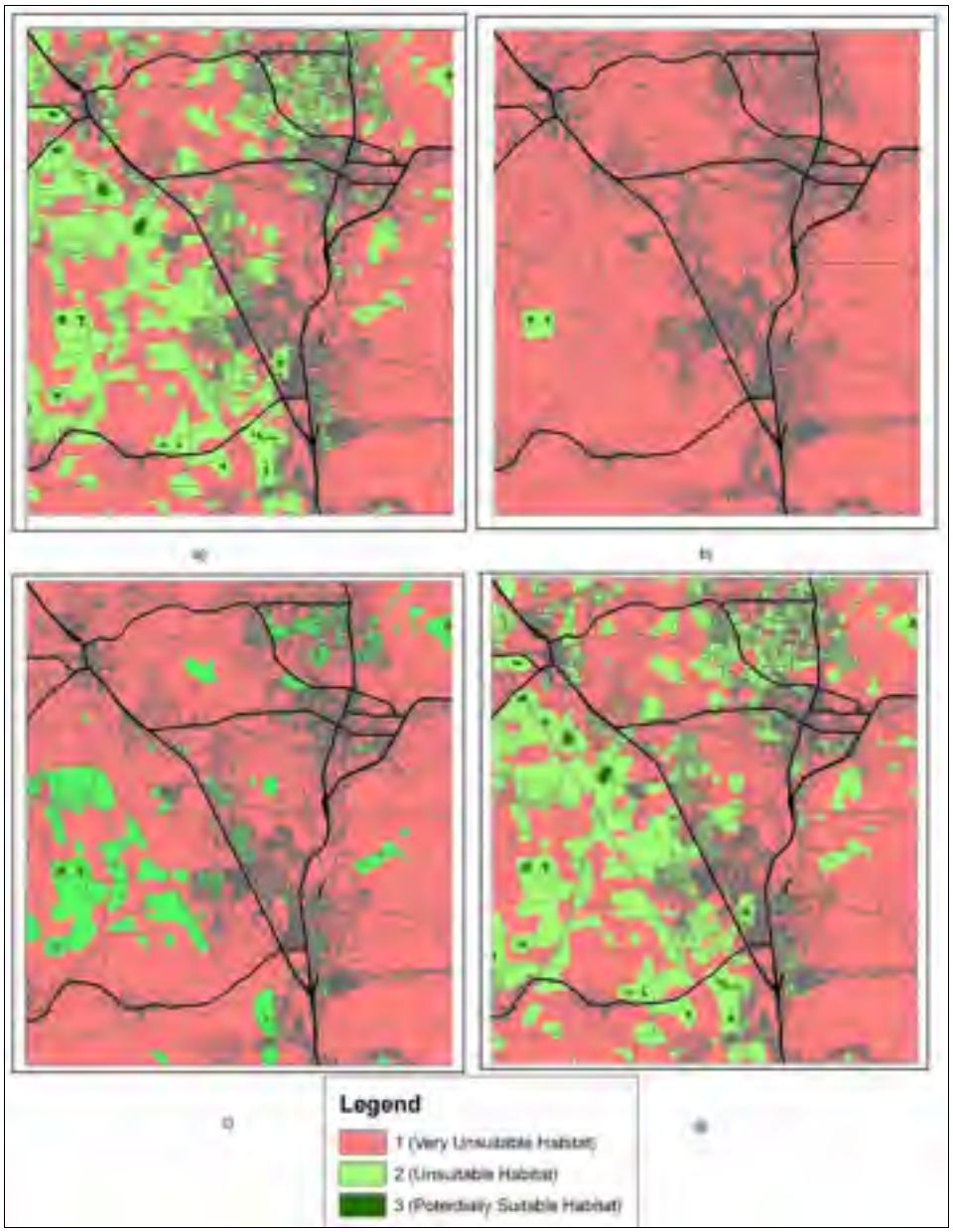

Figure 4.11. Four scenarios of potentially suitable habitat change at parcel level (a) Before development (b) Probability of development≥70% c) Probability of development≥75% and d) Probability of development≥ 80 %.

Results

Data Preparation

We used GIS to create input variables or the five factors and parcel data. Even though, the data were readily available on the web, they required extensive polishing prior to use in the potential development model. For example, we converted coordinate system to WGS 1984 of the entire data set so they would project correctly on the ArcMap, and teased major roads from the combined roads. In addition, we constantly updated road data as there were new roads or intersections being constructed during the course of the project that are still being constructed. For NLCD, we selected 1992 classification system.

The classification schema facilitated selection of already developed lands required for the model. Population data required extensive preparation before it was used for the model. We used excel to create text that was imported to Arc Catalog to convert it to database format file. ArcMap only recognizes the latter file. And for the parcels, we used CAD and converted it to polygons. We used the polygons as zone and the potential development rasters as inputs while calculating development probability mean for individual polygons.

Potential Development Functions

We constructed development potential models to forecast development pattern in the study area. Our results indicate that potential development models are useful in establishing possible locations of change on the landscape. We used a set of predictor variables such as proximity to major and combined roads, LU characteristics obtained from NLCD, and population density obtained from census block data.

As expected, the development probability maps display the patterns intended by the model design. For example, our results indicate commercial development will occur near the densely populated areas, i.e. near towns and close to major roads. Industrial development will occur in close proximity to highways and commercial areas but away from residential areas. Similarly, residential developments tend to occur little further away from the roads, industrial and commercial developments. These maps propose that development occurs in certain areas depending on the need and category. For example, for residential, people tend to select quiet locations away from noisy roads with low traffic volumes and less polluted environment, commercial and industrial developments require easy access to roads and a dense human population nearby to flourish.

Areas near the small towns will see growth in commercial and industrial development. Areas near highways 326, 327, 96, 69 and FM 421 will experience residential growth. Furthermore, use of parcel polygons to study the development pattern provided further ability to pinpoint where and which parcel will convert to a particular development type. These projections illustrate how a potential development model can effectively establish relationship between urbanization and the predictor variables evaluated in Hardin County.

Amount of Habitats Before and After the Development

As mentioned above we quantified the amount of habitat area before and after potential development using total potential development map both as raster and at the parcel level. We used two methods to calculate the amount of habitat: 1) pixel counts, and 2) FRAGSTATS analysis. For pixel counts, we counted the number of pixels that belonged to the three habitat types (Table 4.5). We found the number of pixels for the very unsuitable habitat increased after

the development occurred, i.e. from 384033 to 576990, 518731, and 393441, for 0.70, 0.75, and 0.80 probability scenarios respectively. The highest increase was observed when we removed pixels with more than the 0.7 threshold. And the smallest increase was observed when we removed pixels with more than the 0.8 threshold. This suggests that total development will be highest near the major roads where there was absence of potentially suitable habitats (Please refer to Fig. 4.10 d). Moreover, the increase in the number of pixels for very unsuitable habitat and decrease in the number of pixels especially for potentially suitable habitat patches from 2944 to 332, 568, and 2700, for 0.70, 0.75, and 0.80 probability scenarios respectively. This coincides with the results obtained from landscape metrics as will be discussed in the following paragraphs and pages. The greatest decrease was observed for 70% and 75% development probability.

For the second method, FRAGSTATS analysis, we created four ASCII text files from the raster files. The headers were removed from the ASCII files prior to use in the FRAGSTATS program. First, we determined the current extent of the all habitat types (full method explained in Chapter 3). It showed that, prior to development, the study area contained 265 ha of areas potentially suitable habitat in 27 patches (Table 4.6). There were few patches that contained no data and were not included in the calculation. These 27 patches were scattered across the study landscape (Figure 4.11 a) and physically disconnected, i.e. fragmented, as indicated by COHESION metrics of 92. In contrast, the same metric approaches nearly 100 for the other two habitat types suggesting they are less fragmented. Moreover, the potentially suitable habitat only occupied 0.5% of the total landscape while the other two habitat types occupied nearly half of it. After 70% development, the amount of potentially suitable habitat decreases to merely 29 ha and becomes more fragmented as indicated by COHESION metrics staying at 92 (Table 4.6).

PLAND metrics supports other metric findings – it decreases to 0.06 from 0.5 % showing a 50% decrease.

We used a threshold of 0.70 for the first scenario. The results indicated that the amount of very unsuitable habitat nearly doubles (51,929.1 from 34,562.97 ha) and that there is a drastic reduction in the unsuitable and potentially suitable habitat amounts from 17,543.97 and 265 to 412.92 and 29.88 hectares respectively (Table 4.6). Along with an increasing amount, the COHESION metric of very unsuitable habitat indicates they are still well connected with value approaching 100 (Figure 4.10b). The other two habitat types become more fragmented as indicated by COHESION metric values of 97.54 and 92.33 respectively. In addition, visual inspection indicated potentially suitable habitats are completely engulfed by the development with only about 29.88 ha remaining near Bentura and Sapp Graveyard streets (Figure 4.10b).

Table 4.7

Class Metric Results for First Scenario – More Than 70% Development Probability

TYPE	CA/TA (ha)	PLAND	NP	LPI	COHESION
1	51929.1	99.15	1	99.15	99.99
2	412.92	0.79	10	0.65	97.54
3	29.88	0.06	2	0.032	92.33

For the second scenario –75% threshold the metric results showed an increase in the amount of unsuitable habitat from 412.92 to 5634.99 ha. This sudden increase was the result of removal of pixels with values higher than 0.75 i.e. the developments are more towards the major highways. There was an increase in the amount of potentially suitable habitat types (29.88 to 51.12 ha), and the very unsuitable habitat still increases in size from 34,562.97 to 46685.79 ha.

Similar to the 70% threshold scenario, PLAND, NP, LPI and COHESION metric results showed patchiness of potentially suitable habitat (Table 4.8). Patches near highway 326, 327 and farm-market-to-road 421 highways are the most impacted (Figure 4.10c). The obvious impact was observed in the patches located near FM 421. There were two large potentially suitable habitat patches; one located south of FM 421 and Highway 96 and one located on FM 421 towards the Town of Sour Lake. These patches are completely destroyed for a 75% threshold development. Another patch near HW 327 also completely disappears (Figure 4.10c).

Table 4.8

Class Metric Results for Probability of Development Larger Than 75% – Second Scenario

TYPE	CA/TA (ha)	PLAND	NP	LPI	COHESION
1	46685.79	89.14	27	89.09	99.99
2	5634.99	10.76	128	3.14	98.28
3	51.12	0.1	6	0.03	91.74

Under the third scenario – when the area is under more than 80% development, there are minimal changes in its spatial pattern of the three habitat types. The composition and the configuration remain mostly unchanged. For example, the patch number for potentially suitable habitat merely changes from 27 to 28. However, the amount changes from 265 to 243 ha and is reflected by changes in PLAND and LPI metric results (Table 4.9). In other words, the current situation and third scenario produced similar results indicating most of the developments occurred near the major highways where few potentially suitable habitats exist (Figure 4.10d). In addition, these suggested existing habitats are not severely impacted. Thus, our analysis suggests that development is not further detrimental to habitat if it occurred near the highways.

Table 4.9

Class Metric Results for Probability of Development Larger Than 80% – Third Scenario

TYPE	CA/TA (ha)	PLAND	NP	LPI	COHESION
1	35409.69	67.61	142	62.12	99.93
2	16719.21	31.92	225	16.93	95.51
3	243.	0.46	28	0.09	91.45

We created a graph (Figure 4.12) to represent the amount of habitat pre- and post- development that changes according to the FRAGSTATS analysis from the previous four tables (column CA/TA).

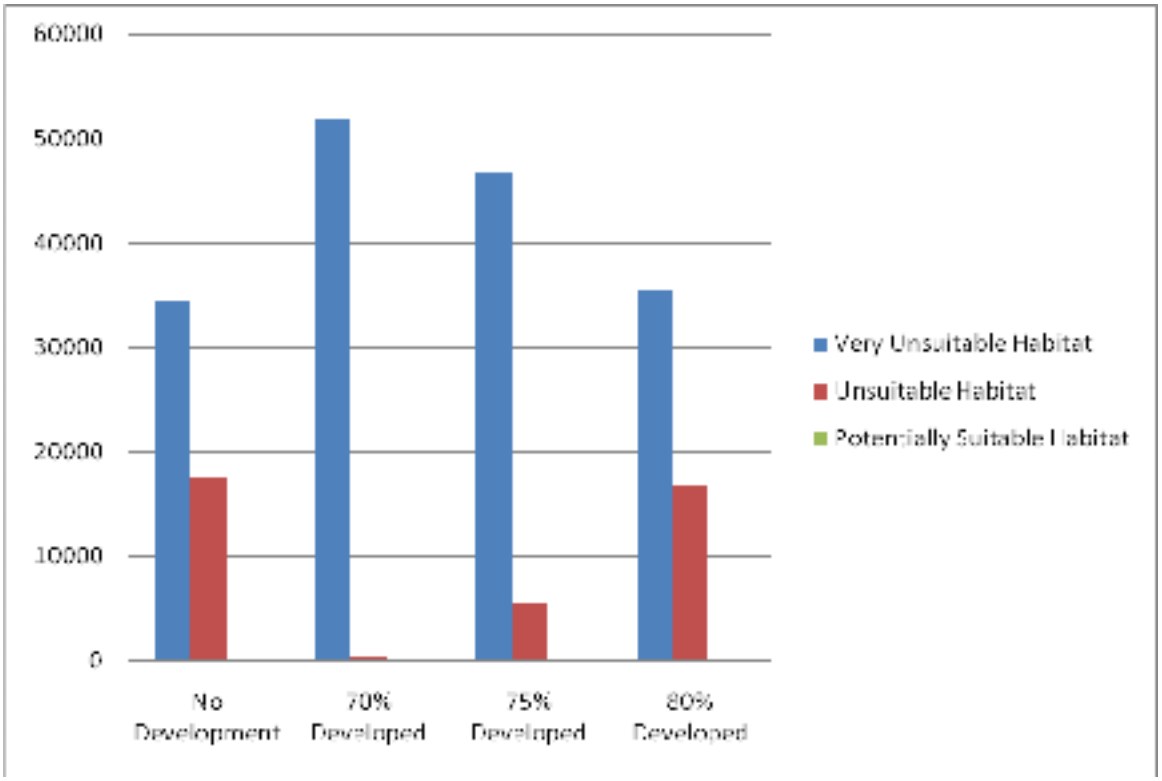

Figure 4. 12. Impact of pre and post development on habitat areas.

Conclusion

The major goals of this work were 1) to build and apply potential development models based on mathematical functions that determined fate of an undeveloped parcel of land based on a set of predictor variables; 2) apply these potential development predictions to assess potential habitat changes for the red-cockaded woodpecker.

We do not study the dynamics of such developments; we assumed that the pattern of each LU predictor variable and their relative effect remained constant. This is of course simplistic, because for example, the values of factors $X1$, $X2$ related to roads are likely to change as new roads and streets are built and they respond to change in LU. This limitation can be removed by including this potential development model in an agent-based simulation as we have done for the North Texas area (Acevedo et al., 2008).

Since we started this work, the study area has experienced substantial growth in population followed by housing units and other developments as explained in the introduction section. The model can be updated to reflect changes in transportation or commercial, industrial and residential if updated layers are available. Thus, given the availability of newer data such as new roads, population estimates, new housing units and more temporal and spatial information about LU change, it is possible to re-examine the model and also study the effects of the assumptions might have on the performance of the potential development model.

This work provided critical data for the coupled human-nature system models of the larger interdisciplinary project Integrating Models of Natural and Human Dynamics in Forest Landscapes across Scales and Cultures, a Biocomplexity in the Environment project funded by the National Science Foundation (Acevedo et al., 2008).

With further efforts, the model can be improved to produce more realistic results. For example, we could use higher resolution images coupled with rigorous field work to improve the habitat analysis conducted here and in Chapter 3. Further field work and use of higher resolution images would provide vital data on pine tree age, diameter at breast height, identification of cavity and non-cavity trees and most importantly, we can have the current data collected in real-time. Such pool of data can be very useful during classification and other analysis. For example, we could use these data to investigate maximum values – why they are 0.89 instead of 1 for initial neighborhood analysis of binary pine tree image? Or why they are 0.76 for total potential development maps? For this project, we had to rely on several assumptions for such low maximum or high minimum values. Also future improvements of the potential development model entails analysis of empirical information to validate the mathematical functions employed. Overall we conclude that the methods employed here resulted useful to study LU spatial dynamics and its impact on wildlife habitat.

APPENDIX

DATA SEARCH

Data Required

1. Road/Streets

2. NLCD

3. Population data (Census)

Data Searching

- I went to www.tnris.state.tx.us to find required data (Figure A.1). This website also provides other data such as census, roads, hydrology, LiDAR, SPOT, soil etc. I downloaded census block shapefile and road polyline.

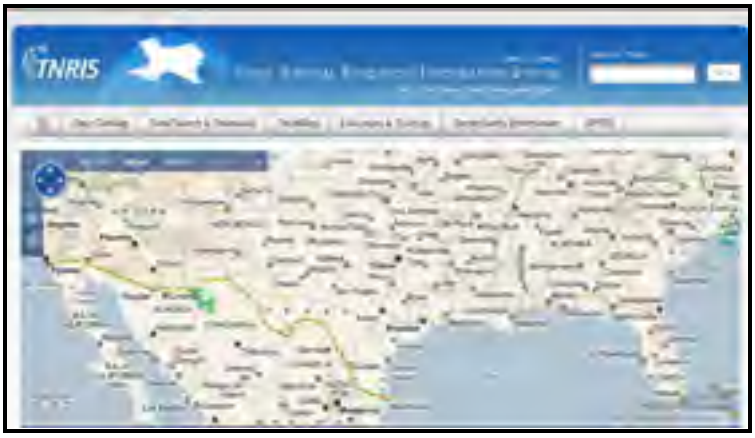

Figure A. 1. Website for road and census data.

Road Data

- The road data resided in 'StratMap ver2' and it contained both minor and major roads. I teased out the major roads and created a separate file as these data were later used for the program to calculate the minimum road distances.
- Then I converted the roads into rasters. I used the following functions as –

  Arc Toolbox → Conversion Tools → To Raster → Polyline to Raster
- After the above procedure, I used the following function on the converted road rasters – CON ([merged_roads] > 0, 1, 0). This is done to select the roads only. Then I used

Spatial Analyst → Raster Calculator → [merged_roads] + 10. This process will make the road cells bigger that facilitated selection of road only (Figure A.2).

Figure A. 2. Selection of road cells only.

- And then I converted the road rasters ASCII text files to use in the C program (Figure A.3).

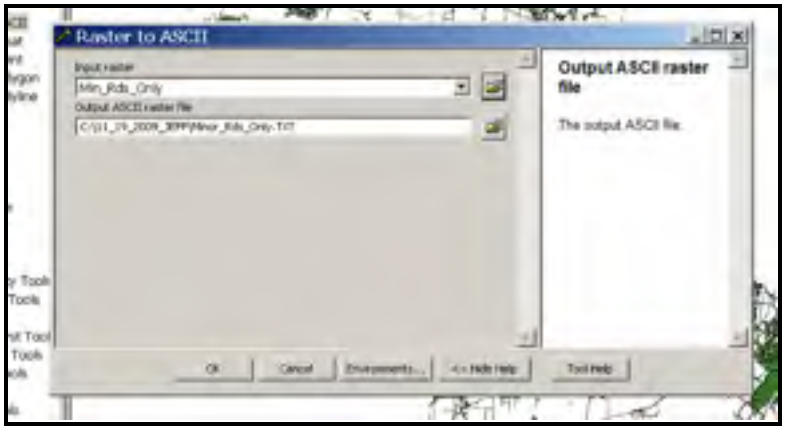

Figure A. 3. Conversion of road raster to ASCII text file.

- After the conversion, the text files were used in program in order to calculate minimum road distance. For this, I used COMMAND PROMPT for the calculation (Figure A.4).

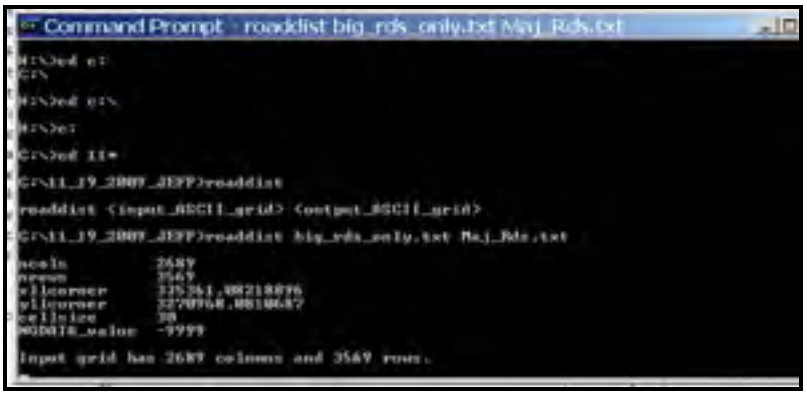

Figure A. 4. Program for calculation of road distance.

- The output was another ASCII text files that were converted back to rasters for visual display. I selected 'Float' as the field data type as the cells contained values in decimals (Figure A.5).

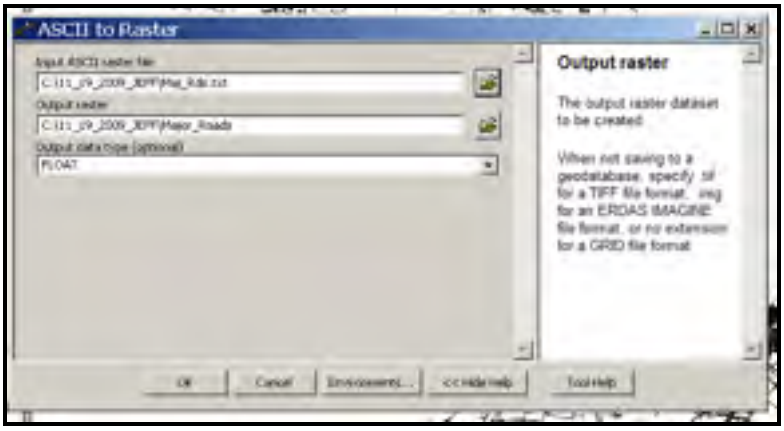

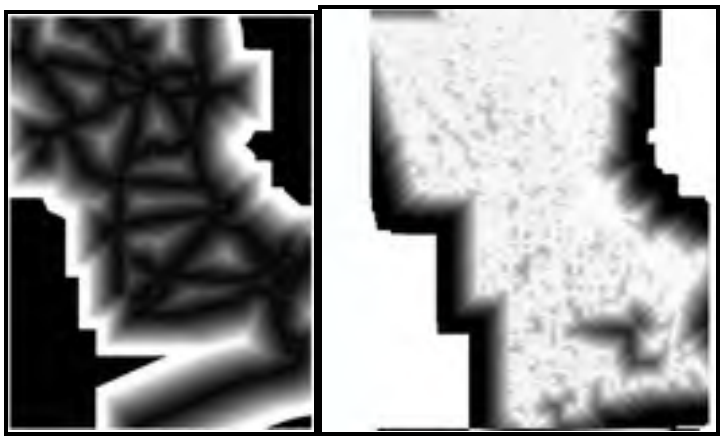

Figure A. 5. Conversion of output ASCII to raster for visual display.

Population Data

- For population data, I went to www.census.gov and clicked on the "American FactFinder" to go to the following page. On this page, I clicked the 'DOWNLOAD CENTER' (Figure A.6).

Figure A. 6. Website to download census data.

- From the download center, I selected census data of 2000 under the file named 'Census 2000 Summary File 1 (SF 1) 100 Percent Data'. This file contains population count of 2000 (Figure A.7).

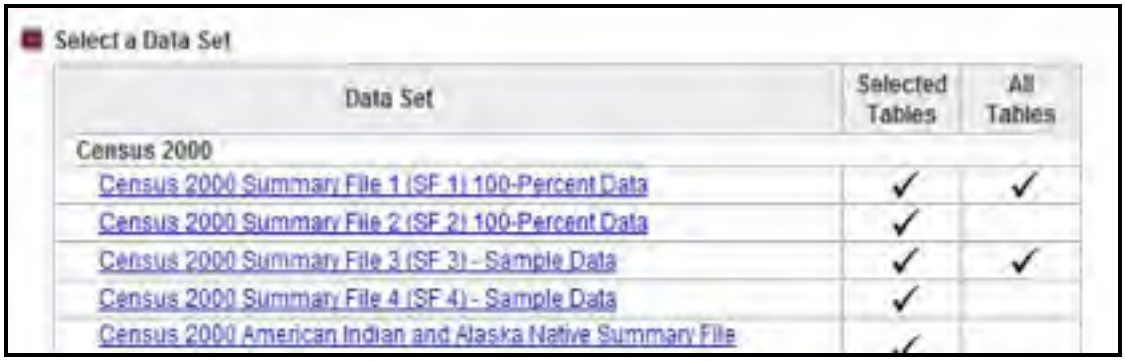

Figure A. 7. Selection of 2000 census data.

- After selecting desired state and county, the population count for block. Other population data such as numbers of specific race such as Asian or Hispanic can be also be downloaded. The block data was downloaded using a zip file (Figure A.8).

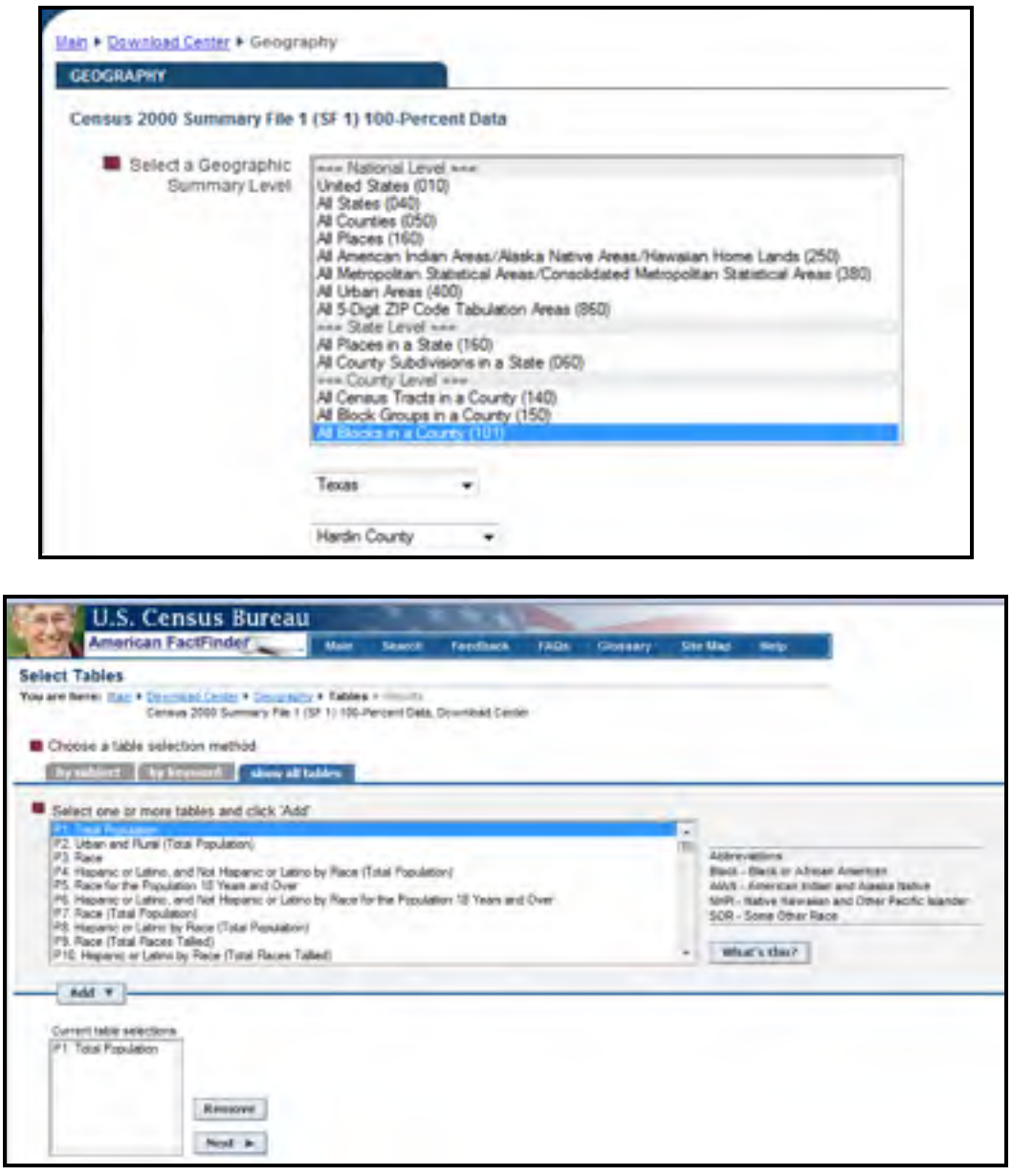

Figure A. 8. Procedures to download block data.

- The block data was then imported to excel for further analysis. I used 'Delimited' and 'Other' before importing the data (Figure A.9).

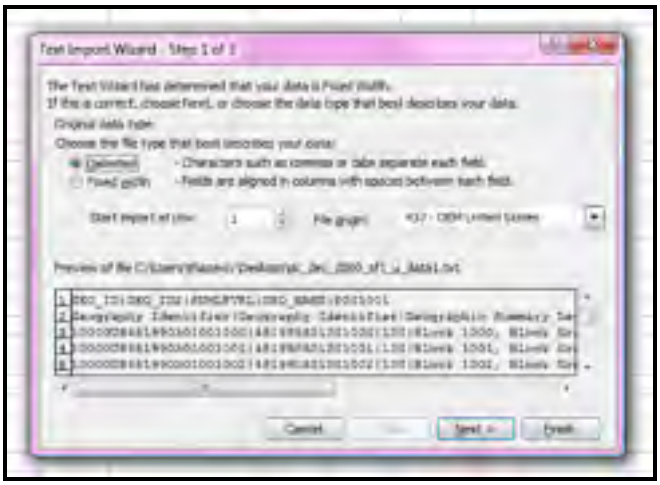

Figure A. 9. Import of block data in Excel.

- I deleted the second row and saved it as a text file. The P001001 contains the population data (Figure A.10).

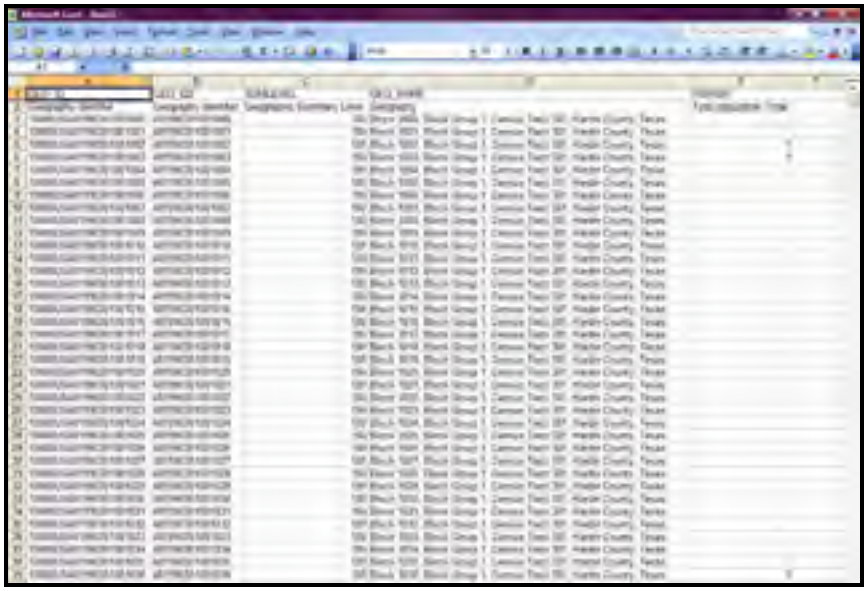

Figure A. 10. Population data import to Excel.

- I imported the text file to ArcGIS and opened it using ArcCatalog. Once opened, I right clicked it and saved it data base format file and suing single (table to table) choice options as shown in Figure A.11.

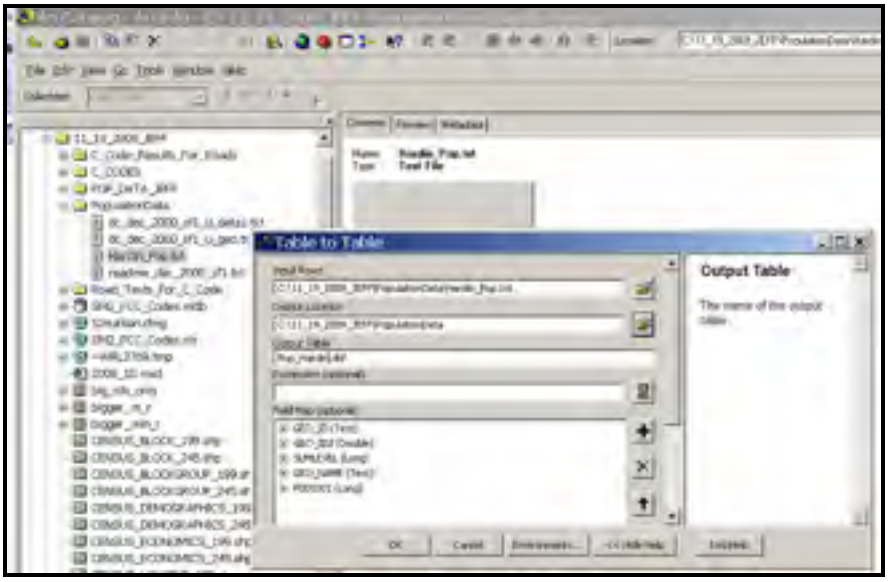

Figure A. 11. Conversion of the text file into dbf file in ArcCatalog.

- After creating the dbf file, I checked the attribute of the census block polygon shapefile to search for appropriate column to use it to with join the newly created population table (Figure A.12).

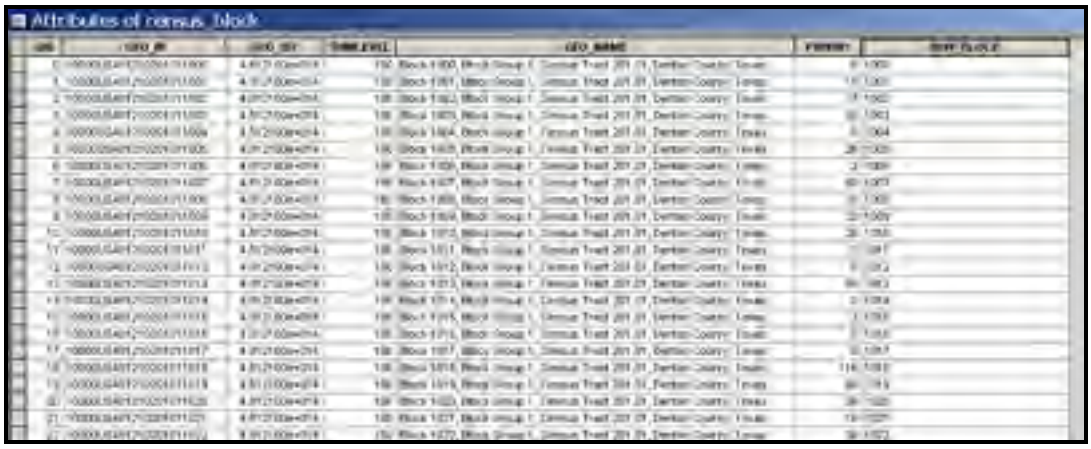

Figure A. 12. Attribute table of the census block shapefile.

- I found a column named ‘BLOCK’ that four numbers. I searched for similar numbers in the population table and found it under GEO_ID column. However, the total numbers were six instead of four. The last four numbers were similar to BLOCK column of census block polygons. Thus, a column with four of these numbers was needed within the population table. I created a new column and named it ‘NEW_BLOCK’ and selected the field type as ‘text.’ I right clicked this new column to get to ‘Field Calculator.’ I used this step in order to populate the new column of NEW_BLOCK and to burrow the last four digits from GEO_ID column. To do this, I selected ‘String’ as ‘Type’ and ‘Right’ from the available functions. This means, out of six, four numbers from the right will be selected in order to match them with the numbers from BLOCK column. In other words, Right () trimming numbers from the right side. I typed Right ([GEO_ID], 4) and derived the four numbers and populated the NEW_BLOCK column. Then I joined the two tables using these four matching numbers (Figures A.13 and A.14).

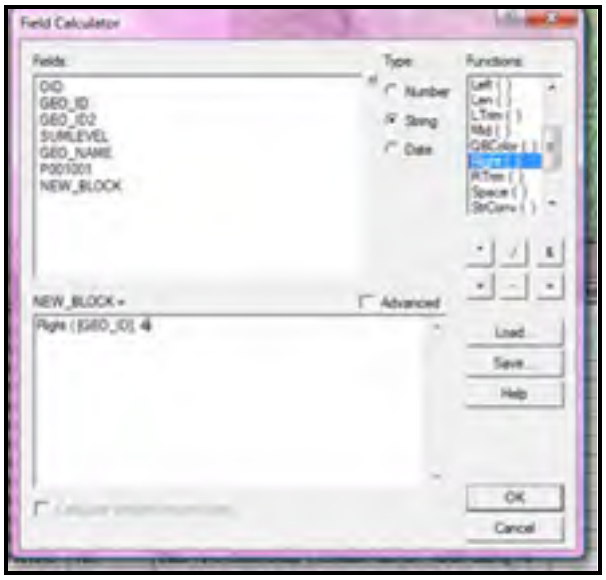

Figure A. 13. Selection of the four numbers from GEO_ID column.

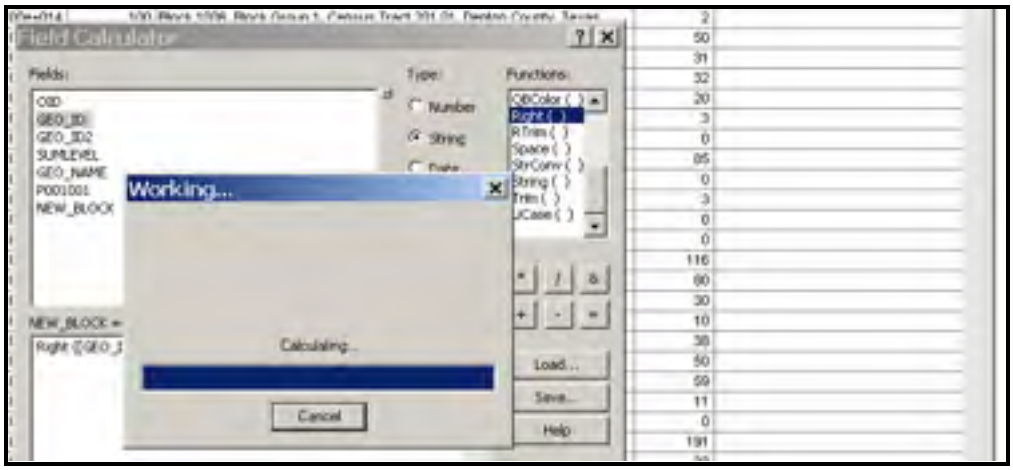

Figure A. 14. Populating the new NEW_BLOCK column with the four numbers burrowed from GEO_ID column.

- Then I created two additional fields in the census block shapefile that now contained newly created 'NEW_BLOCK' column. They were POP_DENSE and AREA respectively. These tables were necessary in order to calculate the population density of the region that in turn was required to create potential development maps. For field data type, I selected 'Float without precision' for POP_DENSE field and 'Double without precision' for AREA field. Float without precision) and AREA (Double without precision). These fields can be created without turning on the 'Editor' function of the ArcMap (Figure A.15).

Figure A. 15. Calculation of AREA.

- And to calculate population density, area of a certain place is required. Thus, I calculate the AREA using ‘Calculate Geometry’ and for unites, square miles was selected (Figure A.16).

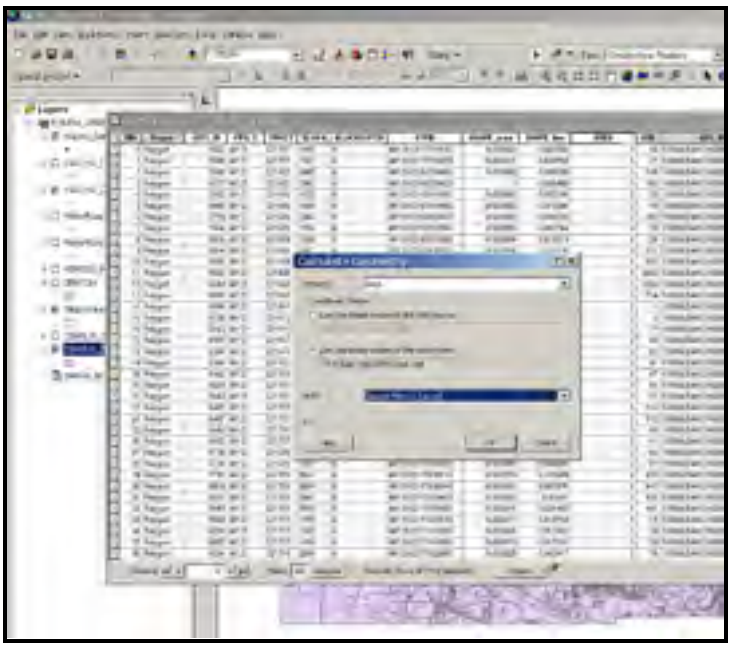

Figure A. 16. Selection of units as square miles to calculate AREA.

- And to calculate population density, I used ‘Field Calculator’ and divide the population by the area as shown in Figure A.17.

Figure A. 17. Calculation of population density.

- After calculating area and population density, I converted the census shapefile to raster. I selected 'POP_DENSE' field as the value field during the conversion (Figure A.18).

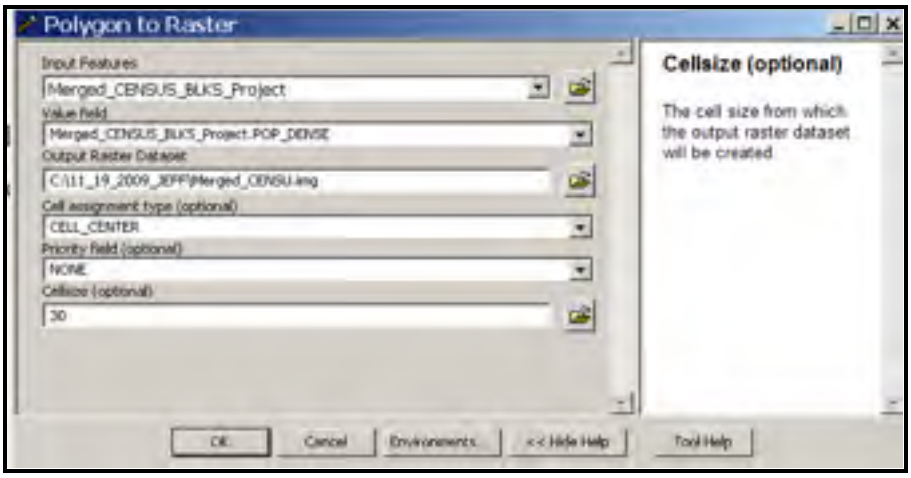

Figure A. 18. Conversion of census blocks to raster.

- The resultant population density raster image was then converted to ASCII text file similar to roads. The ASCII text file was used for c program to calculate the population density using a 7x7 moving window.

Land Use Data of 1992

- I used www.mrlc.gov to download land use and land cover data. I selected 1992 land use data (Figure A.19).

Figure A. 19. Website to download land cover data.

- The raster has 21 land cover categories and are number is assigned to individual category. I extracted land cover categories of 21and 22 for residential and 23 for commercial and industrial. I converted the two rasters directly to ASCII text files and executed the program to calculate the proportion of developed lands around a target cell (Figure A.20).

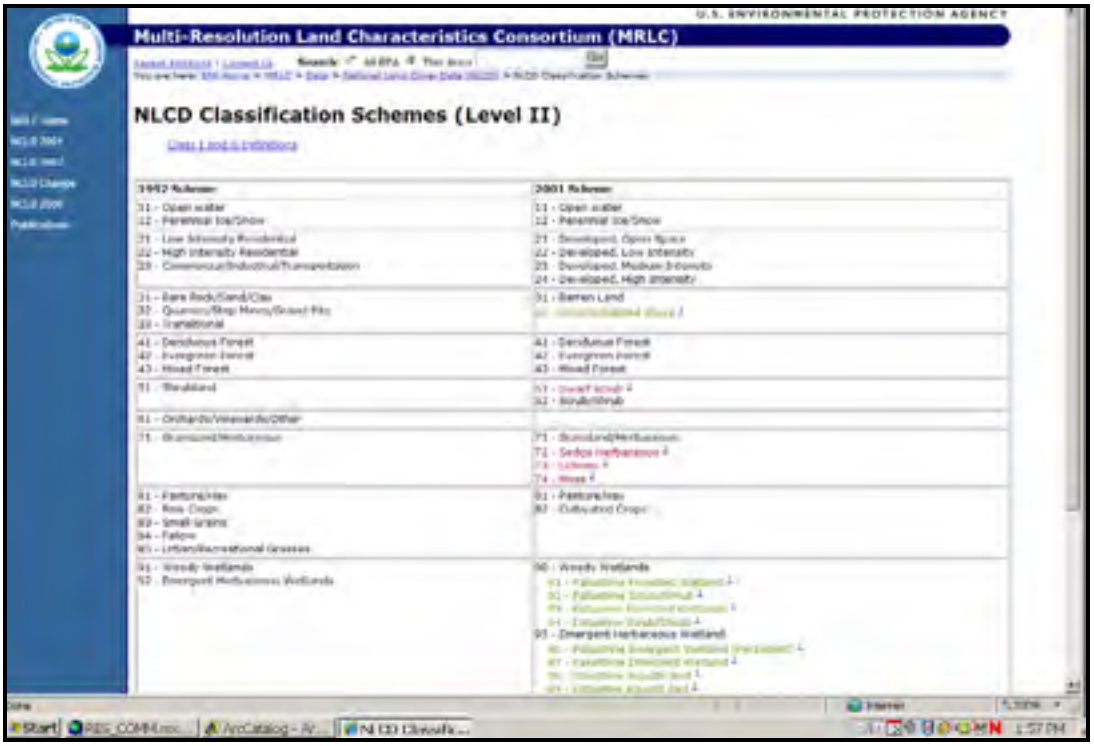

Figure A. 20. Land cover categories for 1992 NLCD.

- The program calculates proportions of land development around a target cell. I used 7 x7 windows similar to population density. Suppose, we have 5 pixels that is 21and 22 (low and high intensity residential areas) in a total of 49 pixels neighborhood then we have 5/49 = 0.1. The target cell will receive the value of 0.1 and so on. Thus, the pixel with a value of 0.1 indicates it is 10% or 0.1 developed that in turn indicates this pixel will have a high probability for future development. Similarly, in a 7x7 neighborhood, if we have 40 pixels that are already developed to residential areas then 45/49 = 0.81 or 81%. The target pixel will get a value of 0.81. In other words, the pixel is 81% developed and possess less chance of future development. In this way, each pixel is calculated for its probability for future development to either residential or commercial and industrial areas. Most of the high valued pixels were centered near the town, major and minor roads. This indicated these areas are already developed and holds little importance to developers.

Executing Final Program Called Devpots

- To execute the final program and to create potential development maps successfully, the raster images of the five factors should contain equal number of rows and columns. Since I was working on the entire Hardin county data while creating the five factors, I made a polygon that encompassed my study area only. I used this polygon to clip the rasters. This way the five factors had equal rows and columns of 776 and 1000.
- The rasters were then converted to ASCII text files and the final program was executed.

Finding Hydrology Dataset (Streams/Rivers/Wetlands)

- The initial program required six factors including hydrology data. The hydrology data included lakes, ponds, reservoirs, wetlands and rivers. If an area contained any of the aforementioned water bodies, the development is unlikely. In other words, the program recognized such areas as natural impediments where there is less opportunity for development. In addition, the study area contains numerous wetlands and is protected under wetland conservation acts. Once thought to be wastelands, nowadays they have received protections due to their free services they provide to the populations living nearby. The services include natural filter of the agricultural pesticides and habitat for wetland species. I went to www.tnris.state.tx.us/DataDictionary.aspx to acquire the data (Figure A.21).

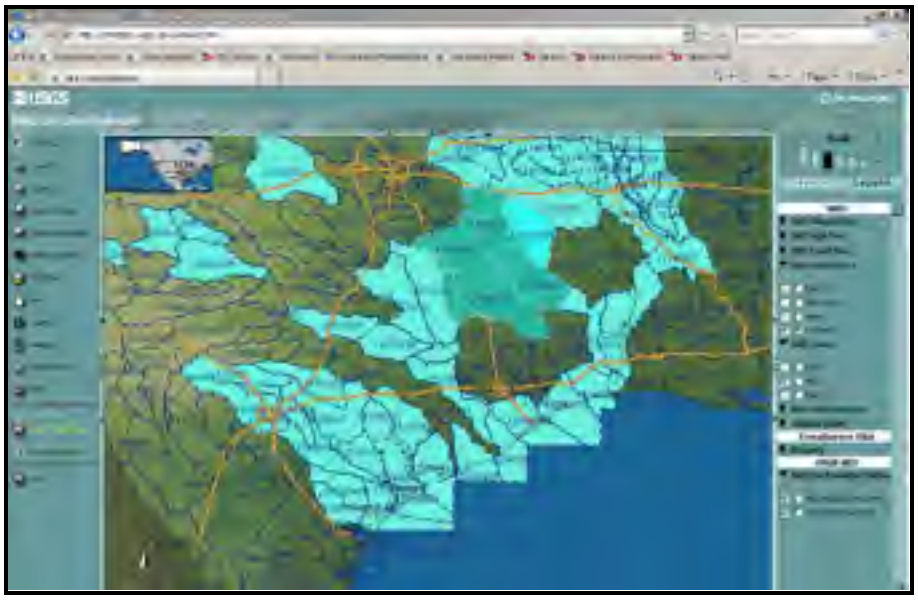

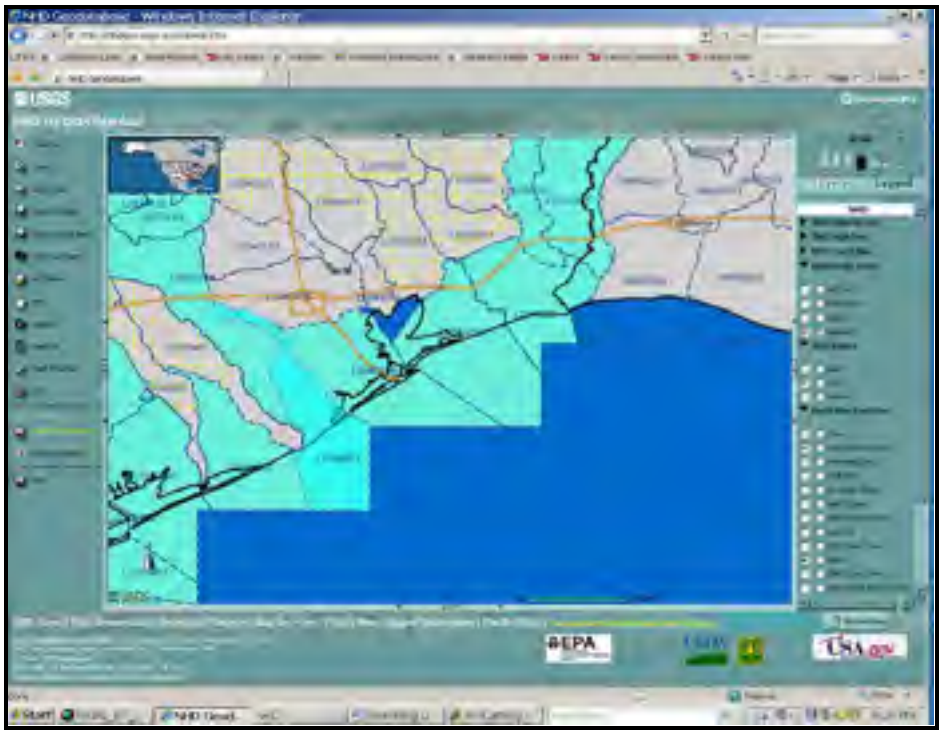

Figure A. 21. Website for hydrology dataset.

- And to find the data, I selected Texas and clicked the sub basin circle. I emailed the selected data.
- However, I had to find another website to find stream data as shown below from TCEQ website and it stands for Texas Commission for Environmental Quality. I downloaded four basins as follows – 5, 7, 8, and 10 (Figure A.22). From these basins, I extracted streams, rivers and major highway data. The website is http://www.tceq.state.tx.us/implementation/water/tmdl/atlas.html#files

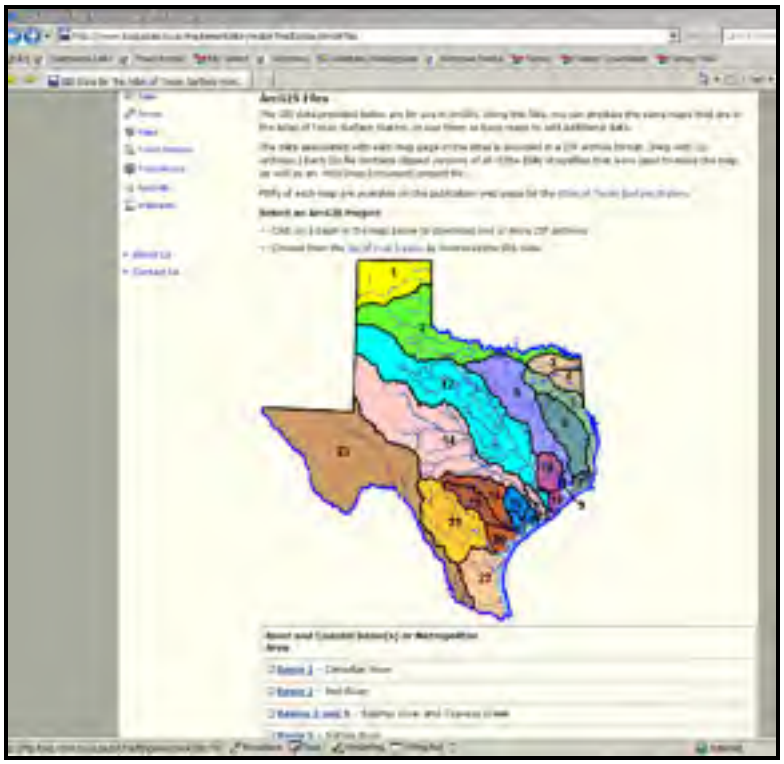

Figure A. 22. Website for stream data.

Parcel Data

- I contacted several personnel's of Hardin County Appraisal District to obtain parcel data. However, finding parcel data for Hardin County was troublesome. They do not have a full-fledged GIS center like the one in Denton County. As suggested by Howard Redfearn, I searched for CAD data and finally, Theresa mailed CD that contained CAD drawings that I used to create parcel polygons. The CAD files were called dgn and converted the polyline into polygons and for input labels, I used annotation. Still, I am missing some parcels. I used Arc Info to convert the CAD polyline to polygons. To do this, the required tool is under ArcToolbox → Data Management → Features → Feature to Polygon (Figure A.23).

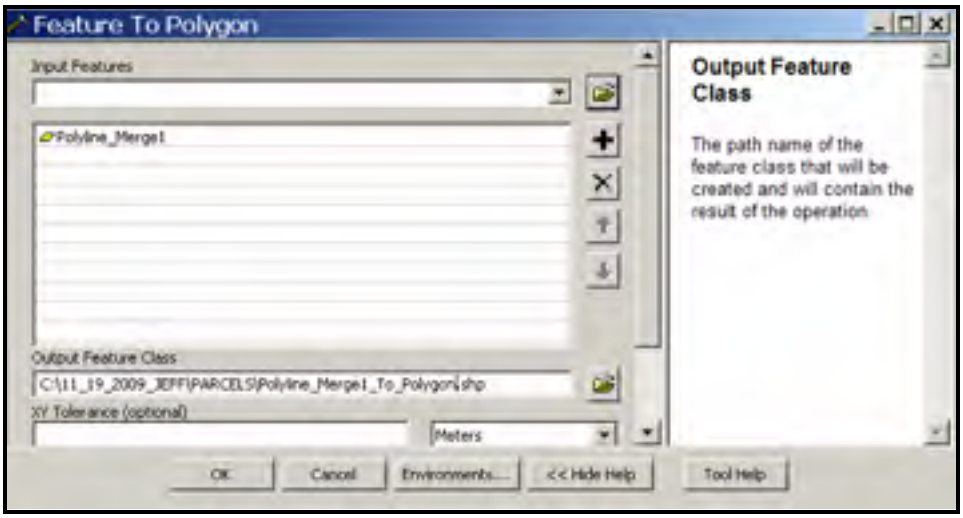

Figure A. 23. Converting CAD polyline to polygons.

- I checked the attribute of the parcel polygons and found the third column empty. The other two columns i.e. FID and Shape contained polygon numbers and shape type respectively. Since we cannot use both first and second column, we needed to populate the third column with FID values. I also changed the coordinate system to WGS 1984 (Figure A.24).

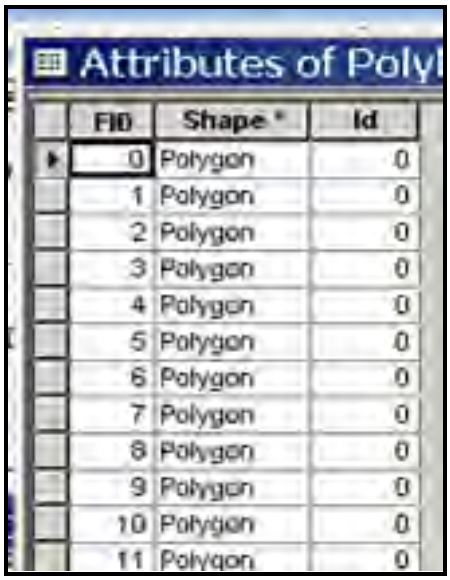

Figure A. 24. Attribute table of CAD converted polygons.

- I used field calculator as shown below to populate the third column. This way I produced parcel polygons with values (Figure A.25).

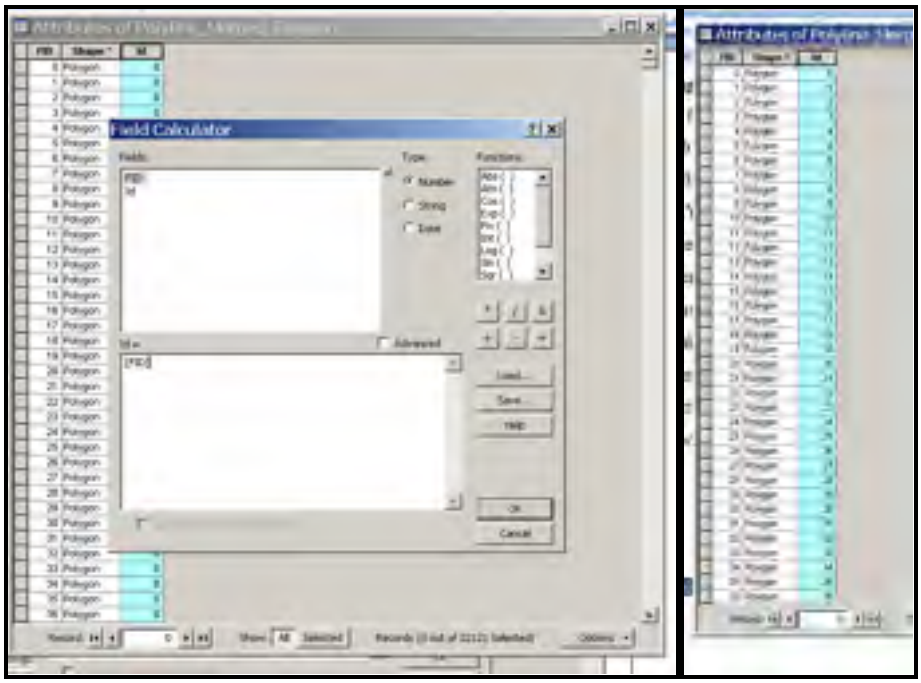

Figure A. 25. Populating third column with FID values.

- After populating the column, I used Spatial Analyst → Zonal → Zonal Statistics tool to calculate the mean value for each polygon. I used the zone field from 'Id' and potential development rasters as input value raster (Figure A.26).

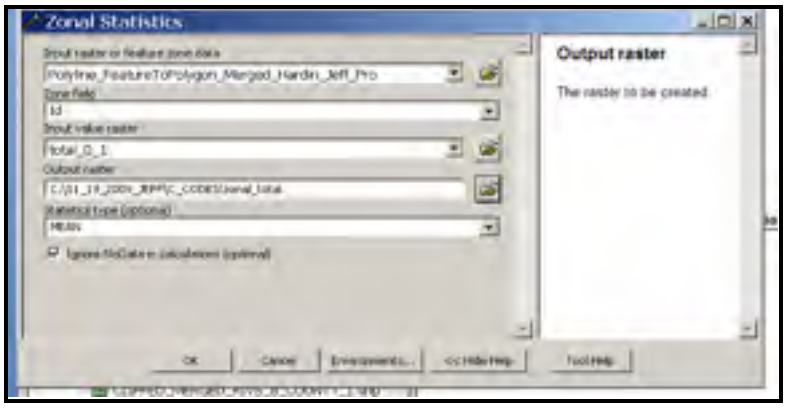

Figure A. 26. Calculation of mean for individual polygons using zonal statistics.

Appendix References

Jenson, J.R. (Ed.). (1996). *Introductory digital image processing: A remote sensing perspective* (2nd ed.). Englewood Cliffs, New Jersey: Prentice-Hall

Luiz, A.B.J. and Garcia, G.J. (1997). A study of habitat fragmentation in Southeastern Brazil suing remote sensing and geographic information systems (GIS). *Forest Ecology and Management, 98*, 35-47.

LITERATURE CITED

Abbott, I. (2001). The Bilby *Macrotic lagotis* (Marsupialia: Perameliadae) in southern Australia: Original range limits, subsequent decline, and presumed regional extinction. *Records of the Western Australian Museum, 20***,** 271-305.

Acevedo, M. F., Callicott, J. B., Monticino, M., Lyons, D., Palomino, J., Rosales, J., Delgado, L., Ablan, M., Davila, J., Tonella, G., Ramirez, H., & ... Vilanova, E. (2008). Models of natural and human dynamics in forest landscapes: Cross-site and cross-cultural synthesis. *Geoforum, 39*, 846-866.

Alberti, M. (1999). Urban patterns and environmental performance: What do we know? *Journal of Planning Education and Research, 19*(2), 151-163. doi:101177/0739456X9901900

Anderson, J.F., Hardy, E.E., Roach, J.T., & Witmer, R.E. (1976). *A land use and land cover classification system for use with remote sensor data*. U.S. Geological Survey Professional Paper 964. Washington, DC: U.S. Geological Survey.

Baker, W. W. (1971). Progress report on life history studies of the red-cockaded woodpecker at Tall Timbers Research Station. 4. 44-60, *in* The ecology and management of the red-cockaded woodpecker (R. L. Thompson, ed.), Bureau of Sport Fisheries and Wildlife and Tall Timbers Research Station, Tallahassee, FL, 188 pp.

Bate, E.F. (1976). *History and reminiscences of Denton County*. Denton, TX: Terrill Wheeler Painting.

Baral, N. & Heinen, J. T. (2005). The Maoist people's war and conservation in Nepal. *Politics and the Life Sciences, 24*, 2-11.

Bawa, K.S. & Dayanandan, K. (1997). Social and economic factors in tropical deforestation. *Nature, 386*, 562-563.

Bell, E. K. & Donnelly, A. M. (2006). Influence of forest fragmentation on community structure of frogs and lizards in northeastern Costa Rica. *Conservation Biology, 20*, 1750-1760.

Bernstein, R. (1983) Image geometry and rectification. *Manual of Remote Sensing, Second Edition*, R. N. Colwell, ed., Falls Church, Virginia: American Society of Photogrammetry, pp. 873-922.

Brandt, J.J.E., Bunce, R.G.H., Howard, D.C., & Petit, S. (2002). General principles of monitoring land cover change based on two case studies in Britain and Denmark. *Landscape and Urban Planning, 62*, 37-51. doi:10.1016/S0169-2046(02)00095-6

Brown, D.G., Page, S.E., Riolo, R., & Rand, W. (2004). Agent-based and analytical modeling to evaluate the effectiveness of greenbelts. *Environmental Modeling & Software, 19*, 1097-1109.

Brooks, T. M., Mittermeier, C. G., Mittermeier, R. A., da Fonseca, G. A. B., Rylands, A. B., Konstant, W. R., Flick, P., Pilgrim, J., Oldfield, S., Magin, G., & … Hilton-Taylor, C. (2002). Habitat loss and extinction in the hotspots of biodiversity. *Conservation Biology, 16*, 909-923.

Botkin, D.B.A. & Keller, E.A. (2003). *Environmental science: Earth as a living planet* (4th ed.). London: John Wiley & Sons, Inc.

Buschbacher, R ., Uhl, C., & Serrao, E. A. S. (1988). Abandoned pastures in eastern Amazonia. II. Nutrient stocks in the soil and vegetation. *J. Ecol*. 76:682 - 699.

Callicott, J. B., Acevedo, M., Gunter, P., Harcombe, P., Lindquist, C., & Monticino, M. (2006). Bicomplexity in the Big Thicket. Ethics, *Place and Environment 9*:21-45.

Callicott, J. B., Rozzi, R., Degaldo, L., Monticino, M., Acevedo, M., Harcombe, P. (2007). Biocomplexity and conservation of biodiversity hotspots: three case studies from the Americas. *Philosophical Transactions of the Royal Society B-Biological Sciences* 362:321-333.

Campbell, J. B. (1996). Introduction to Remote Sensing. Second Edition. The Guilford Press, Ney York, NY. 622 pp.

Charles, J. M., & Howard, H.E. (1996). Foraging habitat of the red-cockaded woodpecker on the D'Arbonne National Wildlife Refuge, Louisiana. *Journal of Ornithology 67*:511-518.

Choi, M., Rae, Y. K., Myeong-Ryong, N., & Hong Oh., K. (2005). Fusion of Multispectral and Panchromatic Satellite Images Using the Curvelet Transform. *Geoscience and remote sensing letters*, *IEEE* 2 (2), 136-140. doi:10.1109/LGRS.2005.645313

Chase, T.N., Pielke, R. A., Kittel, T. G. F., Nemani, R. R., & Running, S.W. (1999). Simulated impacts of historical land cover changes on global climate in northern winter. *Climate Dynamics 16*:93–105.

Cincotta, R.P., Wisnewski, J., & Engelmam, R. (2000). Human population in the biodiversity hotspots. *NATURE 404*:990-992.

Cohn, J. P. (1988). Halting the rhino's demise. *Bioscience 38*:740-744.

Congalton, G.R., & Green, K. (1999). Assessing the accuracy of Remotely Sensed Data: Principles and Practices. Lewis Publishers, New York.

Congalton, G. R. (1991). A review of assessing the accuracy of remotely sensed data. Remote *Sensing of the Environment 37*:35-46.

Congalton, G. R., & Green, K. (1999). Assessing the Accuracy of Remotely Sensed Data: Principles and Practices. CRC Press, Boca Raton, Florida. 137 pp.

Conner, R. N., & Rudolph, D. C. (1989). Red-cockaded Woodpecker colony status and trends on the Angelina, Davy Crockett, and Sabine National Forests. Res. Pap. SO-250, U.S.D.A. Forest Service, 15pp.

Conner, R. N., & Rudolph, D. C. (1991). Forest habitat loss, fragmentation, and red-cockaded woodpecker population. *Wilson Bulletin 103*(3):446-457.

Conner, R. N., Saenz, D., & Rudolph, D. C. (2004). The red-cockaded woodpecker: Interactions with fire, snags, fungi, rat snakes and Pileated woodpeckers. *Texas Journal of Science. 56*:415-426.

Conner, R. N., editor. (1981). Fire and cavity nesters. Pp 61-65. Belle W. Baruch Forest Science Institute of Clemson University., Georgetown, South Carolina.

Conner, R. N., Hooper, R. G., Crawford, H. S., & Mosby, H. S. (1975). Woodpecker nestling habitat in cut and uncut woodlands in Virginia. *Journal of Wildlife Management 39*:144-150.

Conner, R. N., & Locke, B. A. (1982). Fungi and red-cockaded woodpecker cavity trees. *Wildlife Society Bulletin 94*:64 - 70.

Conner, R. N., Miller, O. K., & Adkisson, C. S. (1976). Woodpecker dependence on trees infected by fungal heart rots. *Wildlife Society Bulletin 88*:575-581.

Conner, R. N., & Rudolph, D. C. (1991). Effects of midstory reduction and thinning in Red-cockaded woodpecker cavity tree clusters. *Wildlife Society Bulletin 19*:63 - 66.

Conner, R. N., Rudolph, D. C., Saenz, D., & Schaefer, R. R. (1994). Heartwood, sapwood, and fungal decay associated with red-cockaded woodpecker cavity trees. *Journal of Wildlife Management 58*:728 - 734.

Cozine, J. (2004). Saving the Big Thicket: From exploration to preservation, 1685-2003. Pages xii, 289 p. Big Thicket Association/University of North Texas Press, Denton.

Dale, V., Neill, O., Pedlowski, M., & Southworth, F. (1993). Causes and effects of land use change in Central Rondonia, Brazil. *Photogrammetric Engineering and Remote Sensing 59*:97 - 1005.

Dale, V. H., Pearson, S. M., Oferman, H. L., & O'Neill, R. V. (1994). Relating patterns of land-use change to faunal biodiversity in the central Amazon. *Conservation Biology 8*:1027-1036.

Durrenberger, G., Patzel, N., & Hartmann, C. (2001). Household energy consumption in Switzerland. *International Journal of Environment and Pollution 15*:159-170.

Department of National Parks and Wildlife Conservation. (2007). Shrinking grassland impacts wildlife. In Kantipur. Kathmandu.

Dettki, H., Lofstran, R., & Edenius, L. (2003). Modeling habitat suitability for Moose in Coastal Northern Sweden: Empirical vs. Process-oriented Approaches. Royal Swedish Academy of Sciences. *Ambio. 8. 32*: 549-556 pp.

DeLotelle, R.S., Epting, R.J., & Newman, R.J. (1987). Habitat use and territory characteristics of red-cockaded woodpeckers in Central Florida. *Wilson Bulletin 99*(2):201-217.

Dickman, C. R. (1987). Habitat fragmentation and vertebrate species richness in an urban environment. *Journal of Applied Ecology 24*:337-351.

Dinerstein, E. A., & Wemmer, C. (1988). Fruits Rhinoceros eat: dispersal of Trewia nudiflora in lowland Nepal. *Ecology 69*:1768-1774.

Dinerstein, E. (1989). The Foliage-as-Fruit Hypothesis and the Feeding Behavior of South Asian Ungulates. *Biotropica 21:*214-218.

Dinerstein, E. (2003). The Return of the Unicornis – The Natural History and Conservation of the Greater One – Horned Rhinoceros. Biology and Resource Management Series. World Wildlife Fund, Washington D.C. 320 p.

Dinerstein, E., & Price, L. (1991). Demography and Habitat use by Greater One – Horned Rhinoceros in Nepal. The Journal of Wildlife Management, Vol. 55, No. 3 (Jul., 1991), pp. 401-411.

Dinerstein, E. A., & McCracken, G. F. (1990). Endangered greater one-horned rhinoceros carry high levels of genetic variability. *Conservation Biology 4*:417-422.

Department of National Parks and Wildlife Conservation. (2008). Kathmandu. Retrieved August 26, 2009 from http://www.dnpwc.gov.np/publication/Rhino_Count_2008.pdf (accessed August 2009).

Doster, R.H. & James, D.A. (1998). Home-range size and foraging habitat of red-cockaded woodpeckers in the Ouachita Mountains in Arkansas. *Wilson Bulletin 110*(1):110-117.

Engstrom, R.T., & Sanders, F.J. (1997). Red-cockaded woodpecker foraging ecology in an old-growth longleaf pine forest. *Wilson Bulletin 109*(2):203-217.

Ertep, S.A., & Lee, G.W. (1994). Use of GRASS to facilitate red-cockaded woodpecker management at Fort Benning Military Reservation. Pages 628-633 in 1994 Annual Conference Proceedings, Urban and Regional Information Systems Association, Washington, D.C., USA.

Foster, D.R., Swanson, F., Aber, J., Burke, I., Brokaw, N., Tilman, D., & Knapp, A. (2003). The importance of land-use and its legacies to ecology and environmental management. *BioScience 53*:77-88.

Franzred, K.E. (2006). Implications of home-range estimation in the management of red-cockaded woodpeckers in South Carolina. *Forest Ecology and Management 228*:274-284.

Girvetz, E. H. & Greco, S. E. (2007). How to define a patch: a spatial model for hierarchically delineating organism-specific patches. *Landscape Ecology 22*. 1131-1142.

Gunter, P. A. Y. (1993). The Big Thicket: An Ecological Reevaluation. University of North Texas Press, Denton.

Hall, B.B., Motzkin, G., Foster, D.R., Syfert, M., & Burk, J. (2002). Three hundred years of forest and land-use change in Massachusetts, USA. *Journal of Biogeography 29*:1319-1335.

Hardison, T. (2003). Application of remote sensing and GIS to modeling fire for vegetative restoration in Northern Arizona. Thesis/Dissertation. University of North Texas, Denton.

Harini, N., & Gadgil, M. (1999). Biodiversity assessment at multiple scales: Linking remotely sensed data with field information. *Ecology 96*:9154-9158.

Hatten, J.R., Averill-Murray, A., & van Pelt, W.E. (2005). A spatial model of potential jaguar habitat in Arizona. *Journal of Wildlife Management 69*(3): 1024-1033. doi:10.2193/0022-541X(2005)069[1024ASMOP]2.0.CO;2

Harini, N., Pareeth, S., Sharma, B., Schweik, C. M., & Adhikari, K. R. (2008). Forest fragmentation and regrowth in an institutional mosaic of community, government and private ownership in Nepal. *Landscape Ecology 23*:41-54.

Hansen, A.J., Knight, R.L., Arzluff, J.M., Powell, S., Brown, K., Gude, P.H., & Jones, K. (2005). Effects of exurban development on biodiversity: patterns, mechanisms, and research needs. *Ecological Applications 15*:1893-1905.

Hedrick, L. D., Hooper, R. G., Krusac, D. L., & Dabney, J. M. (1998). Silvicultural systems and red-cockaded woodpecker management: another perspective. *Wildlife Society Bulletin 26*:138-147.

Hooper, R. G., Robinson, A. F., & Jackson, J. A. (1980). The Red-Cockaded Woodpecker: Notes on life history and management in F. S. U.S. Department of Agriculture, Southeastern Area, State and Private Forestry., editor. General Reports.

Hooper, R. G. (1988). Longleaf pines used for cavities by red-cockaded woodpeckers. *Journal of Wildlife Management 52*:392-398.

Hooper, R. G., Robinson, A. F., & Jackson, J. A. (1996). The red-cockaded woodpecker: Notes on life history and management. Gen. report SA-GR9, USDA Forest Service SE area.

Houghton, R. A. (1994). The worldwide extent of land-use change. *Bioscience 44*:305-313.

Huston, M.A. (1993). Biological diversity, soils, and economics. *Science 262*:1676-1680.

Huston, M.A. (1994). Biological diversity: the coexistence of species in changing landscapes. Cambridge University Press, Cambridge, UK.

Huston, M.A. (1995). Saving the planet: report on a farm policy conference. *Bulletin of the Ecological Society of America 76*:97-99.

Huston, M.A. (2004). Management strategies for plant invasions: manipulating productivity, disturbance, and competition. *Diversity and Distributions 10*:167-178.

Huston, M.A. (2005). The three phases of land-use change: implications for biodiversity. *Ecological Applications 6*:1864-1878.

Innes, J. L., & Koch, B. (1998). Forest Biodiversity and Its Assessment by Remote Sensing. *Global Ecology and Biogeography Letters 7*:397-419.

International, C. (2005). The new hotspots. Conservation International. Retrieved November, 2008 from http://www.conservation.org

Jackson, J. A. (1994). Red-cockaded woodpecker. *Birds of North America 85*:1-20.

Jacobs, J. (1984). Cities and wealth of nations. Random House. New York, New York, USA.

Jensen, J. (1996). Introductory digital image processing: a remote sensing perspective. New Jersey: Prentice-Hall.

Jha, S., & Bawa, K.S. (2006). Population Growth, Human Development, and Deforestation in Biodiversity Hotspots. *Conservation Biology 20*:906-912.

Jnawali, S.R., & Wegge, P.W. (1993). Space and habitat use by a small re-introduced population of greater one – horned rhinoceros in RBNP – a preliminary report.

Kaimowitz, D., & Angelson, A. (1998). Economic models of tropical deforestation: a review. Center for International Forestry Research, Bogor, Indonesia.

Kotliar, N. B., & Weins, J. A. (1990). Multiple scales of patchiness and patch structure – a hierarchical framework for the study of heterogeneity. *Oikos 59*: 253-260.

Kummer, D. M., & Turner II, B. L. (1994). The human causes of deforestation in Southeast Asia. *Bioscience 44*:323-328.

Lambin, E. F. (1997). Modelling and monitoring land-cover change processes in tropical regions. *Progress in Physical Geography 21*:375-393.

Landis, J. D. (1994). The California Urban Futures model: a new generation of metropolitan simulation models. *Environment and Planning 21*:399-420.

Larson, M. A., William, D. D., Thompson, F. R., & Millspaugh, J. J. (2003). Landscape-level habitat suitability models for twelve wildlife species in Southern Missouri. Forest Service U. S. Department of Agriculture.

Laurie, W. A. (1978). The Ecology and Behavior of the Greater One – Horned Rhinoceros. Thesis/Dissertation. University of Cambridge.

Laperriere, J., Lent, P. C., Gassaway, W. C., & Nodler, F. A. (1980). Use of landsat data for moose habitat analyses in Alaska. *Journal of Wildlife Management. 44*:881-887.

Lekhmul, J. (1988). The ecology of South Asian tall-grass community. University of Washington, Seattle.

Licht, D.S. (1997). Ecology and economics of the Great Plains. University of Nebraska Press, Lincoln, Nebraska, USA.

Liu, J. G., Linderman, M., Ouyang, Z. Y., An, L., Yang, J., & Zhang, H. M. (2001). Ecological degradation in protected areas: The case of Wolong Nature Reserve for giant pandas. *Science 292*:98-101.

Liu, J. G., Daily, G. C., Ehrlich, P. R., & Luck, G. W. (2003). Effects of household dynamics on resource consumption and biodiversity. *Nature 421*:530-533.

Lobao, L., & Meyer, K. (2001). The great agricultural transition: crisis, change and social consequences of twentieth century US farming. *Annual Review of Sociology 27*:103-124.

Lott, D.F., & McCoy, M. (1995). Asian Rhinos Rhinoceros-Unicornis on the Run – Impact of Tourist Visits on One Population. *Biological Conservation 73*: 23-26.

Lunetta, R. S., Congalton, R. G., Fenstermaker, L. K., Jensen, J. R., McGwire, K. C. & Tinney, L. R. (1991). Remote sensing and geographic information system data integration: Error sources and research issues. Photogram. *Eng. Remote Sens. 57*: 677–687.

Luiz, A. B. J., & Garcia, G. J. (1997). A study of habitat fragmentation in Southeastern Brazil suing remote sensing and geographic information systems (GIS). *Forest Ecology and Management. 98*:35-47.

Lundberg, A. (2002). The interpretation of culture in nature: landscape transformation and vegetation change during two centuries at Hystad, Norway. *Norwegian Journal of Geography 56*:246 -256.

Makse, H. A., Andrade, J. S., Batty, M., Havlin, S., & Stanley, H. E. (1998). Modeling urban growth pattern with correlated percolation. *Physical Review E 58*:7054-7062.

Margules, C. R., & Pressey, R. I. (2000). Systematic conservation planning. *Nature*: 294-373.

Marks, P. L., & Harcombe, P. A. (1981). Forest vegetation of the Big Thicket, Southeast Texas. *Ecological Monographs 51*:287-305.

McGarigal, K. (2002). Landscape pattern metrics. *Enclyopedia of Environmetrics 2*:1135-1142.

McGarigal, K., Cushman, S. A., Neel, M. C., & Ene, E. (2002). FRAGSTATS: Spatial Pattern Analysis Program for Categorical Maps. Department of Natural Resources Conservation, University of Massachusetts, 304 Holdsworth Natural resources Center, Box 34210, Amherst, MA 01003. Retrieved March 11, 2007 from http://www.umass.edu/laneco/research/fragstats_documents.html

McGarigal, K., & Marks, B. J. (1995). FRAGSTATS: spatial pattern analysis program for quantifying landscape structure. USDA Forest Service Technical Reports. PNW-351.

McGarigal, K., & Marks, B. J. (1994). FRAGSTATS: spatial pattern analysis program for quantifying landscape structure. United States Department of Agriculture.

McClain, B.J., & Porter, W. F. (2000). Using satellite imagery to assess large-scale habitat characteristics of Adirondack Park, New York, USA. *Environmental Management 26*: 553-561.

McGarigal, K. (2002). Landscape pattern metrics. A. H. El-Shaarawi and W. W. Peigorsch, eds. *Encyclopedia of Environmetrics 2*:1135-1142.

McNeely, J.A., Miller, K. R., Reid, W. V., Mittermeier, R.A., & Werner, T. B. (1990). Conserving the world's biological diversity. International Union of Conservation of nature and Natural Resources, Conservation International, World Wildlife Fund-US, and the World Bank, Gland, Switzerland, and Washington, D.C.

Medley, K., Okey, B. W., Barett, G. W., Lucas, M. F., & Renwick, W. H. (1995). Landscape change with agricultural intensification in a rural watershed, southwestern Ohio. USA. *Landscape Ecology 10*:161 - 176.

Michael, R. T., Fuchs, V. R. & Scott, S. R. (1980). Changes in the propensity to live alone: 1950 - 1976. *Demography 17*:39-53.

Mitchell, M.S., Zimmerman, J. W., & Powell, R.A. (2002). Test of habitat suitability index for black bears in the southern Appalachians. *Wildlife Society Bulletin 30*:794-808.

Mittermeier, R.A., Myers, N., Thompson, J.B. da Fonseca., G.A.B., & Olivieri, S. (1998). Biodiversity hotspots and major tropical wilderness areas: approaches to setting priorities. *Conservation Biology 12*:516-520.

Monticino, M., Acevedo, M., Callicott, B., Cogdill, T., & Lindquist, C. (2007). Coupled human and natural systems: A multi-agent-based approach. *Environmental Modeling & Software 22*:656-663.

Myers, N., Mittermeier, R. A., Mittermeier, C. G., da Fonseca, G. A. B., & Kent, J. (2000). Biodiversity hotspots for conservation priorities. *Nature 403*:853-858.

National Park Service. U.S. Department of the Interior. Retrieved December, 2009 from www.nps.gov

Nepal, F.R. (1999). Forest Resources of Nepal (1987-1998).

Nepal, S.K., & Weber, K.E. (1995). The Quandary of Local People-Park Relations in Nepal's Royal Chitwan National Park. *Environmental Management 19*:853-866.

North Central Texas Council of Governments. (2003). Demographic Estimates, Denton. Retrieved January, 2008 from www.nctcog.dst.tx.us

North Central Texas Council of Governments. (2005). Demographic Estimates, Denton. Retrieved January, 2008 from www.nctcog.dst.tx.us

North Central Texas Council of Governments. (2008). Demographic Estimates, Denton. Retrieved March, 2009 from www.nctcog.dst.tx.us

Ningal, T., Hartemink, A. E., & Bregt, A. K. (2008). Land use change and population growth in the Morobe Province of Papua New Guinea between 1975 and 2000. *Journal of Environmental Management 87*:117 – 124.

NOAA. National Oceanic and Atmospheric Administration. Retrieved January, 2009 from http://www.ncdc.noaa.gov/oa/climate/research

Owen-Smith, R.N. (1988). Megaherbivores: The Influence of Very Large Body Size on Ecology. Cambridge University Press.

Pearson, S. M., Turner, M. G., Gardner, R. H., & O'Neill, R. V., (1996). An organism-based perspective of habitat fragmentation. Pages 77-95 In R. C. Szaro and D. W. Johnston, eds. Biodiversity in Managed Landscapes: Theory and Practice. Oxford University Press, New York.

Porwal, M.C., Roy, P.S., & Chellamuthu, V. (1996). Wildlife habitat analysis for 'sambar' (Cervus unicolor) in Kanha National Park using remote sensing. *International Journal of Remote Sensing 17*:2683-2697.

Pimm, S.L., Gittleman, J.L., Russell, G.J., & Brooks, T.M. (1995). The future of diversity. *Science* 269-347.

Pijanowski, B. C., Brown, D. G., Shellito, B. A., & Manik, G. A. (2002). Using neural networks and GIS to forecast land use changes: a Land Transformation Model. *Computers, Environment and Urban Systems 26*:553-575.

Ramankutty, N., Foley, J.A., & Olejniczak, N.J., (2002). People on the land: changes in global population and croplands during the 20th century. *Ambio 31* (3), 251–257.

Rawat, G. S. (2005). Vegetation dynamics and management of Rhinoceros habitat in Duars of West Bengal: An ecological review. *National Academy Science Letters – India 28*:177-184.

R Development Core Team. (2005). R: A language and environment for statistical computing. Retrieved February, 2007 from http://www.R-project.org

Reed, J. M., Doerr, P. D., & Walters, J. R. (1988). Minimum Viable Population Size of Red-Cockaded Woodpecker. *The Journal of Wildlife Management 52*:385-391.

Roseberry, J.L., & Sudkamp, S.D. (1998). Assessing the suitability of landscapes for northern bobwhite. *Journal of Wildlife Management 62*:895-902.

Rozzi, R., Massardo, F., Silander Jr, J., Anderson, C., & Marin, A. (2003ª). Conservacio´n iocultural y e´tica ambiental en el extremo austral de Ame´rica: oportunidades y dificultades para el bienestar ecosocial. In Biodiversidad y Globalizacio´n (eds E. Figueroa & J. Simonetti), pp. 51–85. Santiago, Chile: Editorial Universitaria.

Sala, O.E., Chapin, F. S., Armesto, J. J., Berlow, E., Bloomfield, R., Dirzo, E. Huber-Sanwald, L. F., Huenneke, R. B., Jackson, A., Kinzig, R., Leemans, D. M., Lodge, H. A., Mooney, M., Oesterheld, N. L., Poff, M. T., Sykes, B. H., Walker, M., & … Wall, D.H. (2000). Biodiversity: global biodiversity scenarios for the year 2100. *Science 287*: 1770–1774.

Salovaara, K. J., Thessler, S., Malik, R. N., & Tuomisto, H. (2005). Classification of Amazonian primary rain forest vegetation using Landsat ETM plus satellite imagery. *Remote Sensing of Environment 97*:39-51.

Sanjeeb, B. (2008). India's endangered rhinoceros battles for survival. The Thaindian News, Guwahiti.

Santos, M.J, Greenberg, J.A., & Ustin, S. L. (2010). Using hyperspectral remote sensing to detect and quantify southeastern pine senescence effects in red-cockaded woodpecker (*Picoides borealis*) habitat. *Remote Sensing of Environment 114*:1242-1250.

Sarkar, S. (2002). Defining biodiversity: assessing biodiversity. *Monist 85***:** 131–155.

Scott, J.M., Davis, F.W., McGuire, R. G., Wright, R. G., Groves, C., & Estes, J. (2001). Nature reserves: do they capture the full range of America's biological diversity? *Ecological Applications 11*:999-1007.

Sharma, B. D., Clevers, J., Graaf, R. D., & Chapagain, N. R. (2004). Mapping Equus kiang (Tibetan Wild Ass) Habitat in Surkhang, Upper Mustang, Nepal. *Mountain Research and Development 24*:149-156.

Sharma, G. (2005). Poachers killing off Nepal's rhinos. Retrieved September, 2008 from www.indianjungles.com,Kathmandu

Shao, G. & Wu, J. (2008). On the accuracy of landscape pattern analysis using remote sensing data. *Landscape Ecology 23*:505-511.

Shoshany, M., & Goldshleger, N. (2002). Land-use and population density changes in Israel—1950 to 1990: analysis of regional and local trends. *Land Use Policy 19*:123 – 133.

Silveira, P., & Dentinho, T. (2010). Spatial interaction model of land use – An application to Corvo Island from the 16th, 19th and 20th centuries. *Computers, Environment and Urban Systems 34*:91 – 103.

Stepenuck, K.F., Crunkilton, R.L., & Wang, L.Z. (2002). Impacts of urban landuse on microinvertebrate communities in southeastern Wisconsin streams. *Journal of the American Water Resources Association 38*:1041-1051.

Star, J., & Estes, J. (1990). Geographic Information Systems: An Introduction. Englewood Cliffs, New Jersey: Prentice-Hall.

Studsrod, J. E., & Wegge, P. (1995). Park-People Relationships - the Case of Damage Caused by Park Animals around the Royal-Bardia-National-Park, Nepal. *Environmental Conservation 22*:133-142.

Thapa, V. (2005). Analysis of one-horned rhinoceros (*Rhinoceros unicornis*) habitat in the Royal Chitwan National Park, Nepal. Thesis, University of North Texas, Denton. 68 pages.

Thomlinson, J. R. (1993). Landscape ecological characteristics of habitat of the red-cockaded woodpecker (*Picoides borealis*). Dissertation, University of North Texas, Denton.

Tolba, M.K., & El-Kholy, O. A. (1992). The World Environment 1972–1992: Two Decades of Challenge. Chapman & Hall, London.

Turner, M. G., Gardner, R. H., & O'Neill, R. V. (2001). Landscape Ecology in Theory and Practice: Pattern and Process. Springer, New York.

U.S. Forest and Wildlife Services. (2005). Red-cockaded woodpecker (*Picoides borealis*). Northeast Region, U.S. Fish and Wildlife Service, 300 Westgate Center Drive, Hadley, MA 01035. Retrieved December, 2007 from http://www.northeast.fws.org

U.S. Forest and Wildlife Services. (2010). Red-cockaded woodpecker recovery. Retrieved June, 2010 from http://www.fws.gov/rcwrecovery/rcw.html

Vesterby, M., & Heimlich, R., (1991). Land use and demographic change: results from fast-growing counties. *Land Economics 67*:279 - 291.

Waggoner, P.E., & Ausubel, J.H. (2001). How much will feeding and wealthier people encroach on forests? *Population and Development review 27*:239-257.

Wang, L.Z., Lyons, J., & Kanehl, P. (2001). Impacts of urbanization on stream habitat and fish across multiple spatial scales. *Environmental Management 28*:255-266.

Walters, J.R., Daniels, S.J., Carter, J.H., & Doerr, P.D. (2002). Defining quality of red-cockaded woodpecker foraging habitat based on habitat use and fitness. *Journal of Wildlife Management 66*:1064-1082.

Wilcove, D. S., McClellan, C. H., & Dobson, A. P. (1986). Habitat fragmentation in the temperate zone. Conservation Biology: the science of scarcity and diversity. Sunderland, MA: Sinauer Associates: 237-256.

Wilson, E. O. (editor), (1988). *Biodiversity*. National Academy Press. Washington, D.C.

Wiens, J., Sutter, R., Anderson, M., Blanchard, J., Barnett, A., Avery, C., & Laine, S. (2009). Selecting and conserving lands for biodiversity: The role of remote sensing. *Remote sensing of Environment. 113*:1370-1381.

With, K. A., & Christ, T. O. (1995). Critical thresholds in species' responses to landscape structure. *Ecology 76*:2446-59.

Wegge, P., Shrestha, A.K., & Moe, S.R. (2006). Dry season diets of sympatric ungulates in lowland Nepal: competition and facilitation in alluvial tall grasslands. *Ecological Research 21*:698-706.

National Park Services. Big Thicket National Preserve. Retrieved December, 2009 from www.nps.gov

Xulong, L., Chunyang, H., Yaozhong, P., Mingchaun, Y., & Jinshui, Z. (2005). Accuracy Assessment of Thematic Classification based on Point and Polygon Sampling Units, Key laboratory of Environmental Change and Natural Disaster of Ministry of Education of China. College of Resources Science & Technology, Beijing Normal University, Beijing, China, 100875.

Zube, E. (1987). Perceived land use patterns and landscape values. *Landscape Ecology 1*.